

# Hydrogeochemistry of Alat and Khobar Aquifers in Eastern Saudi Arabia

by

Hassan Mohamed Hassan

A Thesis Presented to the

FACULTY OF THE COLLEGE OF GRADUATE STUDIES

KING FAHD UNIVERSITY OF PETROLEUM & MINERALS

DHAHRAN, SAUDI ARABIA

In Partial Fulfillment of the  
Requirements for the Degree of

**MASTER OF SCIENCE**

In

**GEOLOGY**

December, 1992

## **INFORMATION TO USERS**

**This manuscript has been reproduced from the microfilm master. UMI films the text directly from the original or copy submitted. Thus, some thesis and dissertation copies are in typewriter face, while others may be from any type of computer printer.**

**The quality of this reproduction is dependent upon the quality of the copy submitted. Broken or indistinct print, colored or poor quality illustrations and photographs, print bleedthrough, substandard margins, and improper alignment can adversely affect reproduction.**

**In the unlikely event that the author did not send UMI a complete manuscript and there are missing pages, these will be noted. Also, if unauthorized copyright material had to be removed, a note will indicate the deletion.**

**Oversize materials (e.g., maps, drawings, charts) are reproduced by sectioning the original, beginning at the upper left-hand corner and continuing from left to right in equal sections with small overlaps. Each original is also photographed in one exposure and is included in reduced form at the back of the book.**

**Photographs included in the original manuscript have been reproduced xerographically in this copy. Higher quality 6" x 9" black and white photographic prints are available for any photographs or illustrations appearing in this copy for an additional charge. Contact UMI directly to order.**

# **U·M·I**

University Microfilms International  
A Bell & Howell Information Company  
300 North Zeeb Road, Ann Arbor, MI 48106-1346 USA  
313/761-4700 800/521-0600



**Order Number 1354095**

**Hydrogeochemistry of Alat and Khobar aquifers in Eastern  
Saudi Arabia**

**Hassan, Hassan Mohamed, M.S.**

**King Fahd University of Petroleum and Minerals (Saudi Arabia), 1992**

**U·M·I**  
300 N. Zeeb Rd.  
Ann Arbor, MI 48106





**HYDROGEOCHEMISTRY OF ALAT AND KHOBAR  
AQUIFERS IN EASTERN SAUDI ARABIA**

**BY**

**HASSAN MOHAMED HASSAN**

**A Thesis Presented to the  
FACULTY OF THE COLLEGE OF GRADUATE STUDIES  
KING FAHD UNIVERSITY OF PETROLEUM & MINERALS  
DHAHRAN, SAUDI ARABIA**

**In Partial Fulfillment of the  
Requirements for the Degree of**

**MASTER OF SCIENCE  
In  
GEOLOGY**

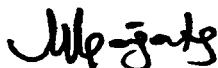
**DECEMBER, 1992**

**KING FAHD UNIVERSITY OF PETROLEUM AND MINERALS**  
**DHAHRAN 31261, SAUDI ARABIA**

**COLLEGE OF GRADUATE STUDIES**

This thesis, written by HASSAN MOHAMED HASSAN under the direction of his Thesis Advisor and approved by his Thesis Committee, has been presented to and accepted by the Dean of the College of Graduate studies, in partial fulfillment of the requirements for the degree of MASTER OF SCIENCE in GEOLOGY.

**THESIS COMMITTEE**



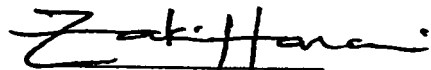
Dr. Mehmet N. Cagatay (Thesis Advisor)



Dr. Mustafa A. Al-Ukayli (Member)



Dr. Abdulatif A. Qahwash (Member)



Department Chairman



Dean, College of Graduate Studies

6-3-93

Date



***Dedicated to  
My Loving Mother  
and  
Family***



## ***ACKNOWLEDGEMENT***

**I thank ALLAH The Almighty for his limitless help and guidance.**

**Acknowledgement is due to King Fahd University of Petroleum and Minerals for providing excellent computing facilities which helped in successful completion of this research.**

**I am deeply indebted to Dr. Mehmet N. Cagatay, my major advisor, for his constant inspiration and guidance in making this research possible. I would also like to thank Dr. Mustafa A. Al-Ukayli and Dr. Abdulatif A. Qahwash, my thesis committee members, for their timely advice and valuable comments.**

**Sincere appreciations are due to Dr. Zaki Y. Al-Harari, Chairman of the Earth Sciences Department, for his continued encouragement. I also wish to thank all the Faculty members of the Earth Sciences Department, my colleagues and friends.**

## TABLE OF CONTENTS

<i>Chapter</i>	<i>page</i>
<i>Acknowledgement</i> .....	<i>iv</i>
<i>List of Figures</i> .....	<i>ix</i>
<i>List of Tables</i> .....	<i>xii</i>
<i>List of Appendices</i> .....	<i>xiii</i>
<i>Abstract</i> .....	<i>xiv</i>
<i>Arabic Abstract</i> .....	<i>xv</i>
<b>1. INTRODUCTION</b> .....	<b>1</b>
<b>1.1 Previous Work</b> .....	<b>1</b>
<b>1.2 Objective of the Study</b> .....	<b>3</b>
<b>1.3 Methods of the Study</b> .....	<b>5</b>
<b>2. GEOLOGICAL AND HYDROGEOLOGICAL SETTING</b> .....	<b>11</b>
<b>2.1 Topography</b> .....	<b>11</b>
<b>2.2 Climate</b> .....	<b>11</b>
<b>2.3 Geology</b> .....	<b>12</b>
<b>2.3.1 Stratigraphy</b> .....	<b>13</b>
<b>2.3.1.1 Rus Formation</b> .....	<b>13</b>
<b>2.3.1.2 Dammam Formation</b> .....	<b>16</b>
<b>2.3.1.2.1 Midra and Saila Shale Member</b> .....	<b>17</b>
<b>2.3.1.2.2 Alveolina Limestone Member</b> .....	<b>17</b>
<b>2.3.1.2.3 Khobar Member</b> .....	<b>18</b>
<b>2.3.1.2.4 Alat Member</b> .....	<b>18</b>

2.3.1.3	<i>Hadrukh Formation</i>	19
2.3.1.4	<i>Dam Formation</i>	19
2.3.1.5	<i>Hofuf Formation</i>	20
2.3.1.6	<i>Recent Deposits</i>	20
2.3.2	<i>Structure</i>	21
2.4	<i>Hydrogeology</i>	21
2.4.1	<i>Rus Aquitard</i>	22
2.4.2	<i>Midra &amp; Saila and Alveolina Limestone Aquitard</i>	22
2.4.3	<i>Khobar Aquifer</i>	22
2.4.4	<i>Alat Marl Aquitard</i>	23
2.4.5	<i>Alat Aquifer</i>	23
3.	<b>DISTRIBUTION OF CHEMICAL CONSTITUENTS</b>	25
3.1	<i>Introduction</i>	25
3.2	<i>Alat Aquifer</i>	25
3.2.1	<i>Calcium</i>	25
3.2.2	<i>Magnesium</i>	27
3.2.3	<i>Sodium</i>	27
3.2.4	<i>Chloride</i>	30
3.2.5	<i>Sulfate</i>	30
3.2.6	<i>Bicarbonate</i>	33
3.2.7	<i>Total Dissolved Solids</i>	33
3.2.8	<i>TDS-EC Relationship</i>	36
3.2.9	<i>Hydrogeochemical Facies</i>	38
3.3	<i>Khobar Aquifer</i>	41
3.3.1	<i>Calcium</i>	41

3.3.2	<i>Magnesium</i> .....	43
3.3.3	<i>Sodium</i> .....	43
3.3.4	<i>Chloride</i> .....	43
3.3.5	<i>Sulfate</i> .....	48
3.3.6	<i>Bicarbonate</i> .....	48
3.3.7	<i>Total Dissolved Solids</i> .....	52
3.3.8	<i>TDS-EC Relationship</i> .....	52
3.3.9	<i>Hydrogeochemical Facies</i> .....	55
3.4	<i>Distributional Comparison between Alat and Khobar Aquifers</i> .....	58
4.	<b>AQUEOUS EQUILIBRIUM STUDIES</b> .....	61
4.1	<i>Aqueous Models</i> .....	61
4.2	<i>Distribution of Saturation Indices in the Alat Aquifer</i> .....	66
4.3	<i>Distribution of Saturation Indices in the Khobar Aquifer</i> .....	68
5.	<b>HYDROGEOCHEMICAL PROCESSES</b> .....	75
5.1	<i>Introduction</i> .....	75
5.2	<i>Alat Aquifer</i> .....	77
5.3.	<i>Khobar Aquifer</i> .....	84
6.	<b>POTABILITY AND AGRICULTURAL USE</b> .....	97
6.1	<i>Domestic use and Public Supply</i> .....	97
6.2	<i>Livestock Consumption</i> .....	99
6.3	<i>Agricultural Use</i> .....	102
6.4	<i>Industrial Use</i> .....	113
7.	<b>CONCLUSIONS</b> .....	115

**REFERENCES .....118**

**APPENDIX.....125**

## LIST OF FIGURES

<i>Figure</i>	<i>page</i>
<i>1.1 Location Map of the Study Area .....</i>	<i>4</i>
<i>1.2 Water Samples Location Map of the Alat Aquifer .....</i>	<i>6</i>
<i>1.3 Water Samples Location Map of the Khobar Aquifer .....</i>	<i>7</i>
<i>2.1 Generalized Lithostratigraphic Sequence of the study area .....</i>	<i>14</i>
<i>2.2 Geological Map of the Study Area.....</i>	<i>15</i>
<i>3.1 Areal Distribution Map of Calcium (mg/l) in Alat Aquifer .....</i>	<i>26</i>
<i>3.2 Areal Distribution Map of Magnesium (mg/l) in Alat Aquifer.....</i>	<i>28</i>
<i>3.3 Areal Distribution Map of Sodium (mg/l) in Alat Aquifer .....</i>	<i>29</i>
<i>3.4 Areal Distribution Map of Chloride (mg/l) in Alat Aquifer.....</i>	<i>31</i>
<i>3.5 Areal Distribution Map of Sulfate (mg/l) in Alat Aquifer.....</i>	<i>32</i>
<i>3.6 Areal Distribution Map of Bicarbonate (mg/l) in Alat Aquifer .....</i>	<i>34</i>
<i>3.7 Total Dissolved Solids Map of Waters in the Alat Aquifer .....</i>	<i>35</i>
<i>3.8 EC versus TDS Plot of Waters in the Alat Aquifer.....</i>	<i>37</i>
<i>3.9 Trilinear Plot of Water Samples of Alat Aquifer.....</i>	<i>39</i>
<i>3.10 Hydrogeochemical Facies Map of the Alat Aquifer.....</i>	<i>40</i>
<i>3.11 Areal Distribution Map of Calcium (mg/l) in Khobar Aquifer .....</i>	<i>42</i>
<i>3.12 Areal Distribution Map of Magnesium (mg/l) in Khobar Aquifer...44</i>	
<i>3.13 Areal Distribution Map of Sodium (mg/l) in Khobar Aquifer .....</i>	<i>45</i>
<i>3.14 Areal Distribution Map of Chloride (mg/l) in Khobar Aquifer.....</i>	<i>46</i>
<i>3.15 Sodium   Chloride (meq/l) ratio Map of the Khobar Aquifer .....</i>	<i>47</i>
<i>3.16 Areal Distribution Map of Sulfate (mg/l) in Khobar Aquifer.....</i>	<i>49</i>
<i>3.17 Chloride   Sulfate (meq/l) ratio Map of the Khobar Aquifer.....</i>	<i>50</i>

<b>3.18 Areal Distribution Map of Bicarbonate (mg/l) in Khobar Aquifer ..</b>	<b>51</b>
<b>3.19 Total Dissolved Solids Map of Waters in the Khobar Aquifer .....</b>	<b>53</b>
<b>3.20 EC versus TDS Plot of Waters in the Khobar Aquifer .....</b>	<b>54</b>
<b>3.21 Trilinear Plot of Water Samples of the Khobar Aquifer .....</b>	<b>56</b>
<b>3.22 Hydrogeochemical Facies Map of the Khobar Aquifer .....</b>	<b>57</b>
<b>4.1 Calcite Saturation Index Map of the Alat Aquifer .....</b>	<b>67</b>
<b>4.2 Dolomite Saturation Index Map of the Alat Aquifer .....</b>	<b>69</b>
<b>4.3 Gypsum Saturation Index Map of the Alat Aquifer .....</b>	<b>70</b>
<b>4.4 Calcite Saturation Index Map of the Khobar Aquifer .....</b>	<b>72</b>
<b>4.5 Dolomite Saturation Index Map of the Khobar Aquifer .....</b>	<b>73</b>
<b>4.6 Gypsum Saturation Index Map of the Khobar Aquifer .....</b>	<b>74</b>
<b>5.1 Relation of Sulfate   Chloride ratio to Sulfate (mg/l) in the Alat Aquifer .....</b>	<b>78</b>
<b>5.2 Profiles of Hydrogeochemical Parameters along Alat Aquifer Flowpath .....</b>	<b>81</b>
<b>5.3 Stiff Diagrams Showing Changes in Major Ions Along Alat Aquifer Flowpath. ....</b>	<b>83</b>
<b>5.4 Hydrogeochemical Parameters along Al Hufuf Flowpath in Khobar Aquifer .....</b>	<b>85</b>
<b>5.5 Relation of Sulfate   Chloride ratio to Sulfate (mg/l) in the Khobar Aquifer .....</b>	<b>87</b>
<b>5.6 Stiff Diagrams Showing Changes in Major Ions along Al-Hufuf Flowpath in Khobar Aquifer .....</b>	<b>88</b>
<b>5.7 Hydrogeochemical Profiles along Abqaiq Flowpath in Khobar Aquifer .....</b>	<b>90</b>

<b>5.8 Stiff Diagrams Showing the Major Ions Changes along Abqaiq Flowpath in Khobar Aquifer .....</b>	<b>93</b>
<b>5.9 Hydrogeochemical Profiles along a Flowpath at the North of Jubayl in Khobar Aquifer .....</b>	<b>94</b>
<b>5.10 Stiff Diagrams Showing Changes in Major Ions along a Flowpath at the North of Jubayl in Khobar Aquifer .....</b>	<b>95</b>
<b>6.1 Sodium Adsorption Ratio Map of the Alat Aquifer .....</b>	<b>107</b>
<b>6.2 Sodium Adsorption Ratio Map of the Khobar Aquifer .....</b>	<b>108</b>
<b>6.3 Diagram Showing Irrigation Water Classification of Alat Aquifer .....</b>	<b>109</b>
<b>6.4 Diagram Showing Irrigation Water Classification of Khobar Aquifer .....</b>	<b>110</b>
<b>6.5 Diagram for Quantitative Estimation of SAR from EC and TDS Values of the Khobar Aquifer .....</b>	<b>112</b>



## **LIST OF TABLES**

<b>Table</b>	<b>page</b>
<b>3.1 Comparison between the Hydrochemical Distributions of Alat and Khobar Aquifers.....</b>	<b>59</b>
<b>5.1 Comparison between Khobar and Umm Er Radhuma Aquifers in Abqaiq Area.....</b>	<b>91</b>
<b>6.1 Recommend Concentration Limits for Human Consumption .....</b>	<b>98</b>
<b>6.2 Recommended Concentration Limits for Livestock Consumption.....</b>	<b>101</b>
<b>6.3 Salinity Tolerance Level of Crop Plants.....</b>	<b>103</b>
<b>6.4 Water Classes Based on SAR .....</b>	<b>105</b>
<b>6.5 Recommended Concentration Limits for Some Selected Industries.....</b>	<b>114</b>

## **LIST OF APPENDICES**

<b>Appendix</b>	<b>page</b>
<b>1. Hydrogeochemical Data of the Alat Aquifer .....</b>	<b>125</b>
<b>2. Hydrogeochemical Data of the Khobar Aquifer .....</b>	<b>128</b>
<b>3. Thermodynamic Database of PCWATEQ Computer Program .....</b>	<b>135</b>
<b>4. The Irrigation Classes of Alat Aquifer Water .....</b>	<b>147</b>
<b>5. The Irrigation Classes of Khobar Aquifer Water .....</b>	<b>150</b>

## **ABSTRACT**

**Full Name** : *Hassan Mohamed Hassan*

**Title of Study** : *Hydrogeochemistry of Alat and Khobar  
Aquifers in Eastern Saudi Arabia.*

**Major Field** : *Geology (Hydrogeochemistry)*

**Date of Degree** : *December 30, 1992*

Major ion distribution and computerized equilibrium studies were conducted on Alat and Khobar aquifers of the Eocene age in Eastern Saudi Arabia. Both aquifers are oversaturated with calcite and dolomite, and undersaturated with gypsum. The Piper's trilinear plots show the presence of three different facies in the Alat aquifer and four facies in the Khobar aquifer. The groundwater evolutionary pattern in both aquifers generally follows Chebotarev's sequence. However, the presence of seawater intrusion near Jubayl, cation exchange in Abqaiq, and water mixing on structural highs are the main superimposed processes. The total dissolved solids (TDS) in the aquifers exceeds the recommended levels for most uses, but mostly its range is suitable for municipal, stock farming and some industrial use.

## **MASTER OF SCIENCE DEGREE**

**KING FAHD UNIVERSITY OF PETROLEUM AND MINERALS**

*Dhahran, Saudi Arabia*

*December 1992*

## ملخص بحث

الاسم : حسن محمد حسن

مسمى البحث : كيميائية المياه الجوفية في الطبقات المائية في  
خزاني علات والخير ، المنطة الشرقية ، المملكة  
العربية السعودية .

التخصص : جيولوجيا ( كيميائية المياه الجوفية ) .  
تاريخ الحصول على الدرجة : ٣٠ ديسمبر ١٩٩٢ م .

لقد تم عمل دراسات ومعادلات بالحاسب الآلي حول توزيع الايونات في طبقات المياه الجوفية في خزاني علات والخير في العصر الحديث بالمنطقة الشرقية . واكتشف ان كلا الخزانين مشبعين بالكالسيوم والدولوميت وغير شبعة بالجسيموم مع وجود ثلاث انواع مختلفة من الشحنات الحاوية للمياه في خزان علات واربعة في خزان الخير . ويتبع تطور المياه الجوفية في كلا الخزانين بشكل عام ترتيب شيبوتاريف . ويعتبر وجود متداخلات مياه البحر في المنطقة بالقرب من الجبيل وتغيير الشحنات الموجبة في ابقى واختلاط المياه في البنيات العالية من اكثر العوامل المؤثرة . وجملة المواد الصلبة الذائبة في المياه الجوفية تتجاوز المستويات القياسية بالنسبة لكثير من المستعملين ولكن هذا المعدل في اغلب الاحيان يناسب الاستعمالات الصناعية والبلدية والرعي .

درجة الماجستير في العلوم

جامعة الملك فهد للبترول والمعادن

الظهران - المملكة العربية السعودية

ديسمبر ١٩٩٢ م

## **CHAPTER 1**

### **INTRODUCTION**

#### **1.1 Previous Work**

Groundwater hydrochemical data give important information on basic geochemical processes in an aquifer system, such as water/rock interaction, mineral dissolution-precipitation, ion exchange, and seawater intrusion. In addition, such data provide information on the origin, type, and quality of water in relation to domestic, agricultural, and various industrial uses.

Khobar and Alat aquifers, with underlying Umm Er Radhuma, constitute a very important aquifer system for the Eastern Province of Saudi Arabia. These carbonate aquifers are divided by intervening aquitards. However, some leakage appears to take place between the three aquifers (Rasheeduddin, 1988). The regional hydraulic gradients of the aquifers decrease to the east and to the north (Naimi, 1965).

Alat is a local, karstified and fissured limestone aquifer of limited extent in the northeastern Arabian shelf, around Qatif, Dammam, and Al Hassa (Edgell, 1990). The aquifer's thickness ranges from 10m to 50m, with transmissivity of  $3.1 \times 10^{-4}$  to  $2.3 \times 10^{-3} \text{ m}^2/\text{s}$  and storativity of  $1.5 \times 10^{-4}$  to  $2.6 \times 10^{-4}$  (Italconsult, 1969), indicating its confined nature. Khobar aquifer is a calcarenitic and partly dolomitic limestone, which is locally karstified and fissured. It provides

water for domestic and agricultural purposes in many parts of the Eastern Province. The aquifer's thickness ranges from 20m to 70m with an average transmissivity of  $2.9 \times 10^{-1} \text{ m}^2 / \text{s}$ , indicating high transmissive behavior (Rasheeduddin, 1988). The average storativity value is about  $2.1 \times 10^{-5}$  which indicates the confined nature of the aquifer (Rasheeduddin, 1988).

The water/rock interaction is probably the main control on the water chemistry in the central parts of the aquifers' flow path and in the recharge areas. The water quality, in the aquifers, in some areas is controlled by the regional geological structures (Naimi, 1965).

Groundwater from different aquifers could mix through fissures and semi-permeable layers in the aquitards. Such mixing could locally disturb the chemical evolutionary sequence along the flow paths.

Few hydrochemical studies had previously been carried out to investigate the controls on the water composition and distribution of water quality parameters in the aquifers of Eastern Saudi Arabia. Most studies have focused on the hydraulic properties of the aquifer systems (Rasheeduddin, 1988; Yazicigil et al, 1986). Naimi (1965) discussed the regional hydraulic characteristics and general water quality of the aquifers. Furthermore, he disclosed that the salt content in the aquifers increases from southwest towards northeast. Job (1978) described the mixing of low-mineralized waters from the south near Qatif, with a groundwater stream of highly mineralized waters from the north. Sen and Al-Dakheel (1986) investigated the hydrochemical

characteristics of the underlying aquifer, Umm Er Radhuma, using histograms, equivalent per million percentage histograms, and linear relationships between various composite variables. Their results indicated that the major groundwater types of Umm Er Radhuma aquifer are NaCl and  $CaSO_4$  types. Abderrahman (1990) attributed the increase of TDS values in the Al Hassa oasis to the groundwater development in the overlying Neogene aquifer between 1976 and 1987. Bazuhair, A. A., M. T. Hussein and M. S. Hamza (1990) arranged the springs of the Kingdom into five groups according to the rock from which their water originates. For instance, the Qatif springs were classified under solution-opening springs with high percentage of Na and Cl, and Al-Hassa springs under interstratification springs with Ca and Mg forming 50 % of the major ions.

## ***1.2 Objectives of the Study***

The objectives of the present study are to investigate the geochemistry of groundwater in the Alat and Khobar aquifers by using the chemical data of (347) wells published by the Ministry of Agriculture and Water (MAW, 1984) and Groundwater Development Consultants (GDC, 1980). The study area is located in the Eastern Province of Saudi Arabia. The area is bounded by latitudes 24° 00' and 29° 00' N and by 47° 00' and 51° 00' E (Fig. 1.1).

The specific objectives of this study are to determine the following:

1. Distribution of major ions and their ratios.
2. Distribution of water quality parameters such as total dissolved solids (TDS)

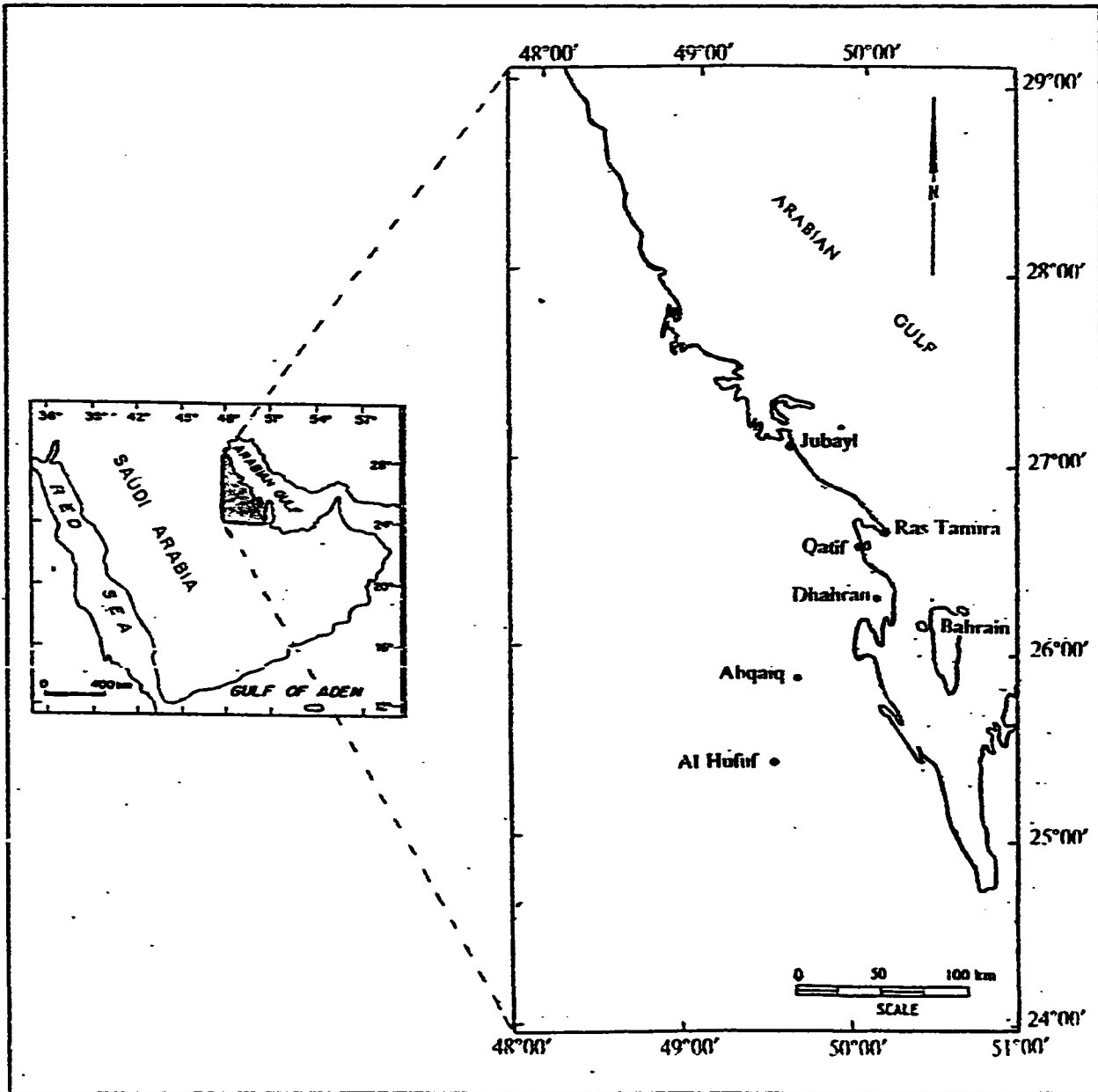


**Figure 1.1** Location map of the study area.



and sodium adsorption ratio (SAR).

3. Distribution of saturation indices (SI) with respect to various aquifer minerals.
4. Chemical evolutionary sequence of groundwaters and the factors affecting the water composition.
5. The quality of waters in relation to domestic, agricultural, and industrial uses.

### ***1.3 Methods of the Study***

Hydrochemical data published by the Department of Water Resources Development of the Ministry of Agriculture and Water (1984) and Groundwater Development Consultants (GDC, 1980) are utilized in this thesis project. The data of Ministry of Agriculture and Water are compiled for 333 samples from 333 wells. Of the 333 wells, 250 wells pump water from Khobar aquifer and 83 from Alat aquifer. The GDC data consists of 14 samples, from 14 wells which are pumping water from Alat and Khobar aquifers (Figures 1.2 and 1.3). The data are mainly distributed along the coastal belt of the Arabian Gulf with few in the western and southwestern parts of the study area. Data on each sample represent concentration of major ions (in mg/l), electrical conductivity, total dissolved solids (TDS), pH, field temperature, minor ions concentrations, and silica contents. Furthermore, each sample is identified by sample number, well location name, geographic coordinates, well depth, and sampling date.

The data of the wells are selected on basis of (1) location of the well, and (2) charge-balance error lesser than about 5%. Most of the analyses used in this study were originally reported in mg/l unit. However, mg/l unit is converted to

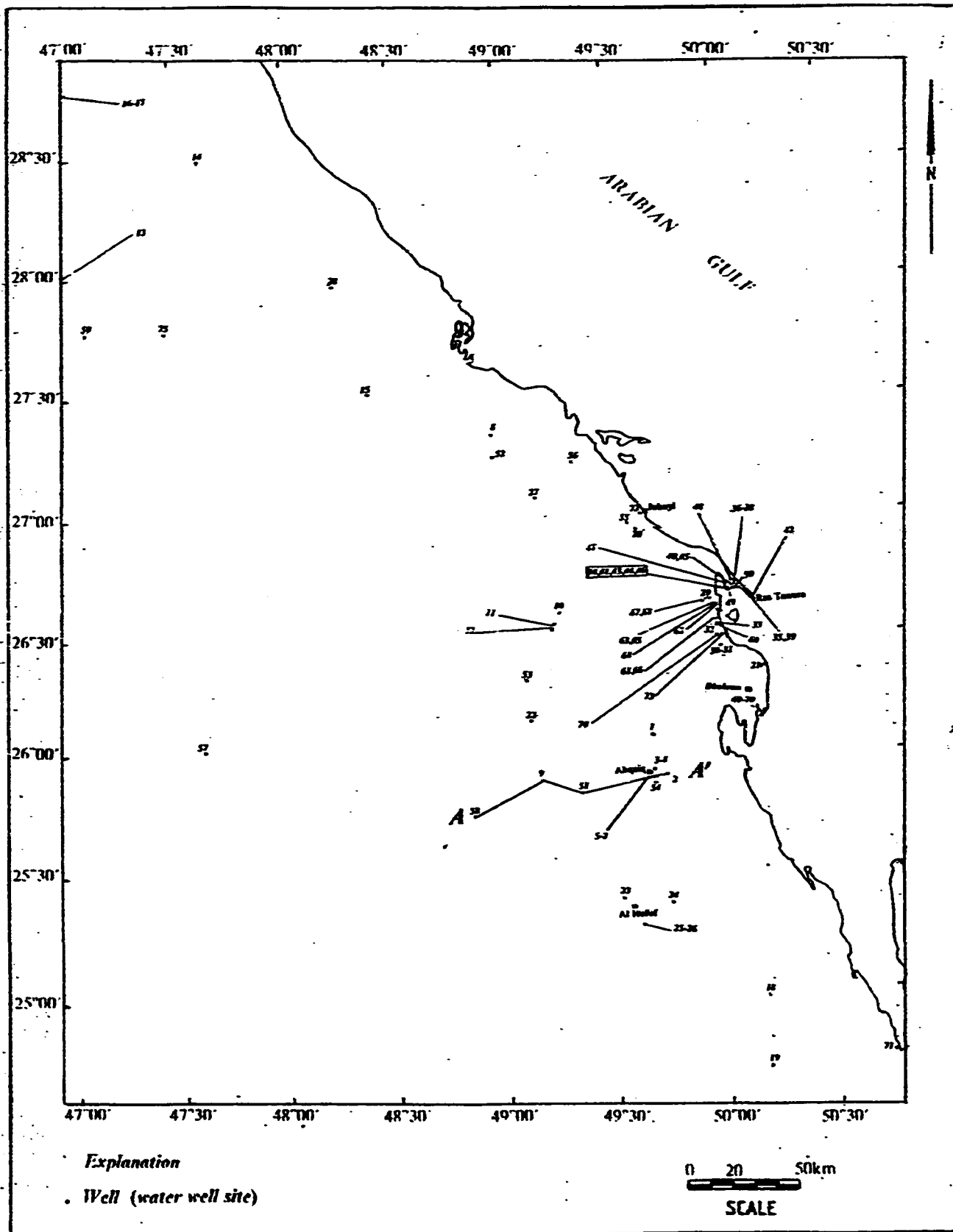


Figure 1.2 Water samples location map of the Alat aquifer.

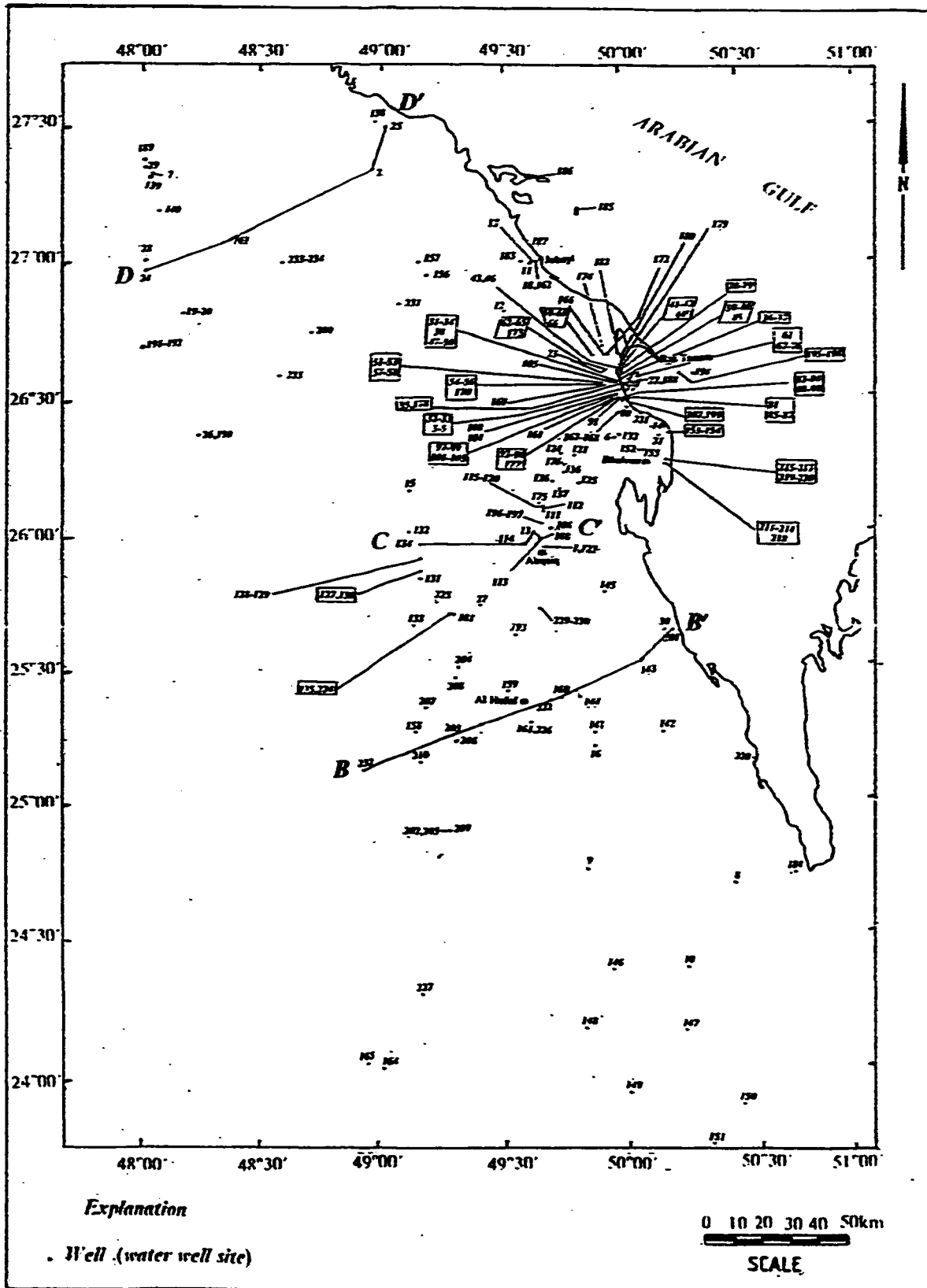


Figure 1.3 Water samples location map of the Khobar aquifer.

the meq/l unit (Appendix 1 and 2).

Raw chemical data give little information about geochemical processes that change the chemistry of groundwater. One of the principal methods of interpreting groundwater geochemistry is by assuming that all dissolved constituents are in equilibrium with the aquifer minerals. The assumption allows the use of thermodynamic models to calculate the distribution of the dissolved species. Such a technique is adopted for this study.

The data is analyzed by using PCWATEQ (Rollins,1990) program which is a special IBM PC modification of WATEQF (Plummer,1984) in the mainframe computer code. Before running PCWATEQ, the data were arranged in a special format by a separate user-friendly data file program (i.e. Datagen; Rollins, 1990). Datagen accepts ion concentration values, water temperature, pH, Eh, and specific gravity of the water. After arranging the data, the PCWATEQ.EXE file was run. The pH values limit PCWATEQ to surface waters where the pressure effect becomes negligible. The program also calculates the redox reactions. Oxidation-reduction equilibria have been treated in the same manner as other reactions in WATEQ (Truesdell et al., 1973).

PCWATEQ solves the equations relevant to the computation of ion activities and the equilibrium pressures of several gases that may be in contact with the water (Rollins, 1990). Moreover, the program computes cation/anion balance and the saturation indices of water with respect to approximately 200 mineral phases. PCWATEQ gives information on the distribution of species and mole ratios of both analytical and computed molalities. A database file,

Pcwateq.dbs, accompanies the package; the database file contains thermodynamic values, such as log equilibrium constants and standard enthalpies for aqueous species (Appendix 3).

A spreadsheet program called SURFER is used for contouring the outputs of PCWATEQ. Parameters such as Total dissolved solids (TDS), saturation index (SI), sodium adsorption ratio (SAR) and areal distribution maps of ions are contoured using the Kriging technique. While using SURFER, the map boundaries were manually digitized. For drawing Pipers' trilinear diagrams and Stiff diagrams, Plotchem PC program is used (TECSOFT, 1987). Besides the above PC programs, the VM (mainframe) programs such as WF77SYS and ICUSYS are used for mathematical calculations and graphical representations.

On basis of the obtained contour maps and hydrogeochemical plots, the water bodies with different qualities in relation to their possible domestic, agricultural and industrial uses are identified. The water quality/geological structures relationships are also investigated by comparing the TDS contour maps with the main geological structures in the region. Due to the scarcity and sometimes absence of data in the western and the southwestern parts of the study area, tentative results are presented by the extrapolation of the contours.

The water samples are classified into different types according to their saturation indices and their locations on the Piper's trilinear diagram (Piper, 1944). To interpret the hydrogeochemical evolution of the groundwater along the flow direction, profiles involving the plots of distance versus total dissolved solids, and distance versus major ions are examined. The possibility of seawater

**intrusion along the coastline is investigated on the basis of the variation in the groundwater chemistry.**

## **CHAPTER 2**

### **GEOLOGICAL AND HYDROGEOLOGICAL SETTING**

#### **2.1 Topography**

The study area is generally flat, rising gradually from the Arabian Gulf towards west, along the edge of As Summan plateau where the elevation reaches about 300m. In general, the transition from coastal zone to the plateau is gradual without any evident boundary. However, near Al Hufuf, there is a steep escarpment which rises more than 100m (Johnson,1978). Two positive topographic features, the Dammam Dome and the Ghawar structure represent isolated highs within the semi-horizontal coastal zone. The Dammam Dome rises to a maximum elevation of 146 m above sea level at Jabal Umm Er Rus which is located a short distance from the Arabian gulf (Tleel,1973).

Unconsolidated clastic sediments are common in the Arabian Gulf coastal zone. There is an area of drifting sand, south of Al Hufuf, called Al Jafurah. Wadis are not common in the area. Another conspicuous feature is the presence of Sabkha deposits. Numerous coastal and inland Sabkhas are found along the Arabian Gulf coast. Previous studies show that these Sabkha deposits are hydraulically independent of the deeper aquifers (Italconsult, 1969).

#### **2.2 Climate**

The climate of the study area varies from scorching summers to cool winters. During the hottest summer months of July and August, the temperature

ranges from 41°C to 44°C. The average temperatures are slightly higher in Abqaiq and lower in Ras Tanura (Naimi, 1965). Winter (December, January and February) is usually cold. However, the temperature never drops below freezing. Snow and hail are uncommon and the minimum temperature ranges from 7°C to 13°C. January is considered as the coldest month (Al Sayyari et al., 1978; Naimi, 1965). As an arid region, precipitation is scarce and rainfall pattern is highly variable. The rainy season is December to May. Measurements by Saudi Aramco for the last 20 years indicate an average rainfall of 72 mm at Dhahran, 88 mm at Ras Tanura, and 82 mm at Abqaiq (Al Sayyari et al. 1978). In Ras Tanura area, a 215.1 mm rainfall recorded in 1955 compared with a 8.9 mm rainfall recorded in 1960, reflecting the variation in precipitation.

Mean monthly and annual relative humidities vary from place to place and from year to year. However, the variability is much lesser compared to the precipitation values (Al Sayyari et al, 1978). In coastal areas, high relative humidity ranges from 65 to 75 % during winter ( December through February) and low relative humidity ranges from 37 to 63 % during summer (June through August). Landward, the high relative humidities vary from 35 to 78 % during winter and low relative humidities vary from 13 to 47 % during summer (Al Sayyari and Zottle, 1978).

### **2.3 Geology**

The following discussion on the geology and hydrogeology of the study area is based on work conducted by Italconsult (1969), BRGM (1977), GDC (1980),



Tleel (1973), Naimi (1965), Powers (1966), Johnson (1978), and Edgell (1990).

### ***2.3.1 Stratigraphy***

The stratigraphic sequence in the study area ranges from Paleocene to Holocene in age (Fig. 2.1) The surface geology of the study area is given in (Fig. 2.2).

Two distinct sedimentary cycles are evident in the study area (Italconsult, 1969). The first cycle is represented by Paleocene - Eocene series and it crops out on the Dammam Dome. It mainly consists of marine carbonate sequence with the intercalation of fine clastics and evaporites. The second cycle, Miocene - Holocene series, lies unconformably over Eocene. The series is mainly formed of continental clastics, with marine and transitional deposits interbedded in lower and middle part.

The Paleogene sequence is subdivided into the Umm Er Radhuma Formation, the Rus Formation, and the Dammam Formation. The Dammam Formation is also subdivided into five members which are Midra and Saila shales, Alveolina Limestone, Khobar, and Alat members.

The Neogene sequence is divided into Hadruk Formation, Dam Formation, and Hofuf Formation.

#### ***2.3.1.1 Rus Formation***

The Rus Formation conformably overlies the Umm Er Radhuma Formation and crops out in the central portion of the Dammam Dome. At the type section

AGE	FORMATION	MEMBER	ROCK UNIT	GENERALIZED LITHOLOGIC DESCRIPTION	THICKNESS (m)	HYDROGEOLOGIC UNIT	
QUATERNARY	SURFICIAL DEPOSITS			Gravel, Sand and silt	3-30	Variable Productivity depending on recharge	
Tertiary	Neogene	Huruf		Sandy marl and sandy limestone	0-95	Neogene Aquifer (LIMITED PRODUCTIVITY)	
		Dam		Sandy marls, silty clays and skeletal limestones	0-100		
		Hadrakh		Silty marls and shales, sandy limestones	0-90		
	Eocene	Dammam	Alat	Limestone	Skeletal Detrital limestones	0-110	Aquifer
				Marl	Dolomitic marls with limestone intercalations (orange color)	0-35	Aquitard
			Khobar		Skeletal, detrital, porous and friable limestones, dolomitic limestones	0-75	Aquifer
			Alveolina Limestone		Limestones interbedded with shales and marls	0-20	Aquitard
			Midra and Saifa shales		Blue and dark grey, fissile shales with gypsiferous lenses	0-20	
			Rus		Chalky limestones; anhydrite, dolomitic limestones & shales	20-110	
	Paleocene	Umm Er-Radhum		Partially dolomitized chalky limestones, detrital, skeletal limestone	average 320	Aquifer	
Cretaceous	Aruma		Variocolored limestone, subordinate dolomite and shale		Poor Aquifer		

Figure 2.1 Generalized lithostratigraphic sequence of the study area (after Italconult, 1969).

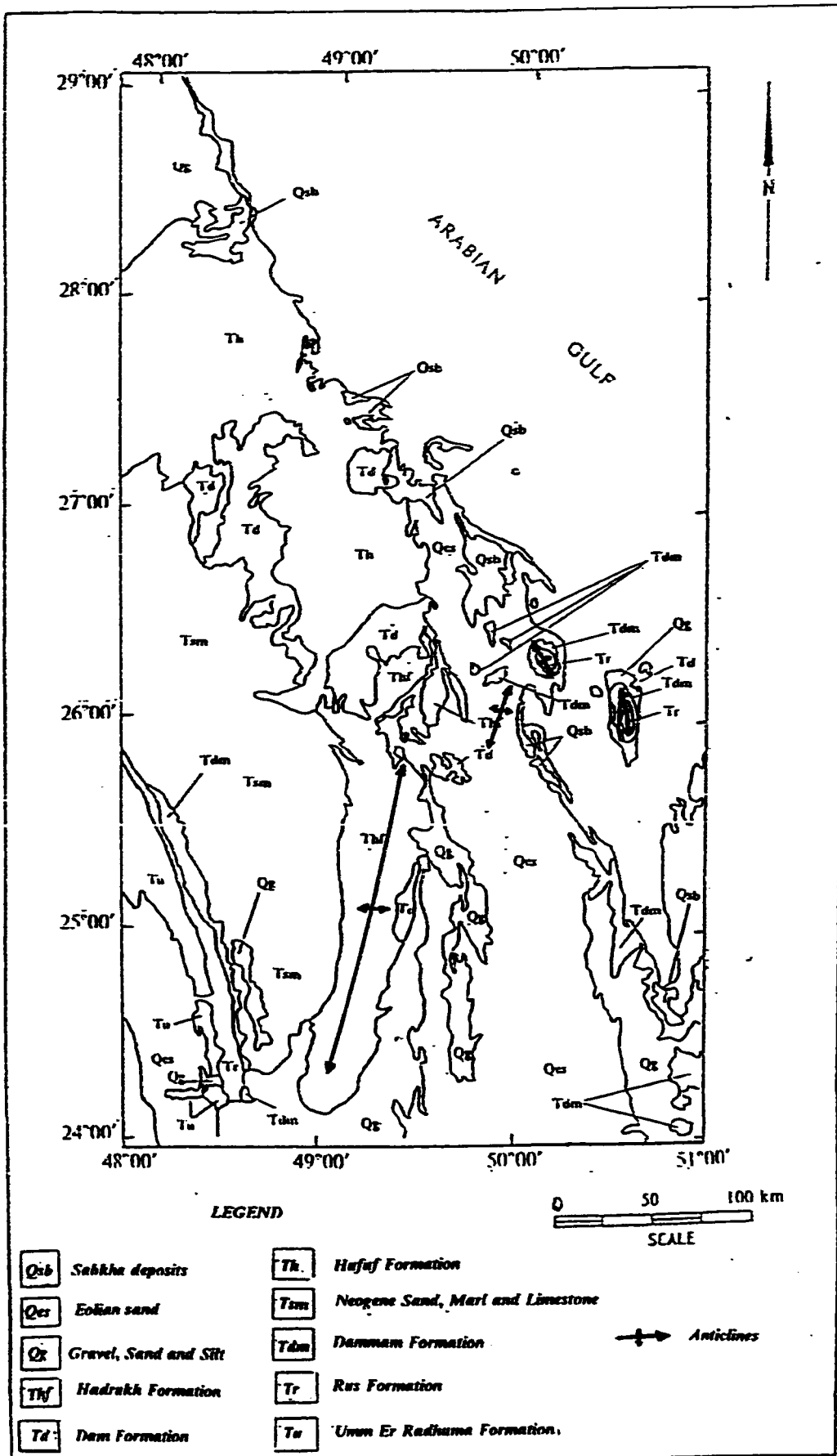


Figure 2.2 Geological map of the study area (after USGS et al, 1963; 1979).

on the Dammam Dome, both Teele (1973) and Powers et al., 1966) divided the formation into three main units : the lower unit is mainly of gray, hard, fine grained dolomitic limestones with intercalation of soft, porous, light colored dolomitic limestones. Upward, the unit is characterized by quartz geodes.

The middle unit consists of evaporites and shallow marine deposits, mainly represented by soft friable cream, buff to pink chalky limestones and gypsum lenses with thin intercalation of gray and buff, fine-grained dolomitic limestones. The upper unit is formed mainly of yellowish microcrystalline, partly dolomitic limestone and white chalky limestone with gypsiferous shale.

#### ***2.3.1.2 Dammam Formation***

Dammam Formation crops out at the circumference of the Dammam Dome and in four smaller patches about 10km to 25km to the west of the dome (Johnson, 1978). The formation conformably overlies the Rus Formation and is bounded at the top by Eocene-Neogene unconformity. It consists mainly of carbonates with intercalation of shales and marls, and subdivided into five members, from older to younger, as follows:

- a) the Midra Shale Member
- b) the Saila Shale Member
- c) the Alveolina Limestone Member
- d) the Khobar Member
- e) the Alat Member

#### ***2.3.1.2.1 Midra and Saila Shale Members***

Due to their lithological similarities, the Midra and Saila shales could be treated as a single lithological unit (Al Tamimi, 1985). The two Members form the basal unit of the Dammam Formation where they are bounded at the bottom by the dolomite of Rus Formation and at the top by the Alveolina Limestone Member.

The Shales consist of blue, blue-gray and tan, fissile and sub-fissile marly shales that are locally gypsiferous with a light gray unit of skeletal, detrital limestone in the central part. These shales consist predominantly of palygorskite and dolomite (Cagatay, 1990). The type section occurs at the Dammam Dome where it is 7-m-thick, having an average thickness of about 10m (Al Tamimi, 1985; Italconsult, 1969).

#### ***2.3.1.2.2 Alveolina Limestone Members***

The Alveolina Limestone Member is bounded at the bottom by blue shales of the Saila unit and at the top by white argillaceous limestone of the Khobar Member. The Member, at the type section, consists of about 1-m-thick yellowish-gray, microcrystalline, partly recrystallized, dolomitized limestone that is locally silicified (Johnson, 1978). It contains common Alveolina elliptica (Sowerby) var. flosculina Silvestri and molds of Lucina pharaonsis (J. W. Tleel, 1973; Johnson, 1978).

#### ***2.3.1.2.3 Khobar Member***

The Khobar Member is subdivided into two units, the lower unit and the upper unit. The lower unit or Khobar Marl consists of 1.5 m of light gray to tan dolomitic marl, whereas the upper unit or the Khobar dolomite consists predominantly of limestone (with 4m of light gray, partly recrystallized, non porous, nummulitic limestone) above which is 1 m of yellowish-brown, soft marly limestone, which is overlain by 3 m of yellowish gray, massive, hard, nummulitic, calcarenitic limestone (Al Sayyari and Zottle., 1978). Tleel (1973) identifies the abundant Nummulites in the calcarenitic limestone as *Nummulites somaliensis*. A thickness of 24 m is encountered at the type section and the average thickness in the subsurface is around 40 m (Al Tamimi, 1985; Tleel, 1973).

#### ***2.3.1.2.4 Alat Member***

Likewise, the Alat Member is subdivided into two units; the lower unit formed mainly of marls and the upper unit composed of predominantly limestone.

The lower unit is known as the Orange Marl or Alat Marl. At outcrops, the lower unit consists of 6 m of light-colored dolomitic marl, which is locally argillaceous. The upper unit is composed of 9 m of cream to tan, chalky, porous, commonly dolomitic limestone with numerous molds of mollusks (Johnson, 1978).

Since the member has been subjected to Pre-Neogene erosion, large variations in its thickness are observed. At the type section, the thickness is 15 m and the average thickness in boreholes is about 70 m.

#### ***2.3.1.3 Hadrukh Formation***

The Hadrukh Formation unconformably overlies the Dammam Formation. The formation extends in a band along the Arabian Gulf Coast from the northern border of the study area as far south as lat 26° 30' N. Also, it occurs in scattered patches beyond Abqaiq. In these areas, the formation is mostly non-marine. However, a small area extending for about 60 km from Al Qatif - Al Alah has marine layers near the top of the formation. The formation consists of sandstone, sandy marl, sand, clay and sandy limestone with abundant chert in some layers and gypsum (Johnson, 1978). Its thickness varies from zero to 90 m.

#### ***2.3.1.4 Dam Formation***

The Dam formation lies conformably over the Hadrukh Formation and near the Arabian Gulf Coast occurs in patches. At Jabal Al Lidam (the type locality), Dam Formation is 90-m-thick consisting of pink, white and gray marl, and red, green and olive clay with intercalation of sandstone, limestone and coquina (Johnson, 1978). The formation thickness in the study area varies from zero to more than 100 m.

#### ***2.3.1.5 Hofuf Formation***

The Hofuf Formation is quite lenticular and heterogeneous; both the thickness and the lithology vary from place to place. At the type locality, the thickness is about 95 m (Johnson, 1978). The lower part is composed of red and white conglomerates, whereas the upper part mainly consists of sandy limestones. Johnson (1978) pointed out that the age might have been late Miocene-Pliocene.

#### ***2.3.1.6 Recent Deposits***

The Recent Deposits in the study area consist of marine terraces, raised beaches, sabkhas and eolian sands. Marine terraces and Raised beaches consist of cross bedded sands and coquina limestones. They occur discontinuously along the Arabian Gulf shoreline having an average thickness of 3-10 m. Their age is Pleistocene (Johnson, 1978).

Coastal as well as inland sabkhas occur in the study area. The largest being sabkhat Ar Riyas which extends from N-NW of Dhahran all the way to the N-NW of Jubayl (Johnson, 1978). The deposits generally consist of silt, clay, and muddy sand associated with evaporites and frequently covered by a salty surface. Eolian sands include areas of dikakah, an irregular surface with bush and grass covered sand and areas of barchan dunes. South of Al Hufuf, there is a narrow drifting sand called Al Jafurah. However, it widens southwardly and merges with Rub al Khali sand dunes.



### **2.3.2 Structure**

The Arabian Gulf Coastal area is part of the Arabian platform, an area that has been generally stable since the Paleozoic era. All the formations are dipping gently ENE, towards the Arabian Gulf. This gentle dip is disrupted, however, by some structures in the region. One prominent structure is the Dammam Dome resulted from a deep seated salt intrusions as indicated by its strong negative gravity anomaly and its oval shape (Powers et al., 1966). The major domal axis trends about N35W with an average dip of 1° on the flanks (Teel, 1973). Teel (1973) noted a few superimposition of minor anticlines and synclines on the dome and the absence of any associated fault system. Qatar arch (Cavalier, 1975) and Bahrain structure (Willis, 1967; Doornkamp et al., 1980), which are similar to Dammam Dome, were positive structures during the Middle Eocene (Cagatay, 1990). Two independently trending fold systems are also present. One system runs parallel to the coast (NE-SW), whereas the other trends N-S (Naimi, 1965). One of the notable N-S trending folds is En Nala structure which includes the Ghawar anticline (Powers et al., 1966).

### **2.4 Hydrogeology**

In relation to the lithostratigraphic units, different aquifers and aquitards could be established. The two aquifers of interest, Alat and Khobar, are associated with the intervening Rus, Midra and Saila, and Alveolina aquitards. These aquitards have an influence on the hydraulic interactions between aquifers as well as on the geochemistry of the adjacent water bodies. These aquifers with the aquitards form a hydrogeological system.

#### ***2.4.1 Rus Aquitard***

The interbedded marl, dolomite, limestone, and anhydrite of Rus Formation caps the groundwater in the underlying Umm Er Radhuma Formation. However, on structural highs, where the formation is mainly composed of dolomite, it could yield small amounts of poor quality water by upward leakage from Umm Er Radhuma aquifer. In structural troughs, it consists of impermeable rocks (Edgell, 1990).

#### ***2.4.2 Midra and Saila Shales, and Alveolina Limestone Aquitards***

The predominantly shaly Midra and Saila members constitute a typical aquitard. Likewise, the relatively impervious Alveolina Limestone Member is another aquitard. The above mentioned members with the Rus Formation make an aquitard package between Umm Er Radhuma and Khobar aquifers.

#### ***2.4.3 Khobar Aquifer***

In the study area, the Khobar Member is karstified and fissured, and provides water for domestic and agricultural purposes (Edgell, 1990). The member forms the Khobar Aquifer which is a dependable and relatively shallow aquifer (Naimi, 1965). The Khobar Aquifer is bounded at the top by Alat Marl Aquitard and separated from underlying Umm Er Radhuma by Alveolina, Midra and Saila, and Rus Aquitards system. Its greatest development takes place in the Qatif oasis and Al Hassa oasis.

The Aquifer's average depth below ground level is 100 m with the maximum

depth being 241 m at Ras Tanura and the minimum being zero near Dhahran. It is absent at the top of the Dammam Dome where the member is eroded (Italconsult, 1969; GDC, 1980).

Khobar Aquifer has an average transmissivity of  $2.9 \times 10^{-1} m^2/s$  indicating highly transmissive behavior and average storativity value of  $2.1 \times 10^{-5}$ . The low storativity value indicates the confined nature of the aquifer (Rasheeduddin, 1988).

#### ***2.4.4 Alat Marl (Orange Marl) Aquitard***

The lower unit of Alat Member which consists mainly of marls and shales, forms an intervening aquitard between Alat (the upper unit) and Khobar aquifers. The aquitard ranges in thickness from 10-40 m (Italconsult, 1969).

#### ***2.4.5 Alat Aquifer***

The porous dolomitized limestone of Alat Member forms the Alat aquifer. The Aquifer is hydraulically separated from the Neogene aquifer by the shales of Hadruk Formation. It is also separated by Alat Marl aquitard from the underlying Khobar aquifer. The depth below ground level ranges from zero at the Dammam Dome to 123 m at Ras Tanura, however, the average depth is 25 m (Italconsult, 1969). Alat Aquifer mainly thickens from Dammam Dome to northeasterly direction. Rashidduddin (1988) has shown a thickness variation ranging from 20 m to 110 m.

Transmissivity values ranging from  $2.6 \times 10^{-4} \text{ m}^2 / \text{s}$  at Wadi Al Miyah to  $2.3 \times 10^{-3} \text{ m}^2 / \text{s}$  at Ras Tanura were reported by the Ministry of Agriculture and Water (1984). Meanwhile, the storativity varies from  $1.31 \times 10^{-4}$  to  $5.34 \times 10^{-4}$ . The low storativity value indicates the confined nature. However, near the erosional surface at Dammam Dome, the Aquifer shows a semiconfined to unconfined behavior (Rasheeduddin, 1988).

## **CHAPTER 3**

### ***DISTRIBUTION OF CHEMICAL CONSTITUENTS***

#### ***3.1 Introduction***

This chapter describes the areal distribution of the major ions and total dissolved solids (TDS), and determines the TDS / EC (electrical conductivity) relations in waters of the Alat and Khobar aquifers. The water-well-samples of the aquifers are concentrated on the coastal belt of the Arabian Gulf where most of the cities and towns of the Eastern Province are located. In the less inhabited interior lands of the study area, water wells are either scarce or absent. Due to this fact, the concentration contours in the western and southwestern parts of the study area are merely extrapolations.

#### ***3.2 Alat Aquifer***

##### ***3.2.1 Calcium***

The calcium content varies from about 100 mg/l up to 1300 mg/l (Fig 3.1). In the southeastern part of the map, the calcium concentration is about 200 mg/l and in the northeast, it reaches its maximum value of 1300 mg/l.

At the Abqaiq area, the calcium concentration is relatively high with a value of 500 mg/l. In Al Hassa area the calcium concentration is uniformly low at a value of about 200 mg/l. In Qatif, the calcium concentration varies in a narrow range between 200 mg/l and 300 mg/l. Farther north, Calcium increases

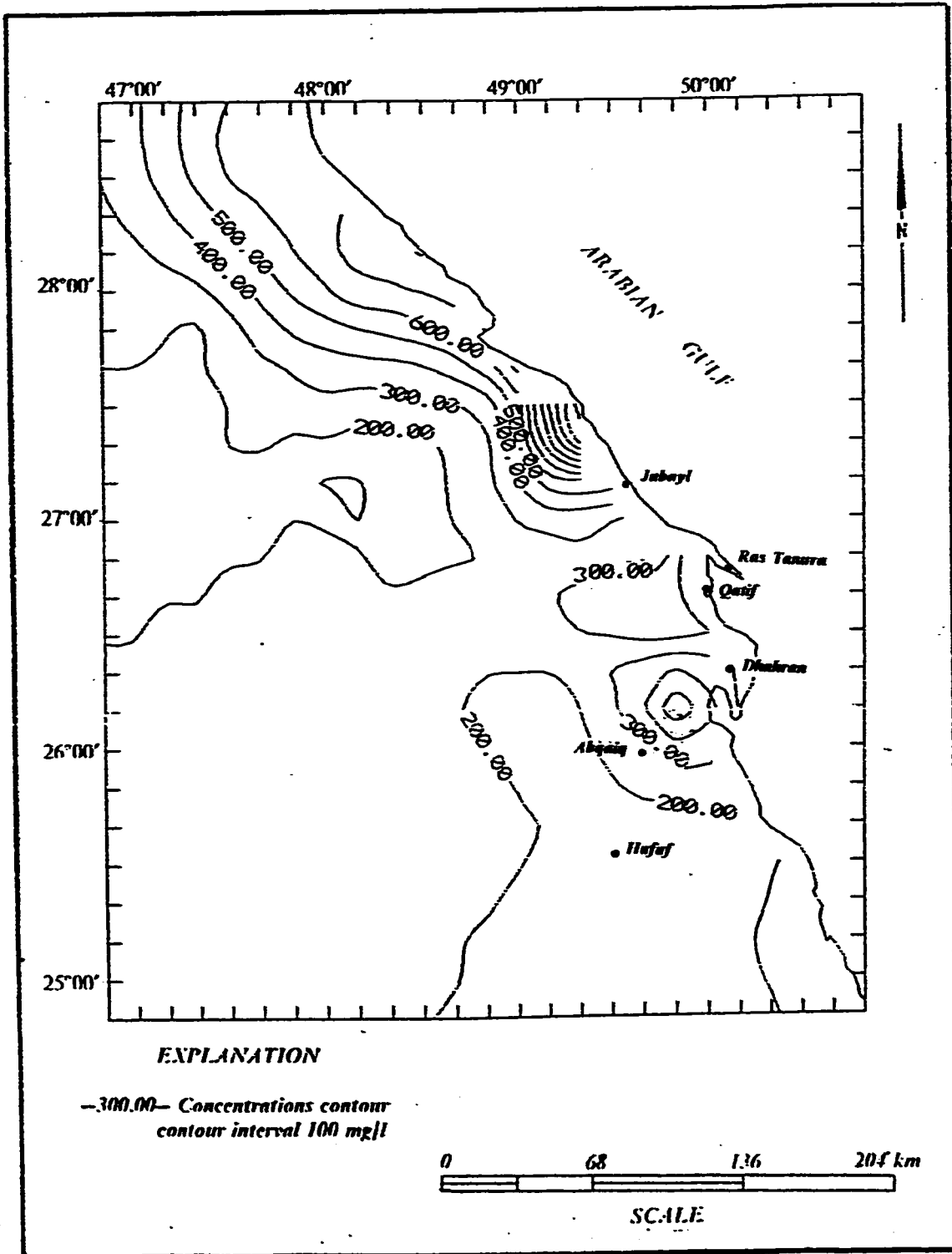


**Figure 3.1 Areal distribution map of Calcium (mg/l) in Alat aquifer.**

seaward reaching a maximum value of 1300 mg/l north of Jubayl.

### **3.2.2 Magnesium**

The lowest magnesium concentration of about 80 mg/l occurs in the southeastern and northwestern part of the map (Fig 3.2). The concentration increases to a maximum value of 480 mg/l north of Jubayl. At Dammam-Abqaiq area, the magnesium concentration is about 120 mg/l. The concentrations in Qatif and Al Hassa are also similar to those in the Dammam-Abqaiq area.

Similar to calcium concentration, magnesium concentration increases further from the north of Jubayl towards the Arabian Gulf. However, the magnesium increase is more gradual compared to the calcium increase.

### **3.2.3 Sodium**

As in the case of the distribution of calcium and magnesium, the sodium concentration in the Alat Aquifer increases from south towards north and from landward to seaward (Fig. 3.3). However, sodium is much more abundant than the other two ions. In the south, low sodium concentration of about 400 mg/l occurs. The 100 mg/l sodium contour in the southwest is less reliable due to insufficient data in this part of the study area.

Dammam-Abqaiq area has about 400 to 600 mg/l of sodium whereas in Qatif, the concentration is higher with a range of 700 mg/l. The maximum

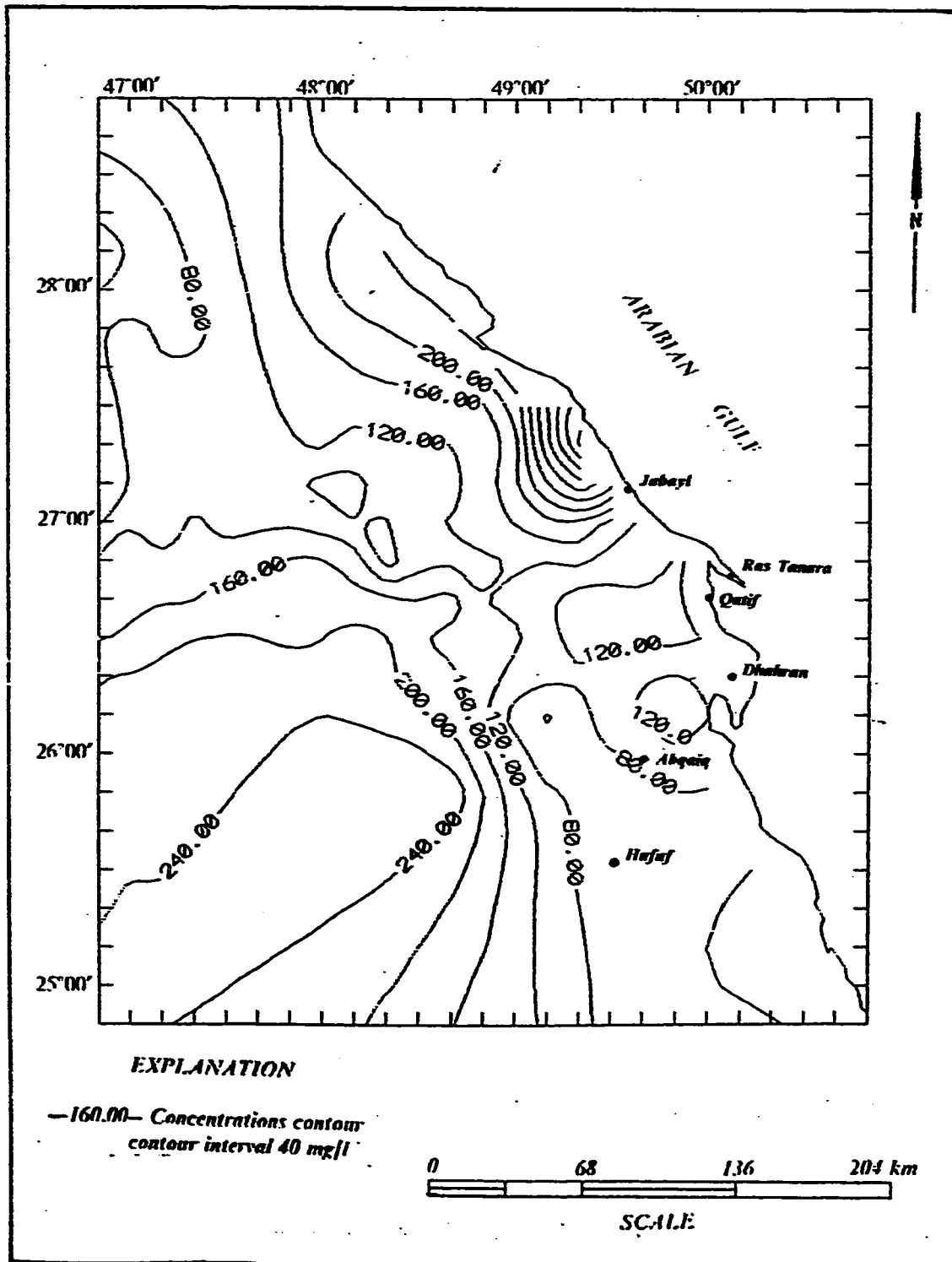


Figure 3.2 Areal distribution map of Magnesium (mg/l) in Alat aquifer.



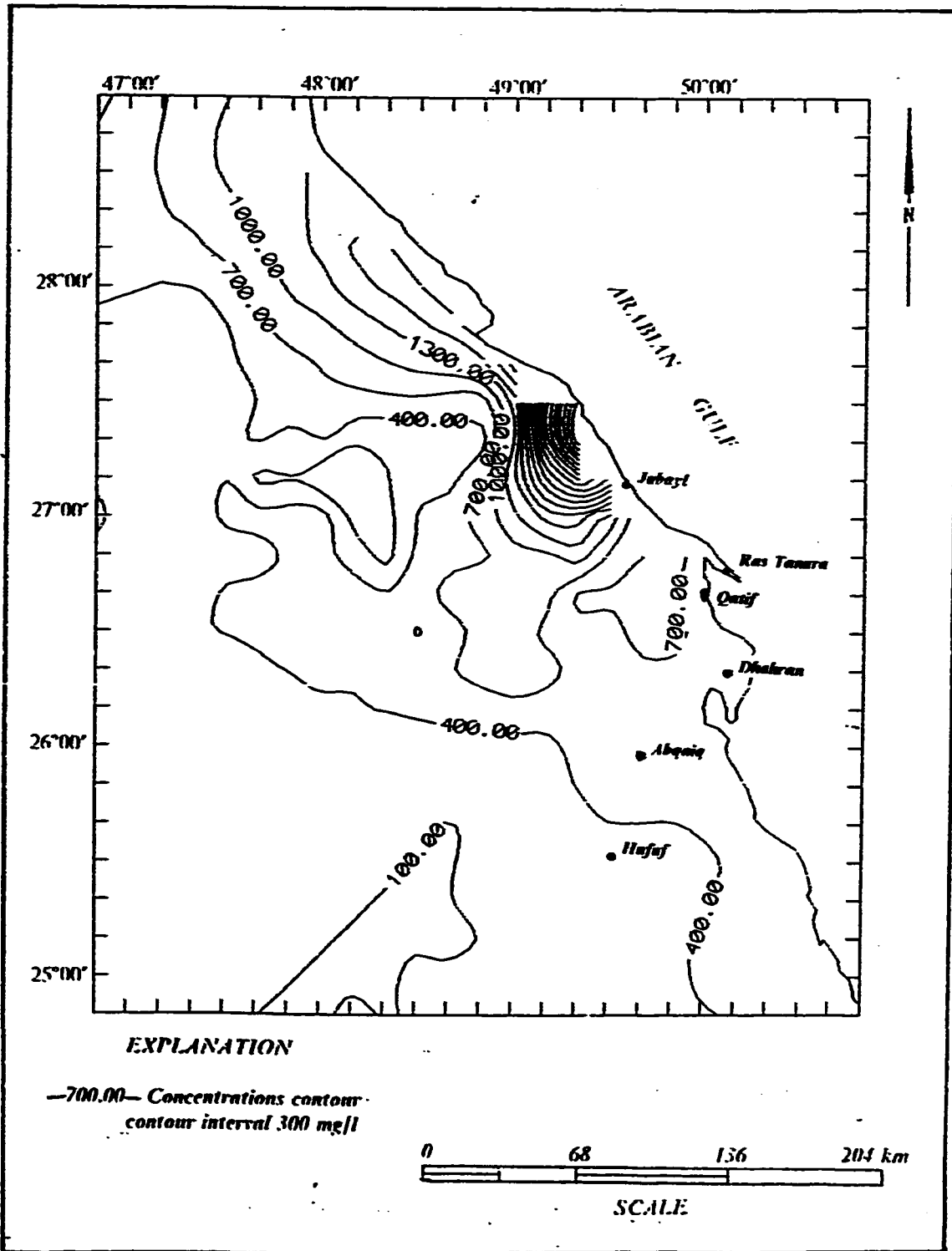


Figure 3.3 Areal distribution map of Sodium (mg/l) in Alat aquifer.

value of 5800 mg/l sodium occurs near Al-Jubayl. The concentration contours in the north follow the pattern of the coastline and reach a maximum contour value of 1900 mg/l. The sodium distribution differs from the distribution of the other major cations in the absence of an evident increase in sodium around Dammam - Abqaiq area.

#### ***3.2.4 Chloride***

Relatively low concentration of 500 mg/l chloride is located in the south (Fig 3.4). The maximum chloride concentration of more than 5000 mg/l occurs in the north of Jubayl. In the Dammam - Abqaiq area, chloride concentration ranges between 500 - 1000 mg/l, but near Qatif it drops below 500 mg/l. The concentration maintains the 1000 mg/l value in Ras Tanura, where the development of Alat Aquifer is reasonably high. In the north of Ras Tanura, at Jubayl, a high chloride concentration of more than 5000 mg/l occurs but the concentration decreases to lower values farther north and northwest.

#### ***3.2.5 Sulfate***

The sulfate concentration varies from 400 mg/l to 1800 mg/l. The lowest concentration of 400 mg/l occurs at Al-Hassa in the southern part of the study area (Fig 3.5). Generally, the concentration increases northward and seaward. However, this pattern is interrupted in the Dammam Dome, Qatif area, and in the north of Jubayl. High concentrations of sulfate are found in the Dammam - Abqaiq area and in the north of Jubayl. These two highs are separated by a narrow zone of low sulfate concentration, in the Qatif area. Farther north, the

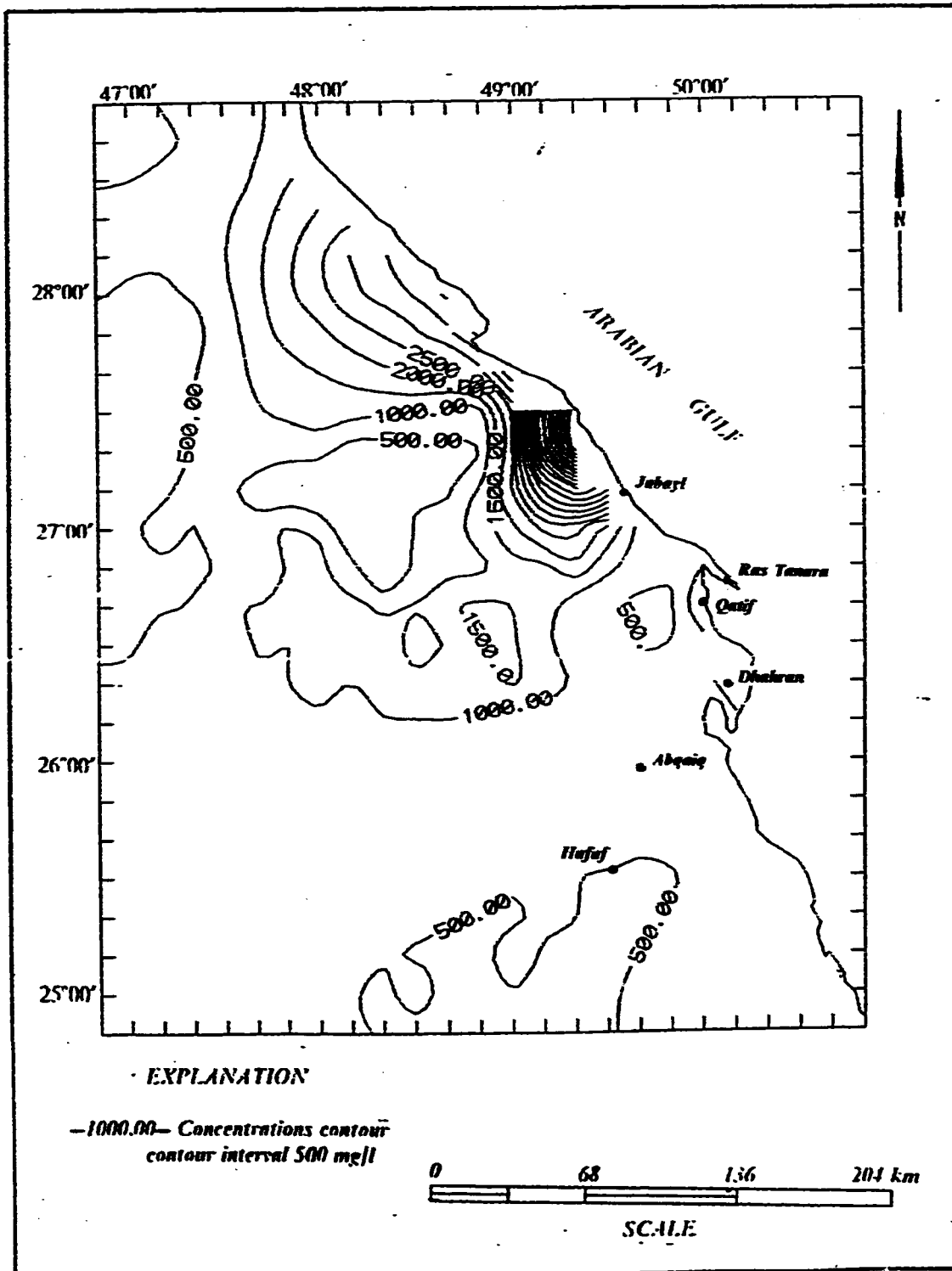


Figure 3.4 Areal distribution map of Chloride (mg/l) in Alat aquifer.

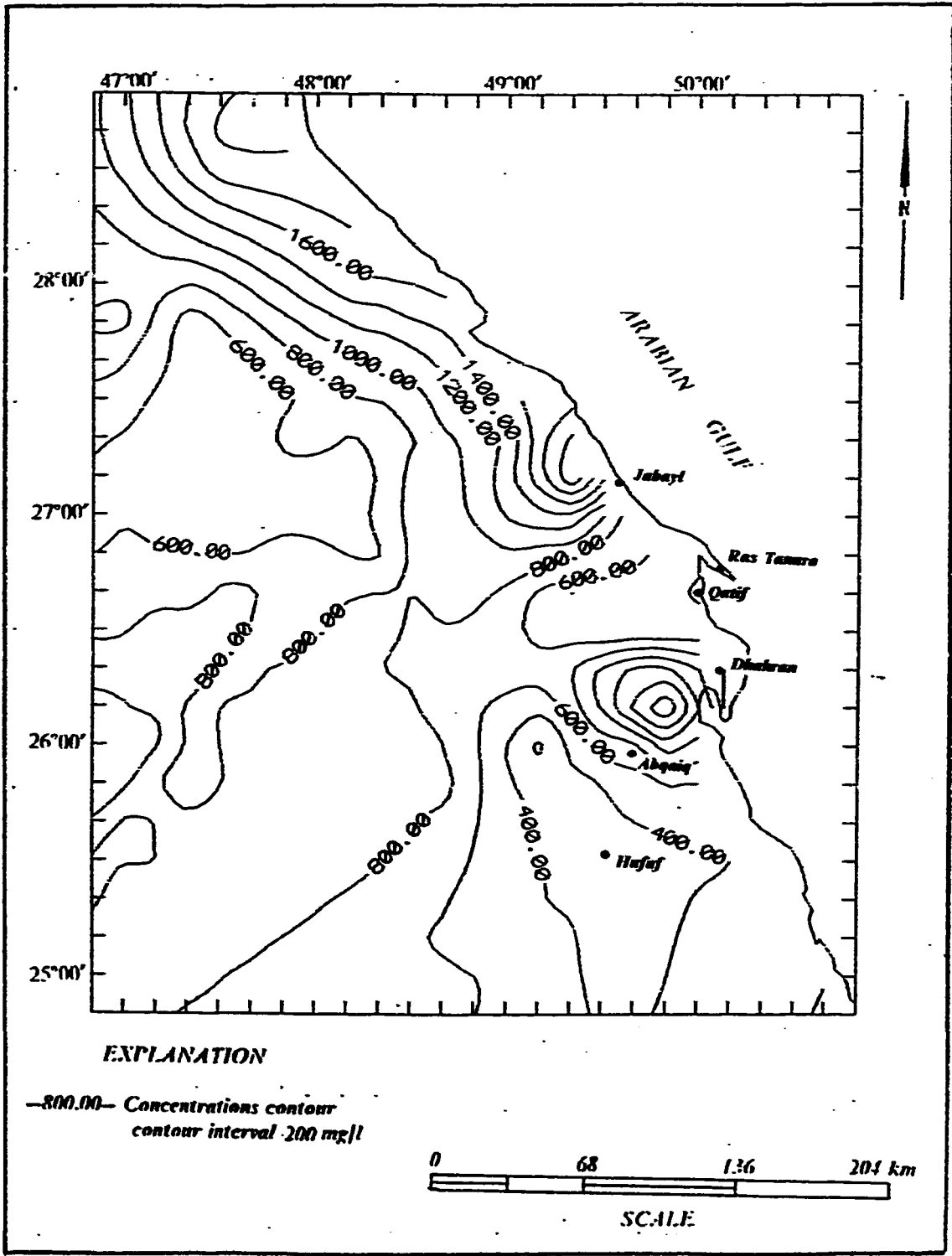


Figure 3.5 Areal distribution map of Sulfate (mg/l) in Alat aquifer.

pattern assumes the general trend where the concentration increases seaward and northward.

### ***3.2.6 Bicarbonate***

The areal distribution pattern of the bicarbonate is quite different from the other major anions. The lowest bicarbonate concentration is located at the extreme north of the map (Fig 3.6). Moreover, the contour patterns of the other ions which run parallel to the coastline is absent in the case of the bicarbonate distribution. The lowest concentration value less than 150 mg/l is situated in the extreme north and in the Dammam-Dhahran area, whereas the highest concentration of more than 400 mg/l, occurs in Abqaiq area (Fig 3.6).

The bicarbonate concentration around Qatif and Ras Tanura is about 200 mg/l. This zone is bounded in the north and south by a relatively lower bicarbonate areas.

### ***3.2.7 Total Dissolved Solids***

The total dissolved solids (TDS), in Alat Aquifer, varies from 2000 mg/l to more than 9000 mg/l. The lowest TDS value is in the southern part of the study area, meanwhile, the TDS increases northward and seaward. This pattern is interrupted in the Qatif - Ras Tanura area where the TDS value is less than 2000 mg/l. Near Jubayl, The TDS increases abruptly seaward (Fig 3.7). This exceptionally high TDS zone extends in the southwest direction from the coastline and is sandwiched between two low TDS areas.

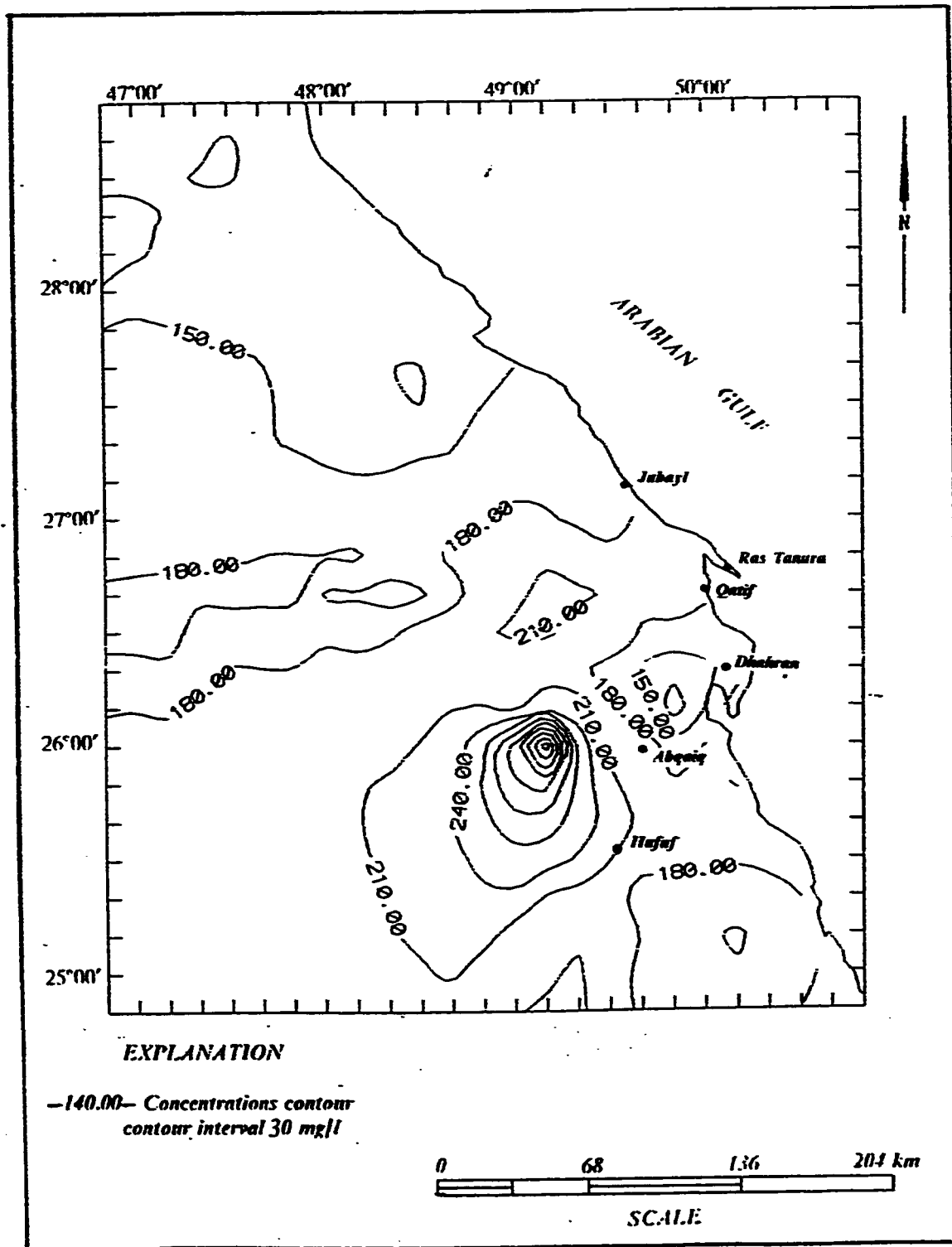


Figure 3.6 Areal distribution map of Bicarbonate (mg/l) in Alat aquifer.

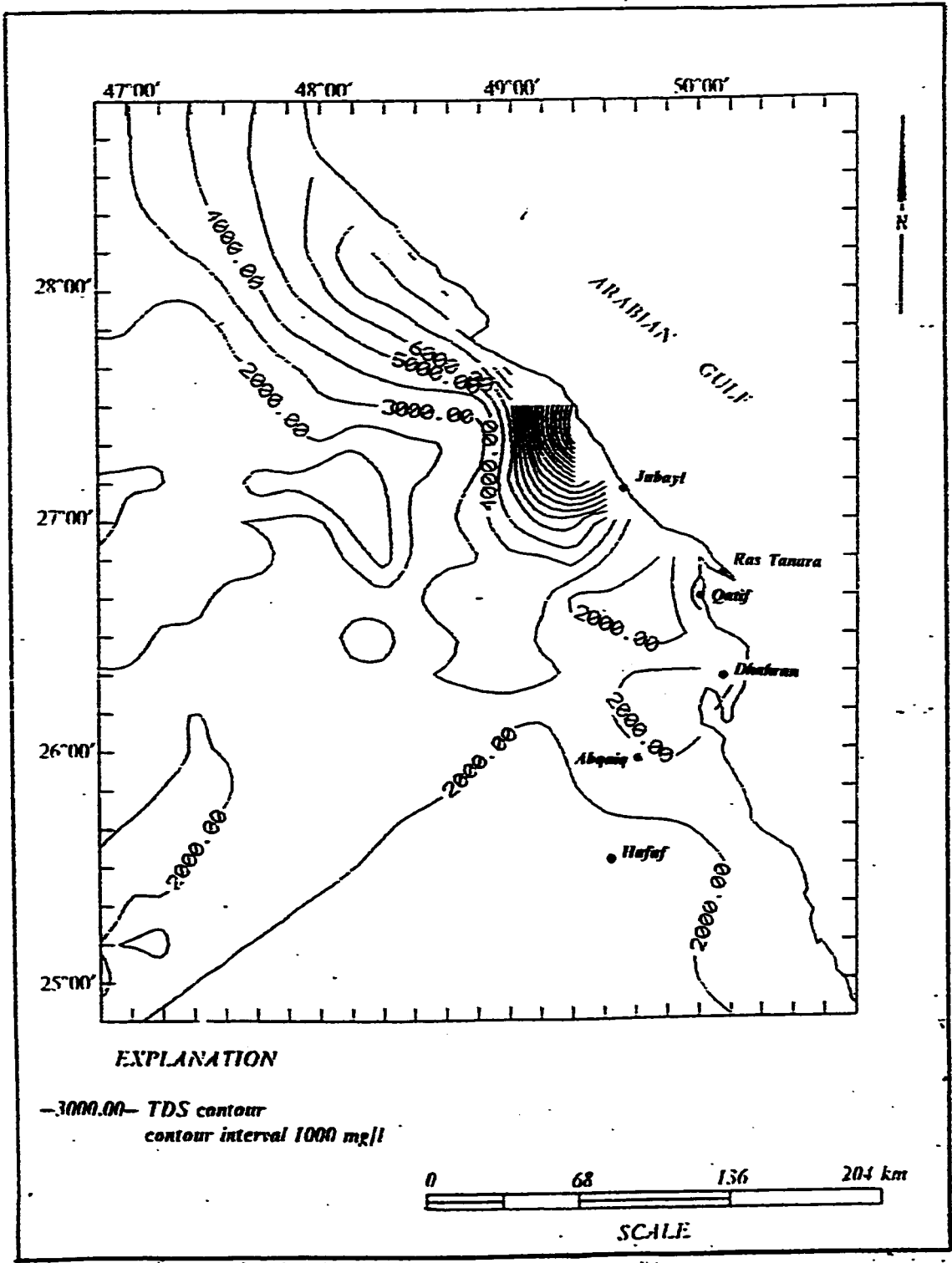


Figure 3.7 Total Dissolved Solids Map of Waters in the Alat Aquifer.

### **3.2.8 Total Dissolved Solids - Electrical Conductivity Relationship**

The electrical conductance is not simply related to ion concentrations or dissolved solids. However, most groundwaters display the following linear relationship between total dissolved solids (TDS) and electrical conductance (EC):

$$KA = S$$

where K is the EC in micromhos/cm, S is the TDS in mg/l, and A is a conversion constant. The value of A is usually between 0.55 and 0.75; the higher values generally being associated with sulfate-rich waters (Hem, 1989). The relationship is expressed in this study as follows :

$$TDS = A \times EC$$

where A is the Hem's conversion factor.

The data from Alat aquifer shows a reasonable straight line regression as shown in (Fig. 3.8). The correlation coefficient ( $r^2$ ), which indicates a strong relationship, and the equation of the fitting line are expressed as:

$$r^2 = 0.93$$

$$TDS = 0.64 EC$$

The slope represents Hem's conversion factor (i.e. 0.64). The equation may be used for practical estimation of the TDS using measurements of EC, since the



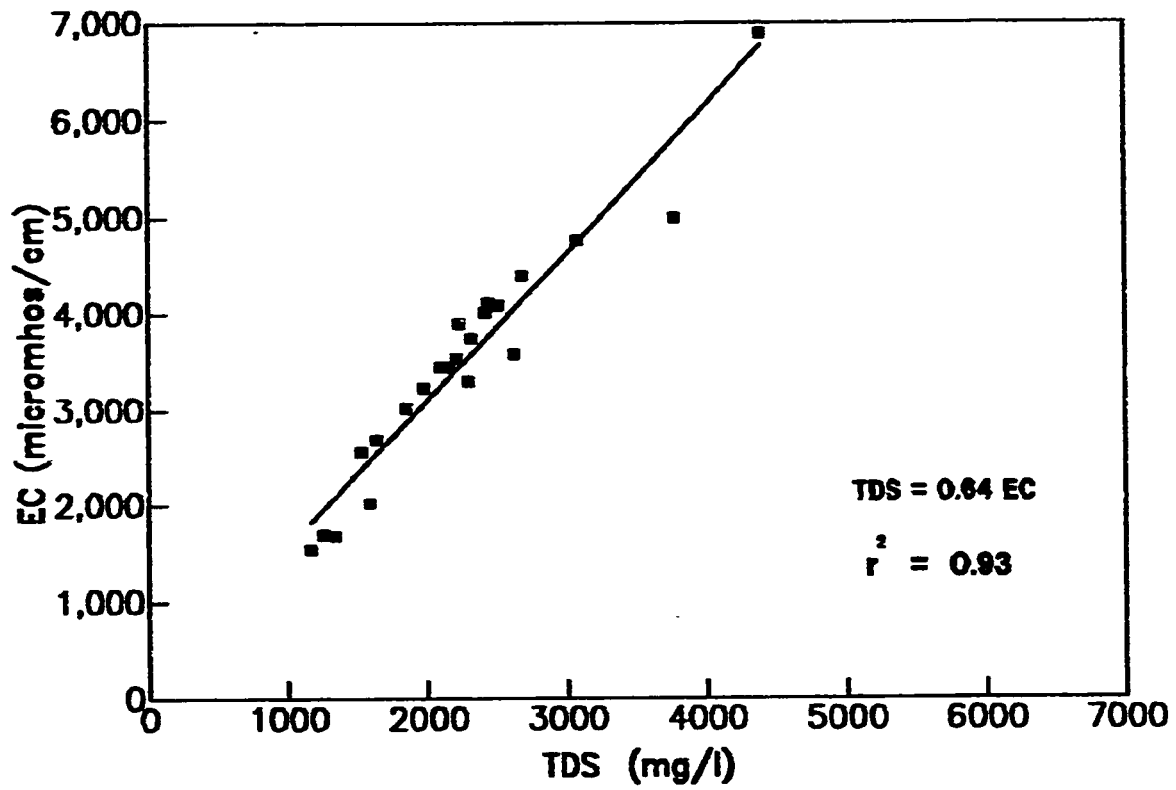


**Fig. 3.8 EC versus TDS plot of waters in Alat aquifer.**

latter property is much easier to determine than the former.

### **3.2.9 Hydrogeochemical Facies in the Alat Aquifer**

To classify the Alat aquifer waters into different hydrogeochemical facies, the hydrochemical data were plotted on Piper's trilinear diagrams (Piper, 1944). The Piper plot suggests the presence of three major hydrogeochemical facies in the Alat aquifer (Fig. 3.9). The three facies are :

1. Na-Cl-Ca-  $SO_4$  facies
2. Na-Ca-Cl facies
3. Na-Cl facies

These facies were then plotted on the map to identify their distribution (Fig. 3.10). However, due to the limited nature and uneven distribution of the existing data, it is difficult to give a precise picture of the facies distribution of groundwaters in the Alat aquifer. Therefore, the water facies distribution in the Alat aquifer represents oversimplified and generalized patterns. The Na-Cl-Ca- $SO_4$  facies is present in the west of Al Hufuf. In terms of areal extent, this facies is smaller than the other two facies being absent around the coastal area. The average TDS of the water type is 2000 mg/l (Fig. 3.7). This area is also characterized by a relatively high  $HCO_3^-$  and low  $Cl^-$ .

The northern part of the study area is characterized mainly by a Na-Ca-Cl facies. Around Manifa, north of Jubayl, however, the water changes into a Na-Cl facies. The TDS in the Na-Ca-Cl facies ranges between 3000 and 5000

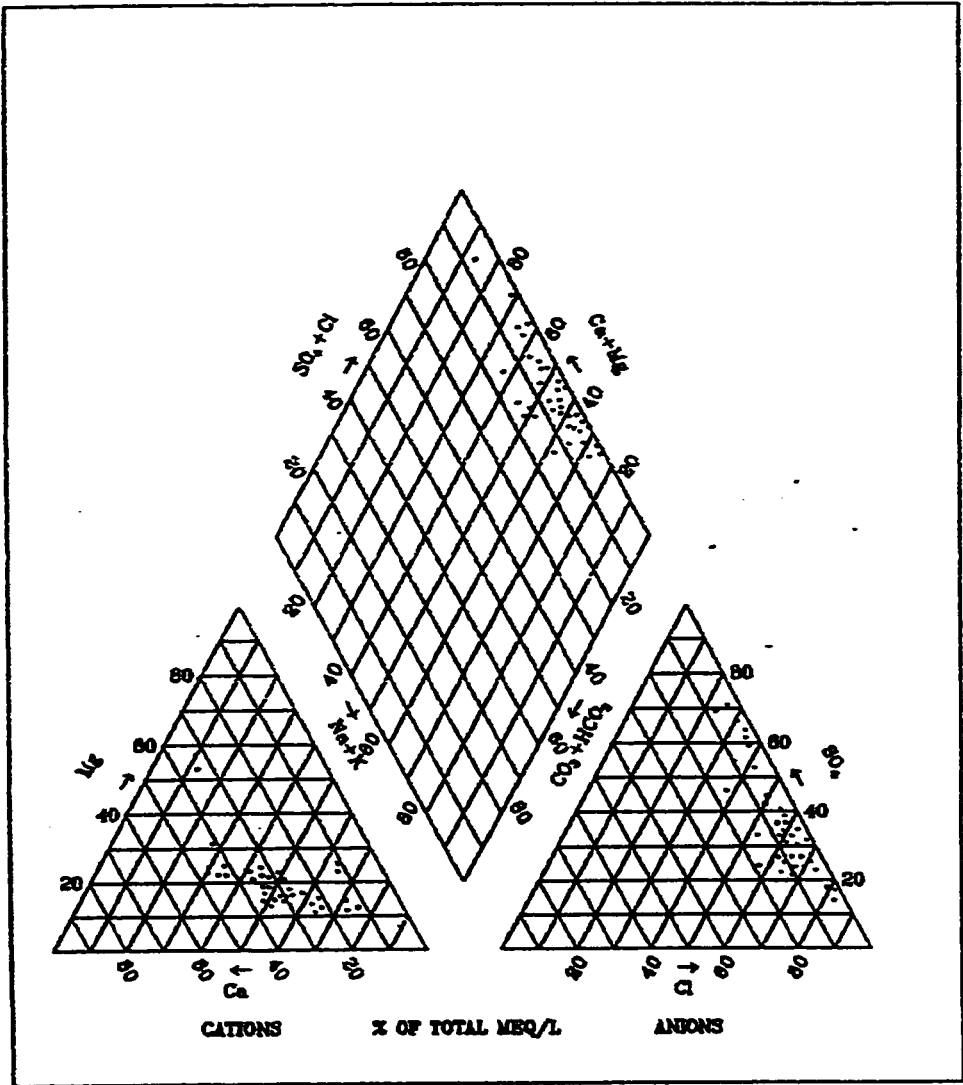


**Figure 3.9** Trilinear plot of water samples of Alat aquifer.

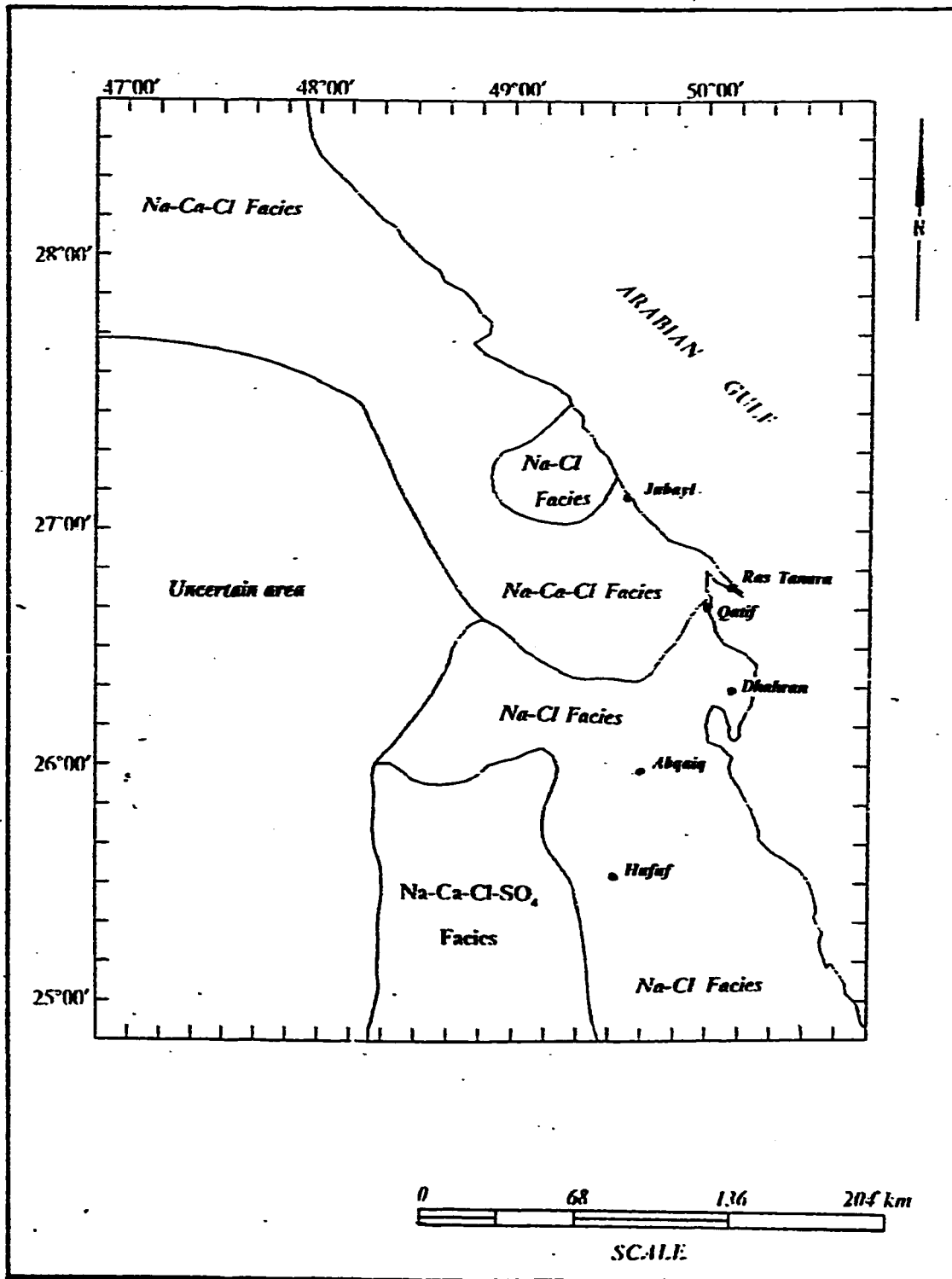


Figure 3.10 Hydrogeochemical facies map of the Alat aquifer.

mg/l. Calcium and sodium constitute more than 50 % of the major cations, whereas chloride makes up more than 50 % of the major anions. Bicarbonate is generally low , even though, there is a relative increase in the west of Jubayl.

The Na-Cl and the Na-Ca-Cl facies are the most widely distributed in the study area. In fact, in the coastal area, the aquifer water is composed of these two facies. The Na-Cl facies is predominant in the southern coastal area and present as an inlier in the Jubayl area within the Na-Ca-Cl facies.

### **3.3 *Khobar Aquifer***

#### **3.3.1 *Calcium***

The calcium concentration varies from about 200 to 1200 mg/l. Three distinctive areal distribution patterns of calcium are evident in the study area (Fig. 3.11). The southern part of the study area is characterized by low concentration of calcium. Near the coast, however, the calcium concentration increases gradually where it reaches 500 mg/l. In the central zone, there are two highs of calcium concentration; one is near Hufuf and the other is around Dhahran - Abqaiq area, where it reaches 500 mg/l. Between these two highs, there is a low calcium concentration zone of less than 200 mg/l. Likewise, there is another area of low calcium concentration of 200 to 300 mg/l in the Qatif area. In contrast with southern and central zones, the northern zone is characterized by high calcium concentration of more than 1100 mg/l.

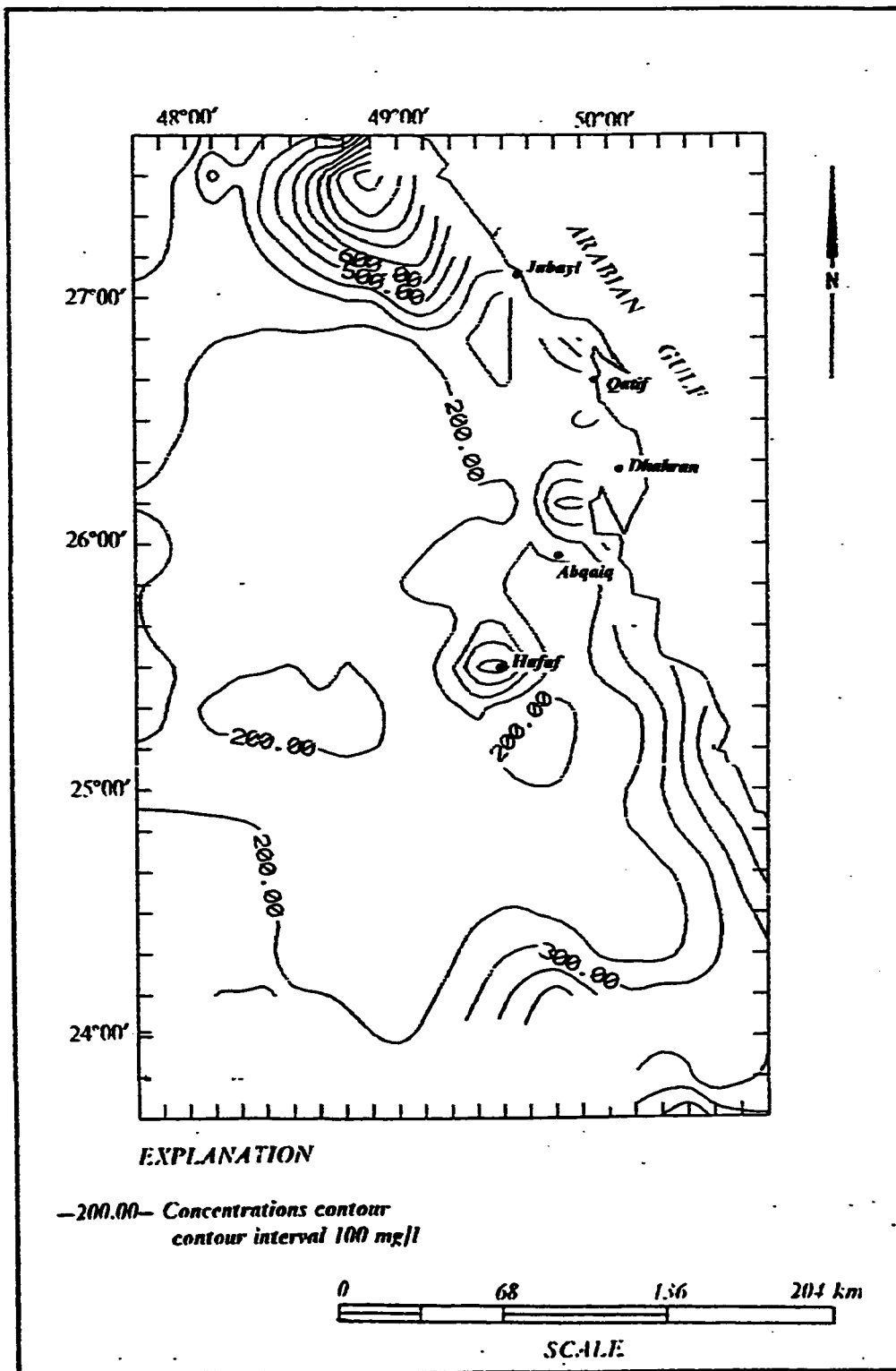


**Figure 3.11 Areal distribution map of Calcium (mg/l) in Khobar aquifer.**

### **3.3.2 Magnesium**

Magnesium follows the distribution pattern of calcium in the study area (Fig. 3.12). The lowest magnesium concentration of less than 60 mg/l occurs mainly in the south. The magnesium contents are also low in Qatif with about 100 mg/l. Along the southern coastal line and near Dammam Dome, magnesium increases up to about 200 mg/l and reaches the maximum concentration of 420 mg/l at the north of Jubayl.

### **3.3.3 Sodium**

Sodium is the most abundant cation with an areal distribution pattern similar to those of calcium and magnesium (Fig. 3.13). Sodium increases gradually seaward at the south of Dammam. A zone of low sodium extends from Qatif westward. This zone is bounded in the north and south by areas of high sodium concentration. The highest sodium concentration of more than 3000 mg/l occurs in the north of Jubayl, whereas around Jubayl the concentration drops to 300 mg/l (Fig. 3.13).

### **3.3.4 Chloride**

The chloride distribution in Khobar aquifer is identical to the sodium distribution (Fig. 3.14). Chloride like sodium reaches its highest concentration of more than 3000 mg/l at the north of Jubayl.

The difference between the distribution of the two ions is shown on the Na/Cl ratio map (Fig. 3.15). Generally, chloride is more abundant than sodium

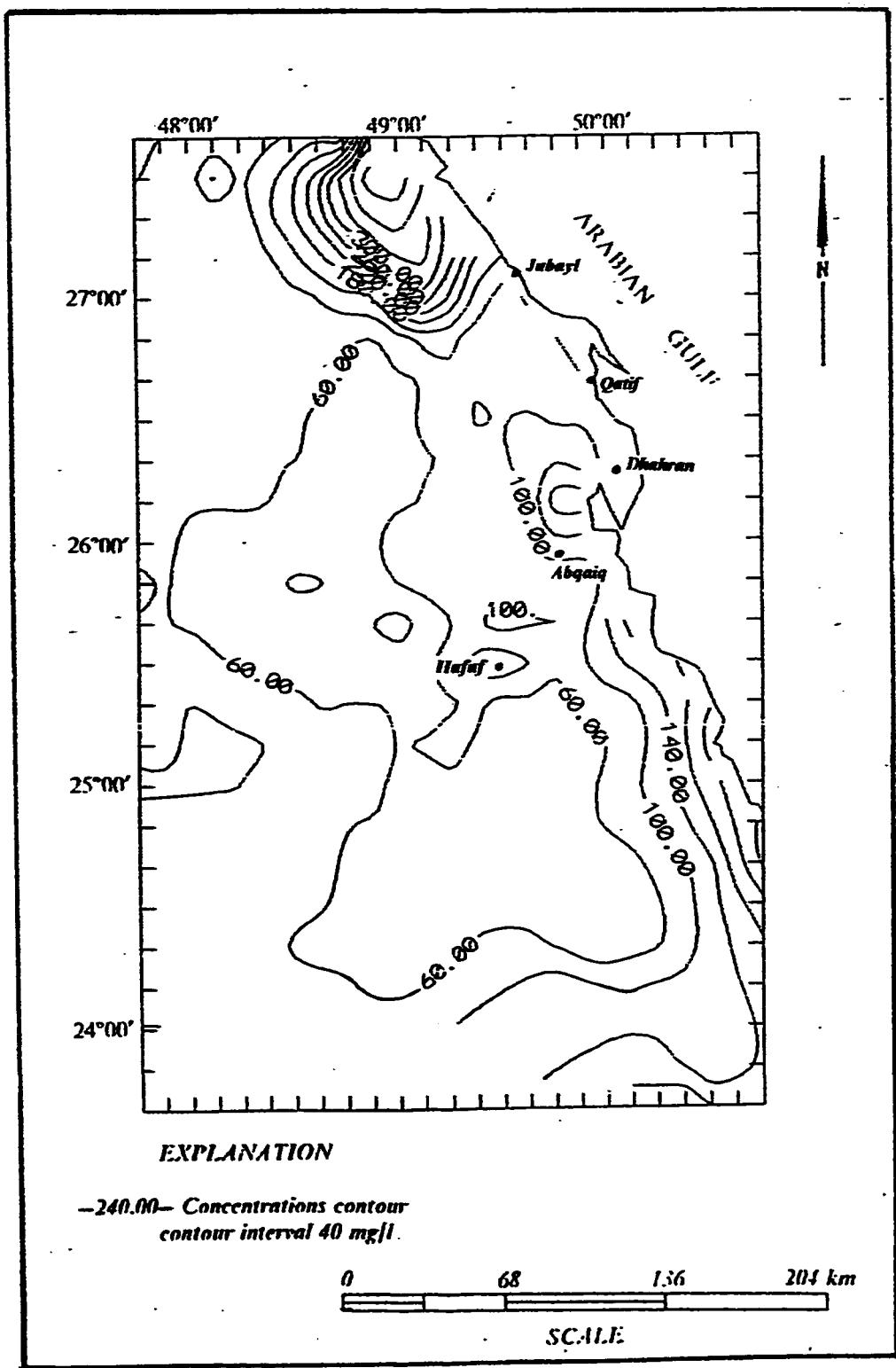


Figure 3.12 Areal distribution map of Magnesium (mg/l) in Khobar aquifer.



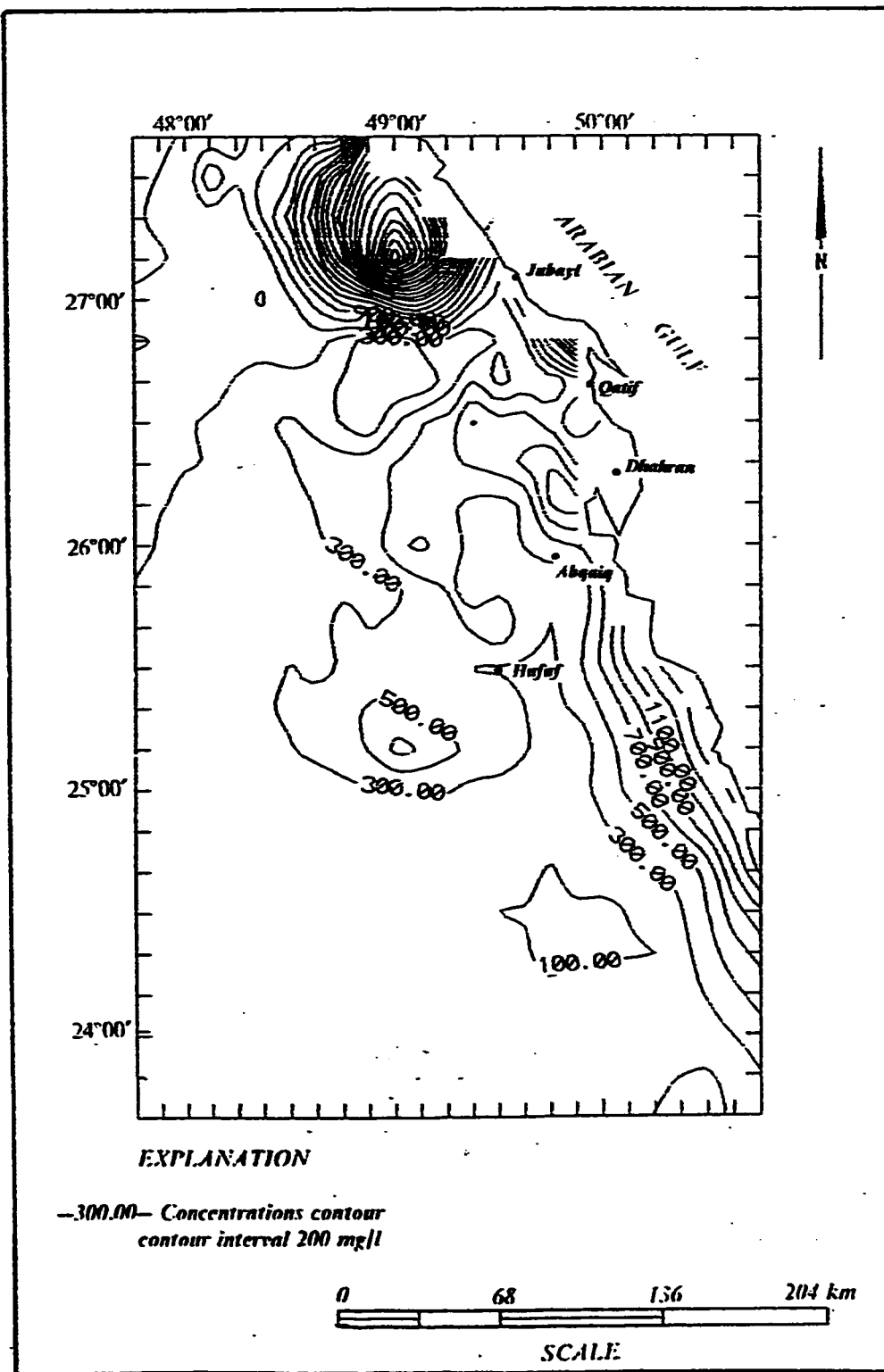


Figure 3.13 Areal distribution map of Sodium (mg/l) in Khobar aquifer.

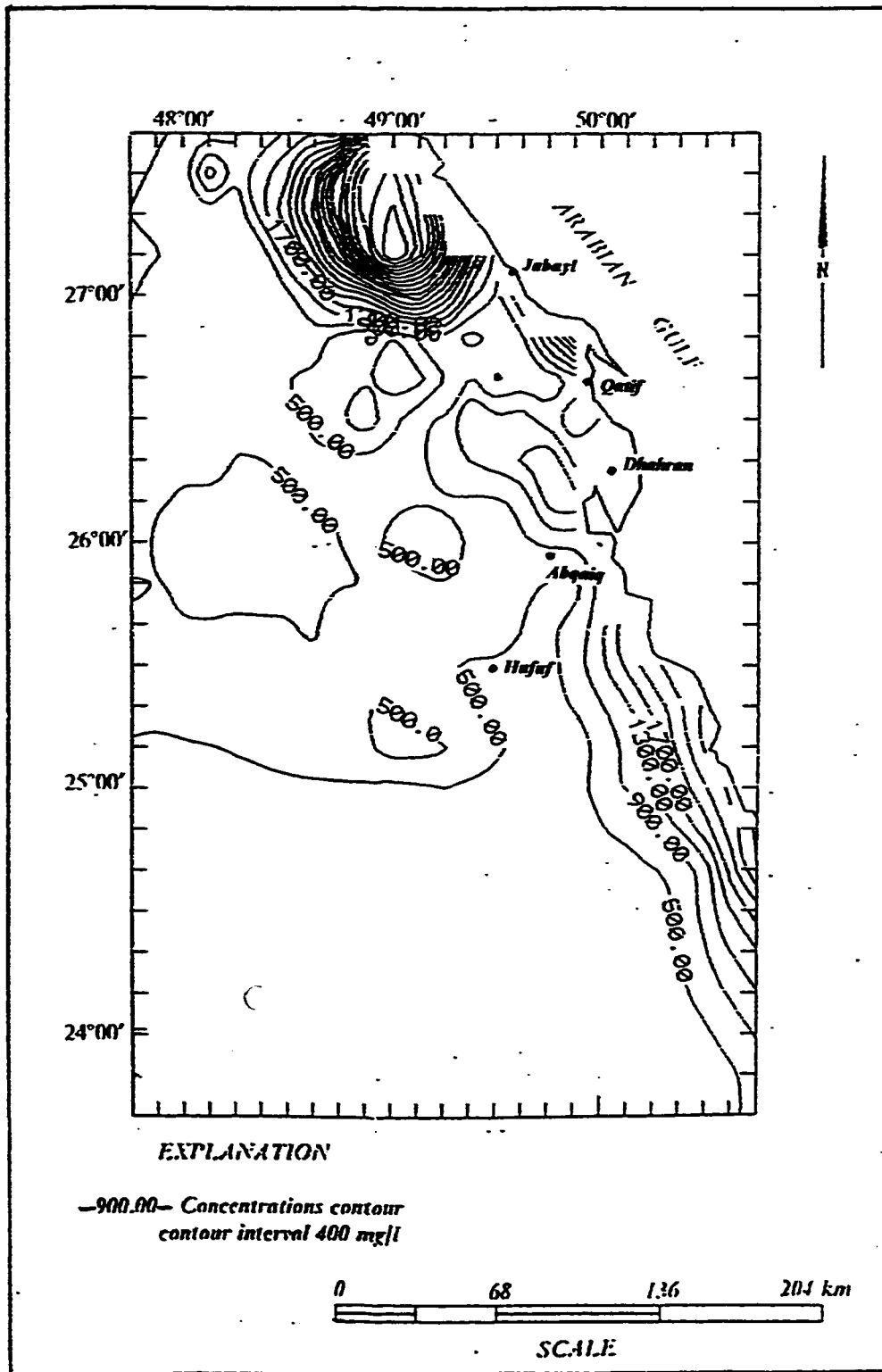


Figure 3.14 Areal distribution map of Chloride (mg/l) in Khobar aquifer.

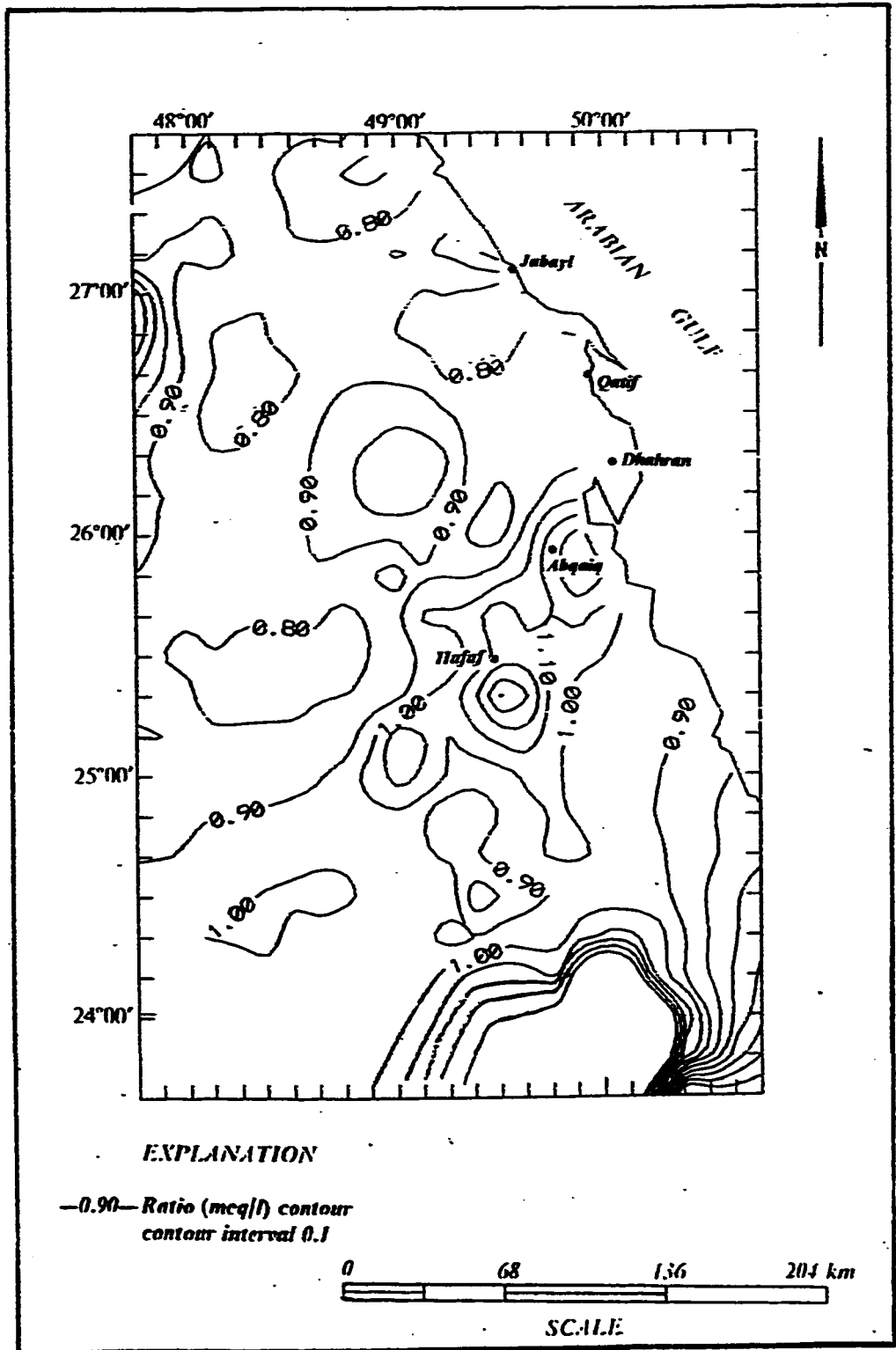


Figure 3.15 Sodium / Chloride (meq/l) ratio map of the Khobar aquifer.

in the whole study area. However, there is an elongated zone of high sodium with NE-SW direction. This zone extends from Abqaiq, where the Na/Cl ratio is 1, to near Hufuf, where the Na/Cl ratio is 1.3. Qatif and Dhahran are characterized by a Na/Cl ratio of 0.9.

### **3.3.5 Sulfate**

The sulfate concentration in Khobar aquifer varies from 400 to 1600 mg/l (Fig. 3.16). The concentration increases seaward. However, in Qatif and in the surrounding coastal land, sulfate is low of about 400 mg/l.

Sulfate concentration increases near Hufuf and in Dhahran - Abqaiq area. In the area north of Jubayl, sulfate increases with a rate similar to that of chloride. Although high sulfate concentration accompanies high chloride in the north, it is much lesser than chloride. The ratio of  $Cl/ SO_4$  (Fig. 3.17) is about one in the south and increases sharply northward, reaching a value of about eight.

### **3.3.6 Bicarbonate**

Khobar aquifer has an average bicarbonate of 180 mg/l ( Fig. 3.18). The bicarbonate concentration is anomalously high near Hufuf, with a value of 480 mg/l. This high concentration zone extends north to Qatif and drops sharply seaward. North of Jubayl, as well as in the southern part of the study area, a very low bicarbonate concentration occurs. This pattern contrasts with the distribution pattern of the other anions, chloride and sulfate, which increases

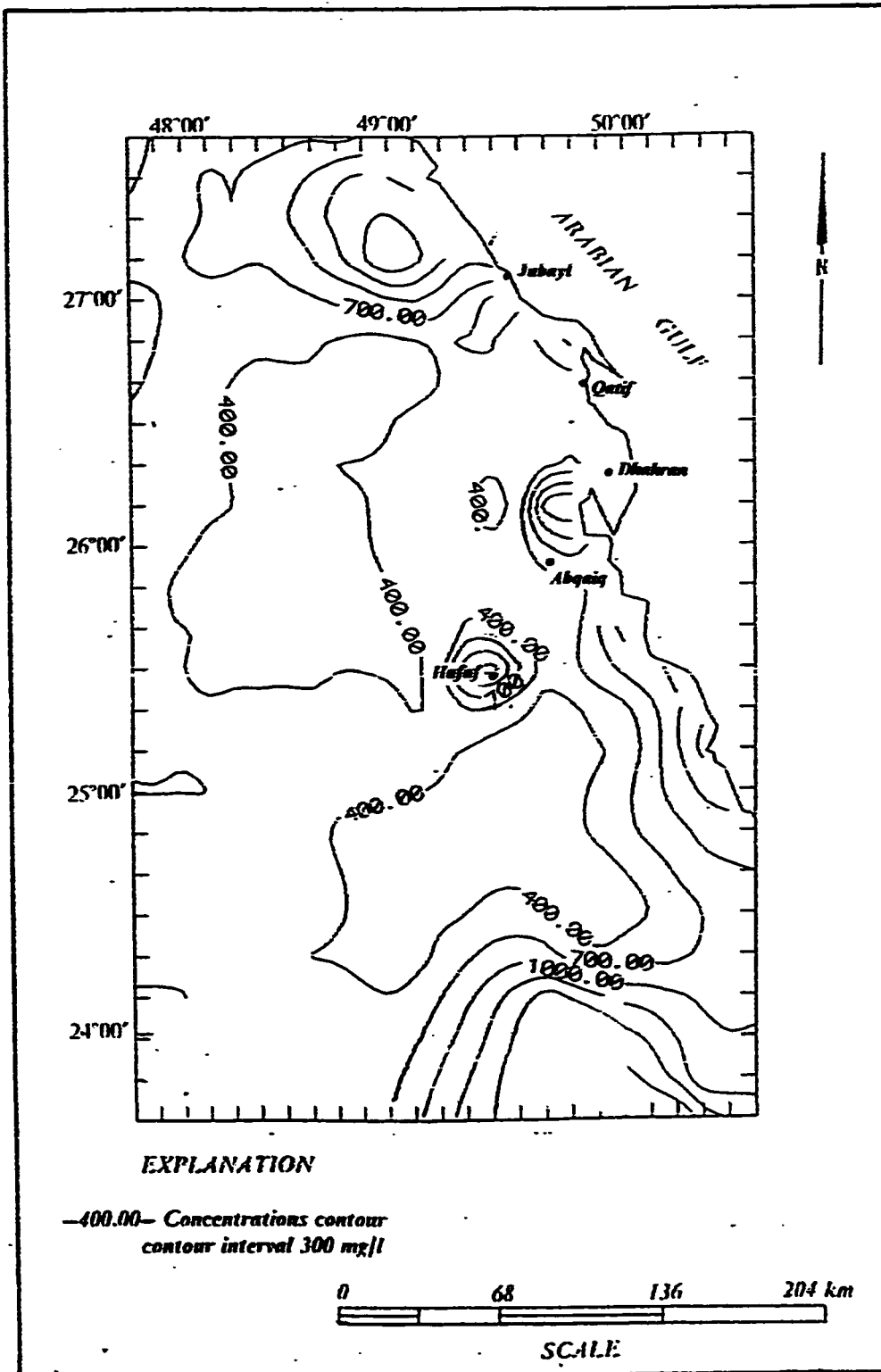


Figure 3.16 Areal distribution map of Sulfate (mg/l) in Khobar aquifer.

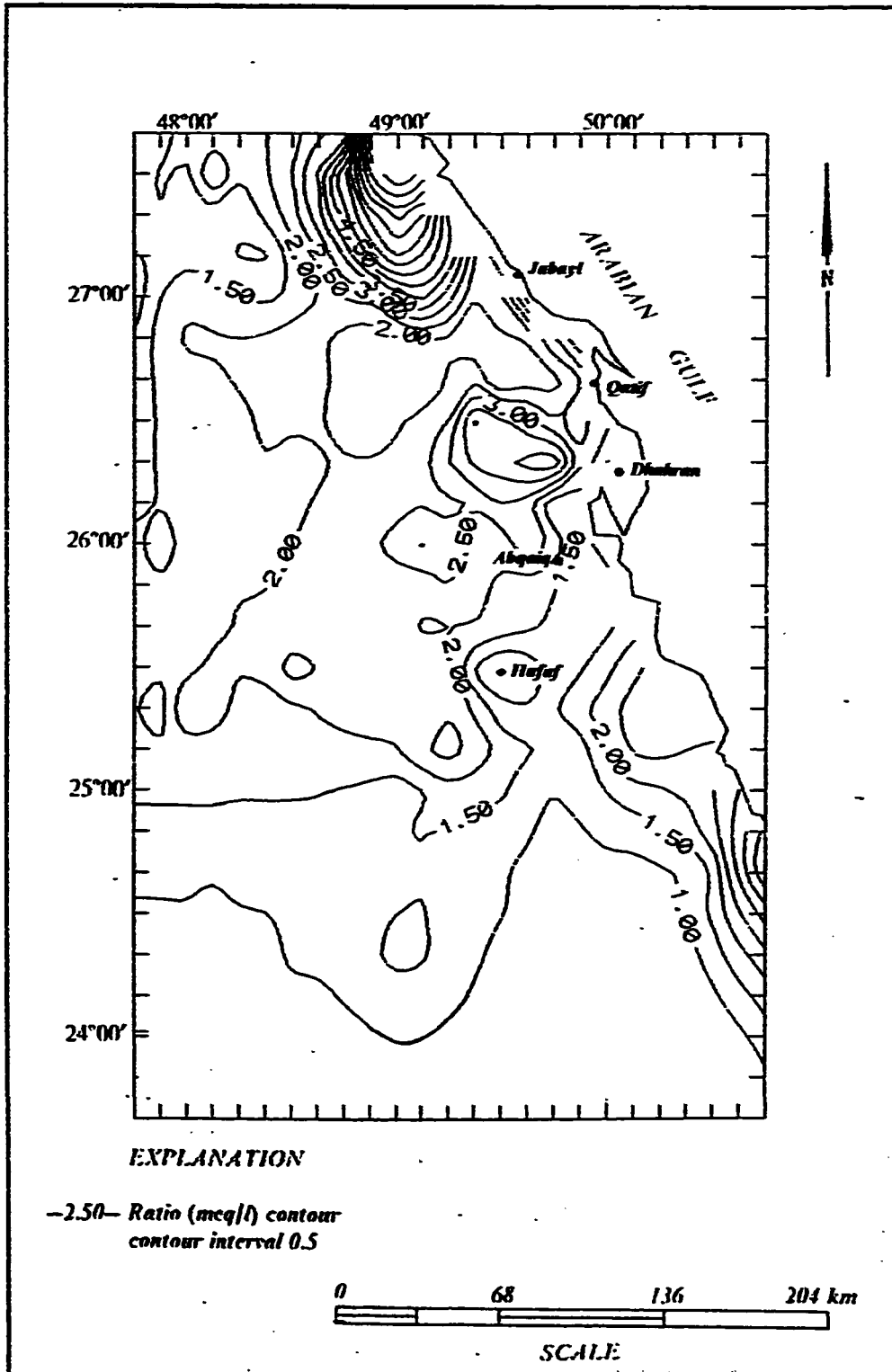


Figure 3.17 Chloride | Sulfate (meq/l) ratio map of the Khobar aquifer.

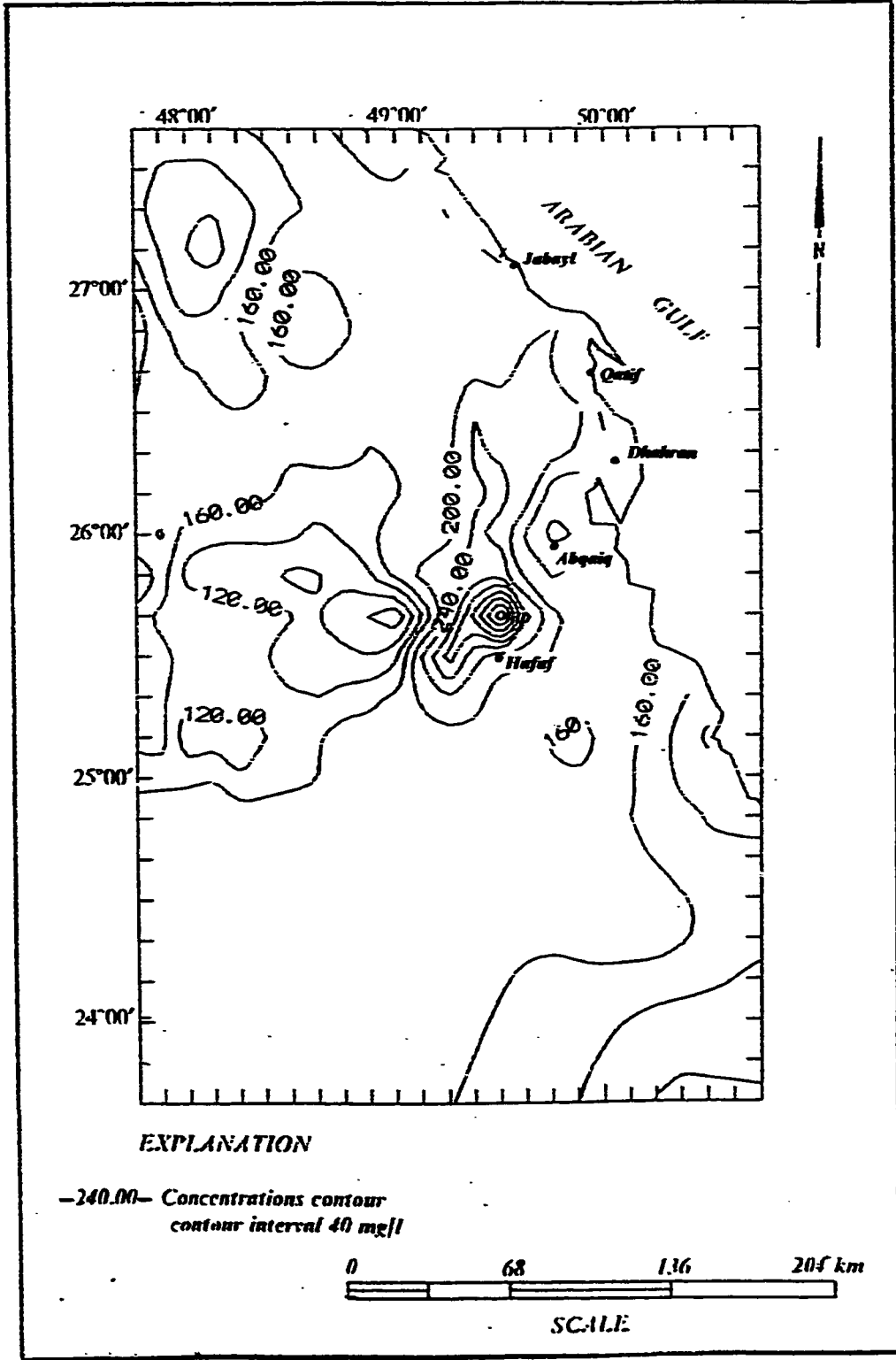


Figure 3.18 Areal distribution map of Bicarbonate (mg/l) in Khobar aquifer.

from south to north and occurs in very high concentrations to the north of Jubayl.

### ***3.3.7 Total Dissolved Solids***

Total dissolved solids (TDS) in Khobar aquifer varies from less than 1000 mg/l in the southern portion of the study area to more than 7000 mg/l in the north (Fig. 3.19). A zone of low TDS extends from Hufuf northward to Abqaiq. Another zone of low TDS having an east - west trend occurs around Jubayl.

The coastal area of the Arabian Gulf is characterized by an increase in TDS, however, this general trend is interrupted in two areas, around Qatif and near Jubayl.

### ***3.3.8 TDS-EC Relationship***

As in the Alat aquifer, the TDS - EC relationship in Khobar aquifer has been approximated by a straight line regression (Fig. 3.20). The equation of the fitted straight line could be utilized to estimate the TDS in Khobar aquifer. The equation with Hem's conversion factor value of  $A = 0.65$  is as follows :

$$\text{TDS} = 0.65 \text{ EC}$$

The correlation factor ( $r^2 = 0.87$ ) and the linear fitting equation are given on the lower right margin (Fig. 3.20).



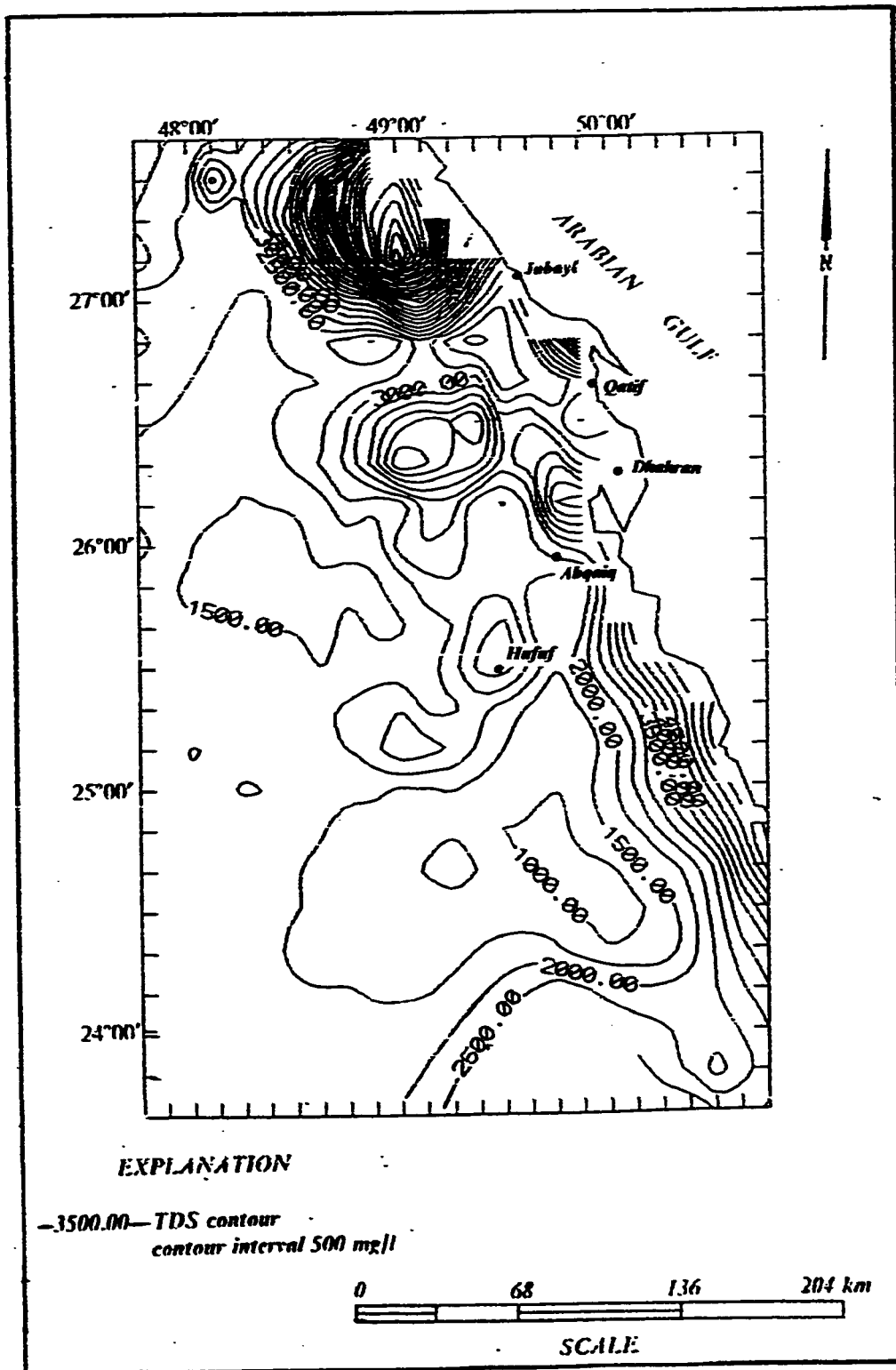
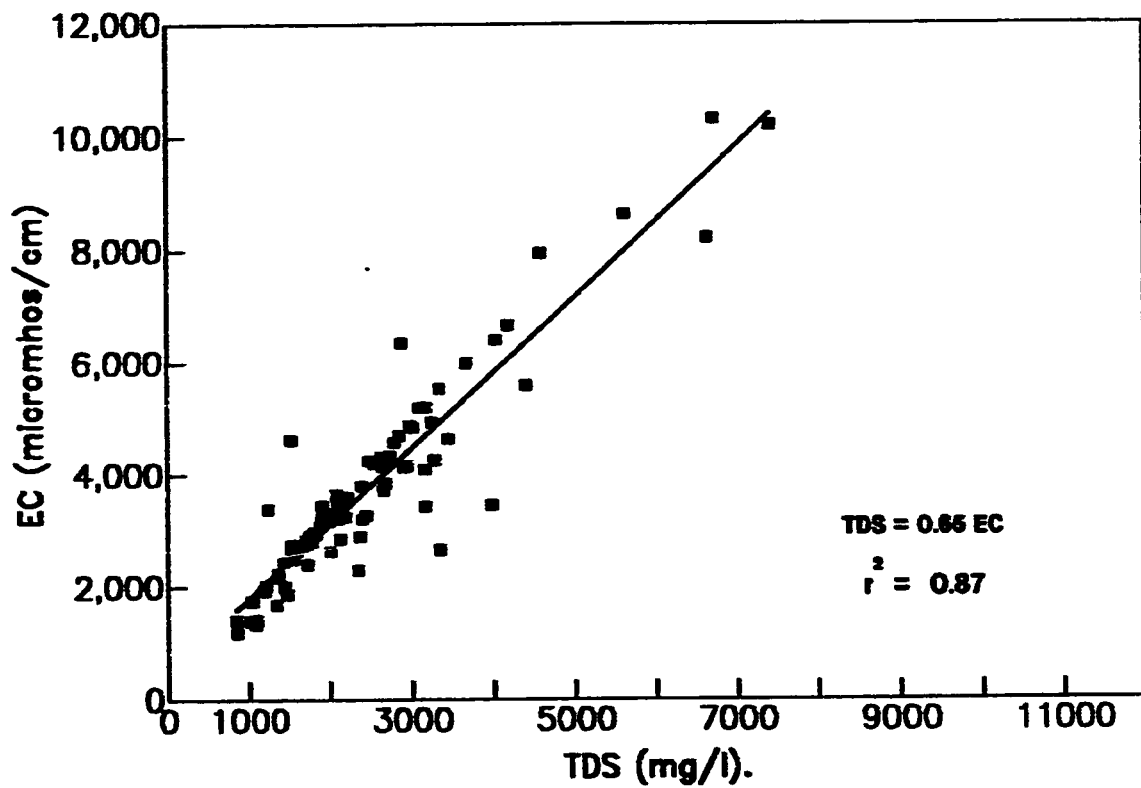


Figure 3.19 Total dissolved solids map of waters in the Khobar aquifer.



**Fig. 3.20 EC versus TDS plot of waters in the Khobar aquifer.**

### **3.3.9 Hydrogeochemical Facies**

The following four hydrogeochemical facies are identified in Khobar aquifer (Fig. 3.21):

1. Ca-  $SO_4$  facies
2. Na-Cl-Ca-  $SO_4$  facies
3. Na-Ca-Cl facies
4. Na-Cl facies

The Ca-  $SO_4$  facies is present at the extreme south of the study area (Fig. 3.22). In the trilinear diagram, more than 70 % of the anions of this water type are sulfate and more than 50 % of the cations are calcium. The TDS ranges from less than 1000 mg/l to more than 3000 mg/l.

The second (Na-Cl-Ca-  $SO_4$  ) facies is as widely distributed as the first facies; the two water types cover adjacent areas in the south. Sodium and calcium are the most abundant cations, and chloride and sulfate together comprise more than 50 % of the anions. Magnesium is relatively low and bicarbonate, although low, increases south of Al Hufuf. For this facies the TDS is generally low.

The third (Na-Ca-Cl) facies is abundant in the NE of the study area and it extends into the sea at the latitude of Jubayl. The facies divides two Na-Cl type waters which are located at the south and north of Jubayl. The dominant cations are sodium and calcium; meanwhile, chloride constitutes more than 50 % of the anions. The average TDS in the area is 2500 mg/l. Bicarbonate is

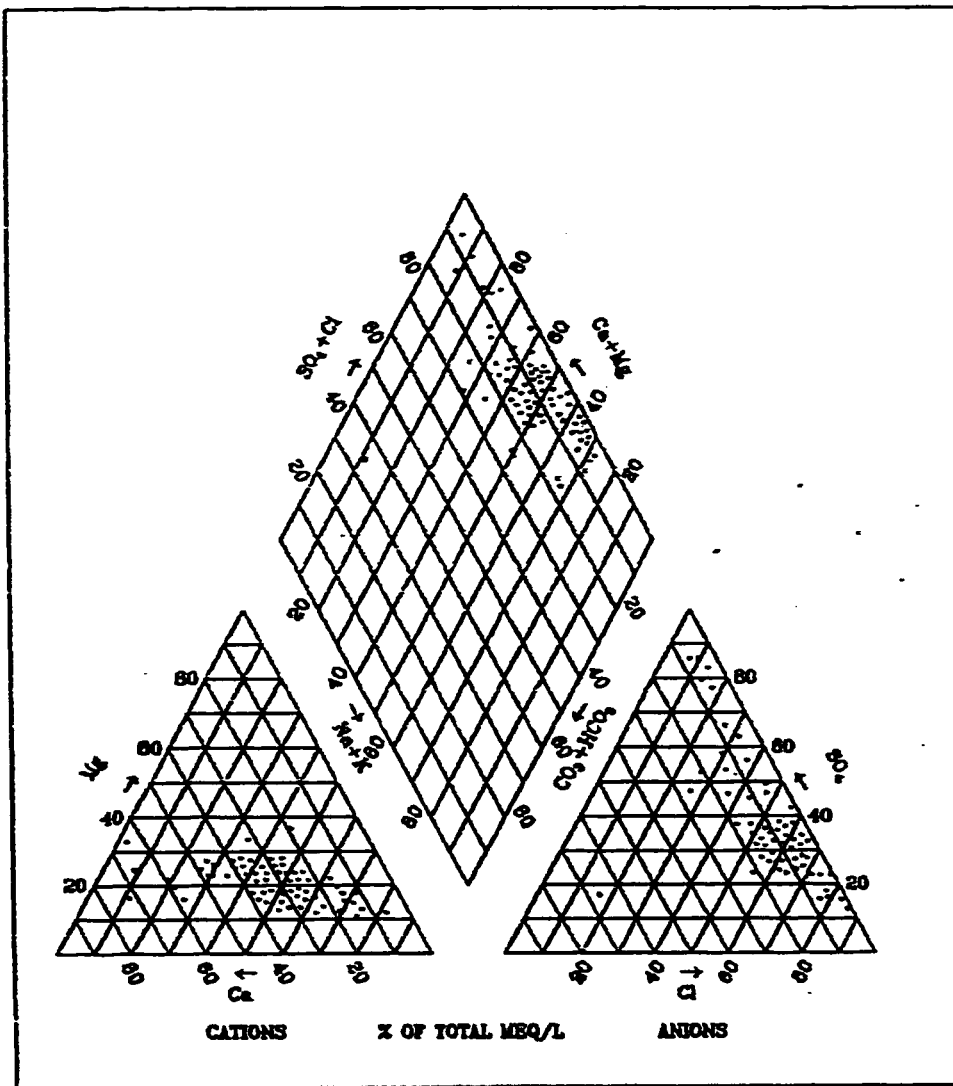


Figure 3.21 Trilinear plot of water samples of the Khobar aquifer.

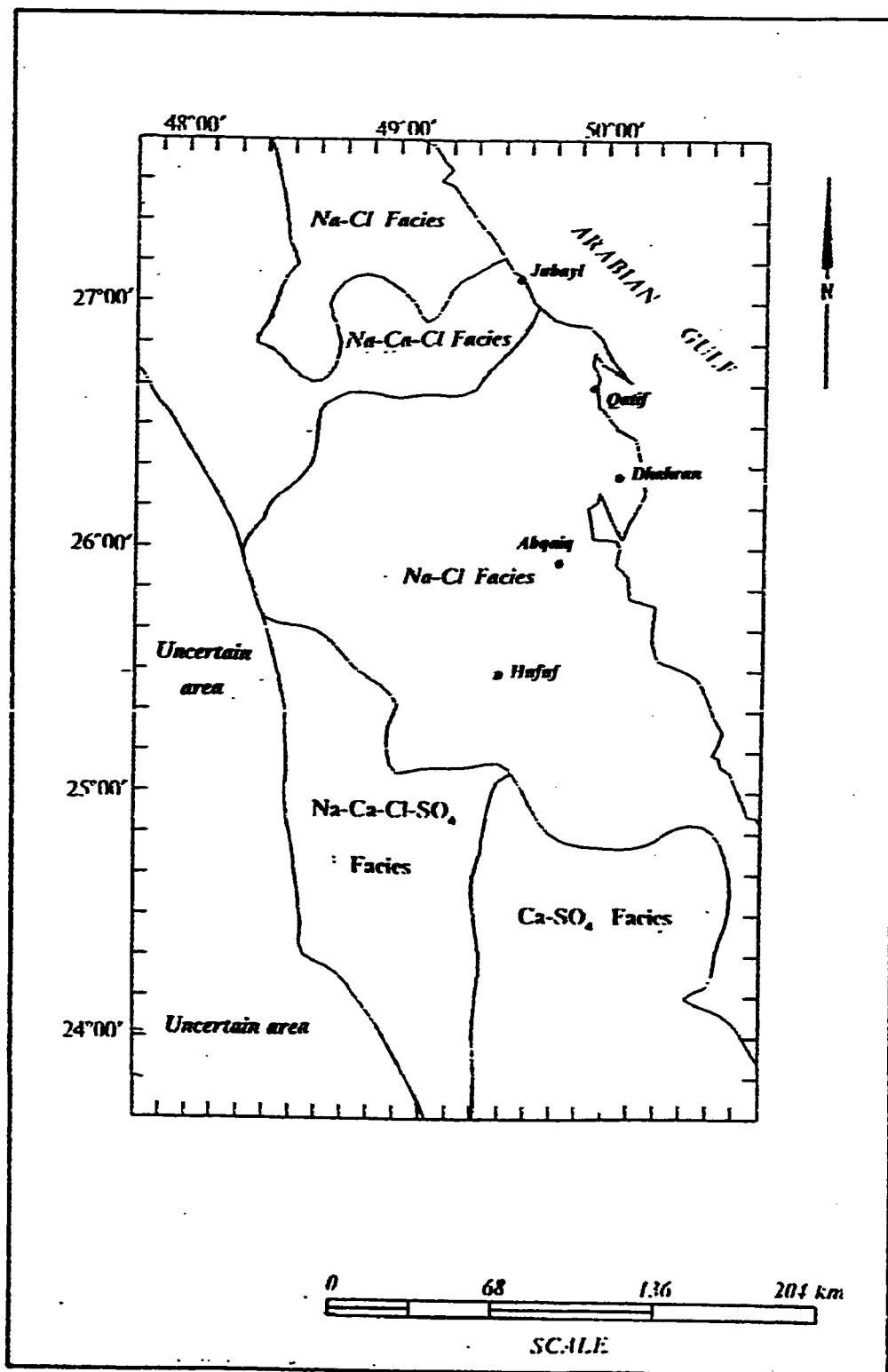


Figure 3.22 Hydrogeochemical facies map of the Khobar aquifer.

relatively high while the sulfate concentration is half the chloride concentration.

The fourth (Na-Cl) facies represents the most abundant water type. It is present in two distinctive areas, at the north of Jubayl and at the central part of the study area. This water type is common in areas along the Arabian Gulf, except around Jubayl. Almost all the areas on which the big cities are situated in the Eastern Province are characterized by this water type.

Quantitatively, sodium and chloride are the most abundant ions, whereas the other major ions constitute less amount in the fourth facies. The TDS increases gulfward, except around Qatif where the pattern seems disturbed.

The Na-Cl type water seems to be associated with the Na-Cl-Ca-  $SO_4$  facies and Na-Ca-Cl facies. However, it seems that the latter two water types are related geochemically to the Ca-  $SO_4$  in two different ways. The calcium in facies Na-Cl-Ca-  $SO_4$  and Na-Ca-Cl facies could be generated by dissolution of aquifer minerals. The anomalous sulfate in the Na-Cl-Ca-  $SO_4$  facies might have been introduced to the system by local gypsum dissolution or regional geochemical evolution.

### ***3.4 Distributional Comparison Between Alat and Khobar Aquifers***

To compare the two aquifers, the overlap area between  $25^{\circ}30' N$  latitude and  $27^{\circ}00' N$  latitude is considered. Table 3.1 show a comparison between the major ions and TDS in Alat and Khobar aquifers. Three major areas located north of Jubayl, Qatif-Dhahran and Abqaiq- Al

**TABLE 3.1 Comparison between the Hydrochemical Constituents Distribution of Alat and Khobar Aquifers.**

Const.	Jubayl Area		Qatif-Dhahran		Abqaiq-Al Hufuf	
	Alat	Khobar	Alat	Khobar	Alat	Khobar
Ca	400-1100	500-1000	300-500	300-500	200-300	200-500
Mg	160-420	260-420	100	100-180	60-80	60-80
Na	1000-5500	1000-5000	400	500-1100	400	500
Cl	> 5000	> 5000	500-1000	900-1700	500	500
SO <sub>4</sub>	1000-2000	700-1600	600-1600	600-1600	400-600	400-1300
HCO <sub>3</sub>	150-180	160	140-180	160-200	210-500	200-500
TDS	> 10000	> 10000	2000	2000-4500	> 2000	2000-3000

Const. = Constituent

**Hufuf are taken in account.**

**There is a similarity in major ion concentration and TDS of the Alat and Khobar aquifers in the Jubayl area. In the area between Qatif and Dhahran, there are differences in sodium and chloride concentration and the TDS. The calcium, sulfate and bicarbonate concentrations are more or less similar in both aquifers. In Abqaiq - Al Hufuf area, the ion concentration and the TDS in both aquifers show a good resemblance. The only exception is the relatively high sulfate concentration.**

**The hydrogeochemical facies distribution of the two aquifers are generally similar. In both aquifers, the Na-Cl water type is a predominant facies. There is a limited extent of Na-Cl facies near Jubayl in both aquifers. Moreover, the main Na-Cl facies in both aquifers falls below the  $26^{\circ}30' N$  latitude. This facies is predominant in Khobar aquifer and covers almost all the major cities in the study area. The extent of the Na-Cl facies in Alat aquifer is reduced and somehow overtaken by the Na-Ca-Cl and the Na-Ca-Cl-  $SO_4$  facies.**



## **CHAPTER 4**

### **AQUEOUS EQUILIBRIUM STUDIES**

#### **4.1 Aqueous Models**

Computerized models, according to their origin and applications could be grouped into generalized and non-generalized types. There are two types of generalized methods: The equilibrium constant approach and the Gibbs free energy minimization approach. The mathematical approach of the equilibrium constant method was derived in general form by Brinkley (1947), and Brinkley and Kandiner (1950). Using digital computers, Feldman et al. (1969), utilized this method to calculate equilibrium conditions. The mathematical formulation of the Gibbs free energy minimization was pioneered by White et al. (1958). Kaprov and Kaz'min (1972) have computed the distribution of species in seawater by a computerized free energy minimization model.

The non-generalized models use the equilibrium constant approach and incorporate individual reactions as part of the program. They apply different approximations to solve equilibrium problems in aqueous geochemistry. One way is the successive approximation that was conveniently described by Wigley (1977). The successive approximation uses either the brute force method or a continued fraction method. In the brute force method, mass action expressions are substituted directly into the mass balance condition and solved for total concentrations which are then compared to the analytical values. In the

continued fraction method, non-linear equations are rearranged to solve for free ion concentrations which are initially assumed to be equal to the total concentrations.

Wigley (1977) had illustrated the two methods by introducing a simple example. Assuming a solution containing free  $Ca^{2+}$  ions,  $CO_3^{2-}$  ions and only one ion pair ( $CaCO_3^0$ ); he established the mass balance conditions as follows:

$$mCa(\text{total}) = mCa^{2+} + mCaCO_3^0 \quad (1)$$

$$mCO_3^{2-}(\text{total}) = mCO_3^{2-} + mCaCO_3^0 \quad (2)$$

Assuming an ideal condition

$$K = \frac{mCaCO_3^0}{(mCa^{2+})(mCO_3^{2-})} \text{ or } mCaCO_3^0 = K(mCa^{2+})(mCO_3^{2-}) \quad (3)$$

Substituting equation 3 into 1 and 2

$$mCa(\text{total}) = mCa^{2+} + K(mCa^{2+})(mCO_3^{2-})$$

$$mCO_3^{2-}(\text{total}) = mCO_3^{2-} + K(mCa^{2+})(mCO_3^{2-})$$

Using the brute force method :

$$mCa^{2+} = mCa(\text{total}) - K(mCa^{2+})(mCO_3^{2-})$$

$$mCO_3^{2-} = mCO_3^{2-}(\text{total}) - K(mCa^{2+})(mCO_3^{2-})$$

For the first estimate

$$mCa^{2+} = mCa(total)$$

$$mCO_3^{2-} = mCO_3(total)$$

Using the continued fraction method, the equations will be rearranged to :

$$mCa^{2+} = \frac{mCa(total)}{(1 + KmCO_3^{2-})}$$

$$mCO_3^{2-} = \frac{mCO_3(total)}{(1 + KmCa^{2+})}$$

There are different computerized programs that employ the successive approximation method. However, the first-generation programs of this type are WATEQ (Trusdell and Jones, 1974), SOLMNEQ (Kharaka and Barnes, 1973) and EQ3 (Wolery, 1978). These programs have been designed to accept water analyses data with pH, Eh and temperature values. SOLMNEQ carries a database of equilibrium constants for the range 0 - 350°C. EQ3 contains equilibrium constant database for 0 - 300°C. WATEQ uses the Vant Hoff equation or analytical expressions for equilibrium constants as a function of temperature and is considered reliable for the range 0 - 100°C (Nordstrom et al., 1979).

WATEQ was originally written in PL/I and has been revised and translated into FORTRAN by Plummer et al., (1976) in a program called WATEQF. Rollins (1990) introduced a new version of WATEQ family which is PCWATEQ. This version is a special adaption for IBM PC's of WATEQF and

it is used in this study.

The extended form of Debye-Huckel and the Davies equations are used in PCWATEQ for the calculation of single ion activity coefficients. The two models are used because single ion activities and single ion activity coefficients can not be defined thermodynamically or measured exactly. Measuring the activity of a single charged ion requires a measurement to the finite free energy change of the solution which results from a finite change in concentration of the single ion while holding the concentration of other ions constant. This is impossible and it necessitates the use of non-thermodynamic models to evaluate single-ion activity coefficients. The following two equations are used to calculate the activity coefficients ( $\gamma$ ):

The extended form of Debye-Huckel equation :

$$\log \gamma = \frac{AZ^2\sqrt{I}}{(1 + Ba\sqrt{I})}$$

and Davies equation

$$\log \gamma = \frac{AZ^2\sqrt{I}}{(1 + Ba\sqrt{I})} + bI,$$

where A is a function of the solvent dielectric constant (D) and the absolute temperature (T), (Pagenkopf, 1978). A is expressed as :

$$A = 1.823 \frac{(10^6)}{(DT)^{3/2}}$$

Z is the ion charge, I is the ionic strength, "a" is the size of the hydrated ion,

and  $B$  is a constant which depends upon solvent dielectric constant ( $D$ ) and absolute temperature ( $T$ ), (Pagenkopf, 1978).

$$B = \frac{50.3}{\sqrt{(DT)}}$$

Using mass action and mass balance equations, the concentrations of free ions (molalities) are calculated from the total (analytical) concentrations, the pH, and the activity coefficients of the species. The molalities of free ions are calculated by iteration and when the sums of free ions, complex ions, and weak acids agree with the analytical values within 0.5%, the iteration stops. The activities are calculated from molalities and ion activity coefficients. The calculated activities are combined to produce ion activity products, which are compared with the solubility products in order to find out the degree of saturation (saturation index) with different minerals (Truesdell et al., 1973).

Since experimental determinations of equilibrium constants have been made at 25°C, the equilibrium constant at other temperatures is expressed as a power function of the absolute temperature :

$$\log K = A + BT + C/T + DT^2 + E/T^2 + F \log T ,$$

where  $A$ ,  $B$ ,  $C$ ,  $D$ ,  $E$ , and  $F$  are experimentally-determined constants for a given system. This expression is used in PCWATEQ, whenever it is available in the literature. The full information is shown on Appendix 3.

The PCWATEQ calculates both activities of aqueous species and the

departure from equilibrium (saturation indices) for many solid phases and gases that might be in contact with aqueous phase. The saturation index (S.I) is expressed as :

$$S.I. = \log \frac{IAP}{K_T} ,$$

where IAP is the ion activity product of the components of the solid or gaseous phase, and  $K_T$  is solid or gaseous phase solubility equilibrium product at the specified temperature.

The S.I. value indicates the departure from equilibrium, when it is not equal to zero. The solid or gaseous phase is undersaturated and has thermodynamic potential to dissolve, when the S.I value is less than zero (i.e. negative). When it is greater than zero, the solid or gaseous phase is oversaturated and has the potential to precipitate or volatilize. Sprinkle (1989) mentioned the likeliness of dissolution, although slow, when negative saturation indices are calculated. This indicates an association of undersaturation with mineral dissolution. However, oversaturation does not necessarily mean mineral precipitation. Drever (1982) explained other factors such as mineral surface topography, surface poisoning, and nucleation energy that may inhibit the formation and growth of a mineral.

#### ***4.2 Distribution of Saturation Indices in the Alat Aquifer***

The water of this aquifer is mostly oversaturated with respect to calcite (Fig. 4.1). The calcite S.I. in the Alat aquifer mainly varies from 0.2 to 0.4 . In the southwest of the map the negative S.I. indicates undersaturation and a possible

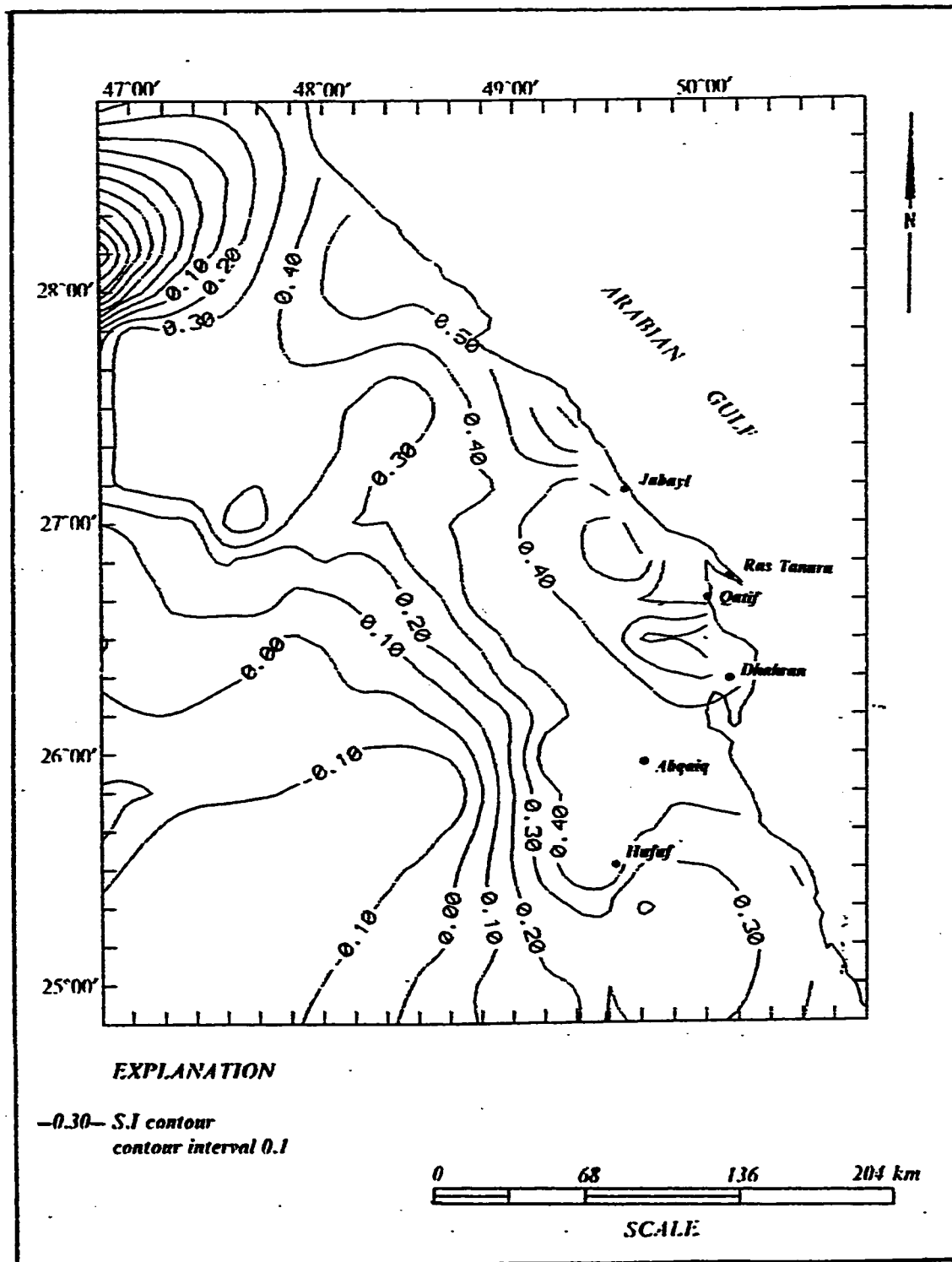


Figure 4.1 Calcite saturation index map of the Alat aquifer.

dissolution of the aquifer minerals. Due to insufficient data, the negative S.I. value might not represent the real value. However, it is a clear indication of decreasing calcite content in the upgradient areas.

The northwestern part of the study area (Fig. 4.1) is characterized by dissolution of calcite. Calcite S.I. values drop landward. Generally, the S.I. values are low inland and increase towards the Arabian Gulf coast.

Alat aquifer is undersaturated with dolomite in the southwest and northwest of the study area. (Fig. 4.2). The degree of saturation increases seaward and a high degree of oversaturation exists in the area stretching from Jubayl to Dhahran. Dolomite S.I. follows the saturation pattern of calcite in the Alat aquifer. However, the dolomite S.I. values are twice those of the calcite. Around Dammam dome, the aquifer water is distinctly oversaturated with dolomite and less oversaturated with calcite.

Negative gypsum S.I. values are obtained for the Alat aquifer indicating an undersaturation with respect to gypsum (Fig. 4.3). However, the degree of undersaturation varies generally from north to south, decreasing northward, where the gypsum S.I. tends to be more closer to equilibrium (saturation). The degree of undersaturation increases near Abqaiq-Dhahran area.

#### ***4.3 Distribution of Saturation Indices in the Khobar Aquifer***

In general, Khobar aquifer is oversaturated with respect to calcite. Although the degree of saturation varies, there is no discernable generalized pattern of the variation.



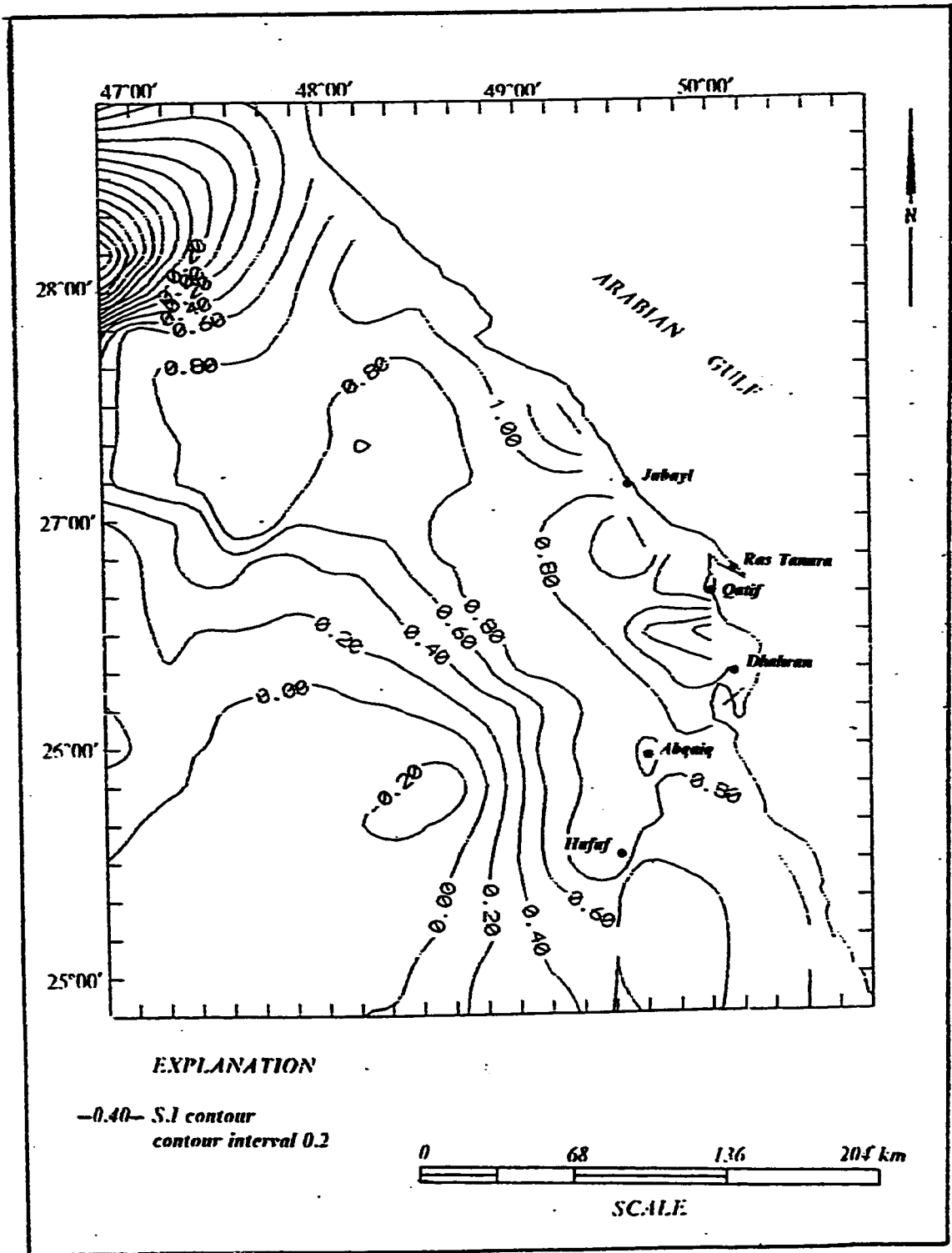


Figure 4.2 Dolomite saturation index map of the Alat aquifer.

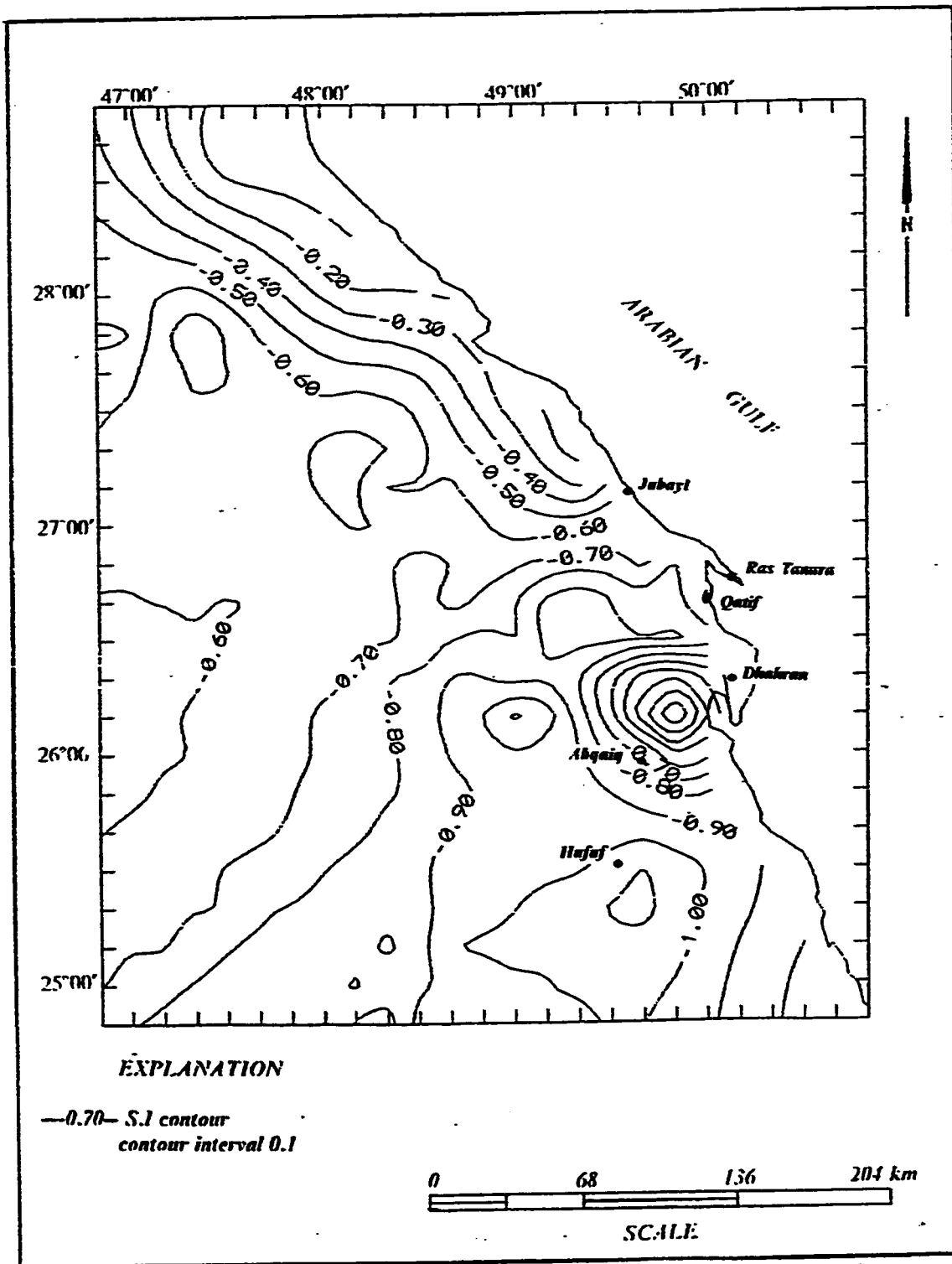


Figure 4.3 Gypsum saturation index map of the Alat aquifer.

The calcite S.I. values in the extreme north increase seaward (Fig. 4.4). The S.I. is about zero at the northwest (landward) and gradually increases seaward where it becomes oversaturated. To the south, the S.I. values decrease from Jubayl all the way to Dammam. South of Dammam, at Al Hufuf, the calcite S.I. values drop rapidly eastward within a short distance. Here the high calcite S.I. values coincide with high bicarbonate contents (Fig. 3.18).

The dolomite S.I. values (Fig 4.5) are similar to those of calcite. The aquifer is generally oversaturated with respect to dolomite. However, in the west-central part of the study area, the aquifer is undersaturated with dolomite.

Khobar aquifer is undersaturated with respect to gypsum (Fig. 4.6). The degree of undersaturation decreases from south towards north and east. Near Abqaiq and Al Hufuf, areas of relatively low undersaturation with gypsum are evident.

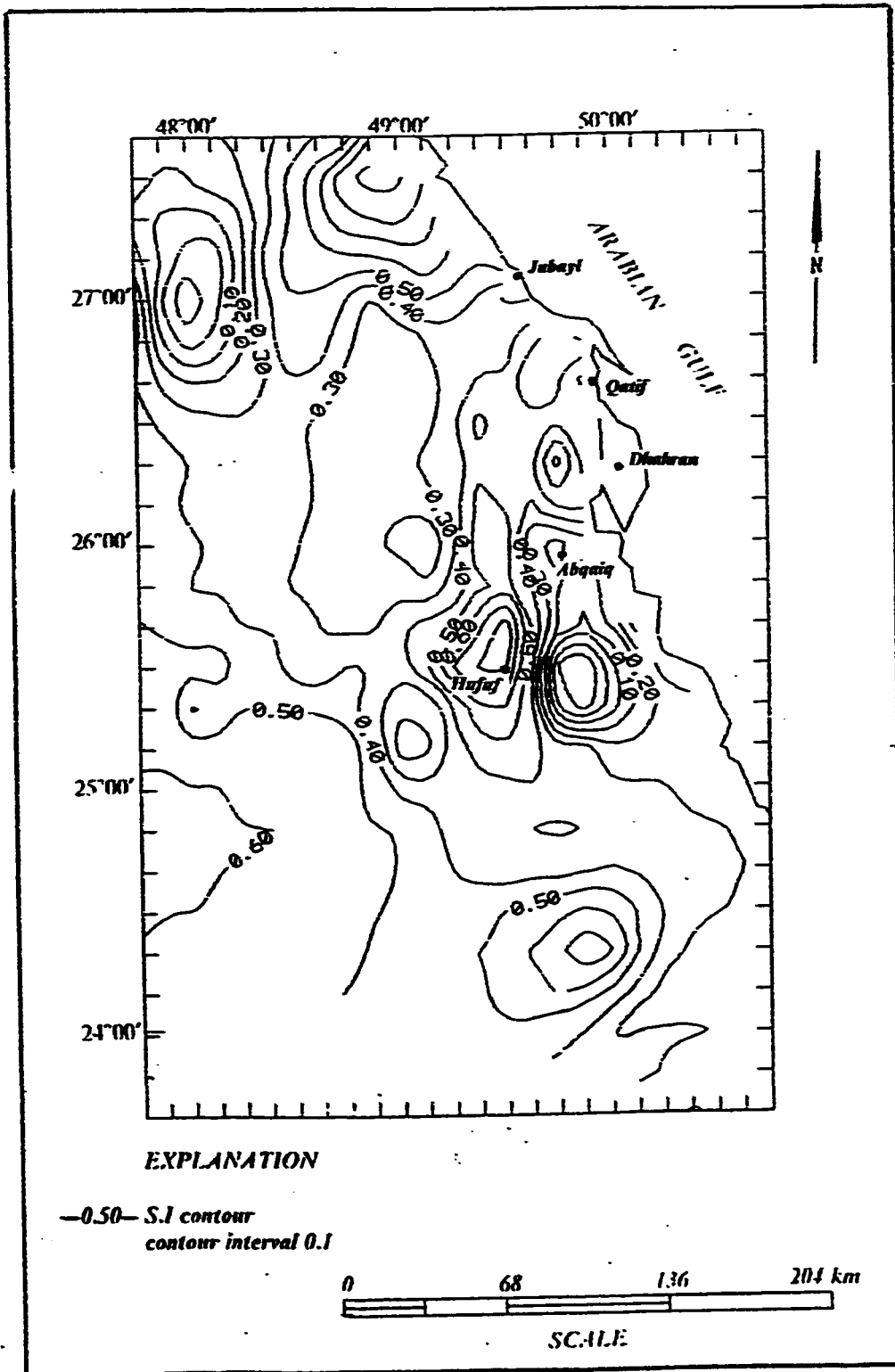


Figure 4.4 Calcite saturation index map of the Khobar aquifer.

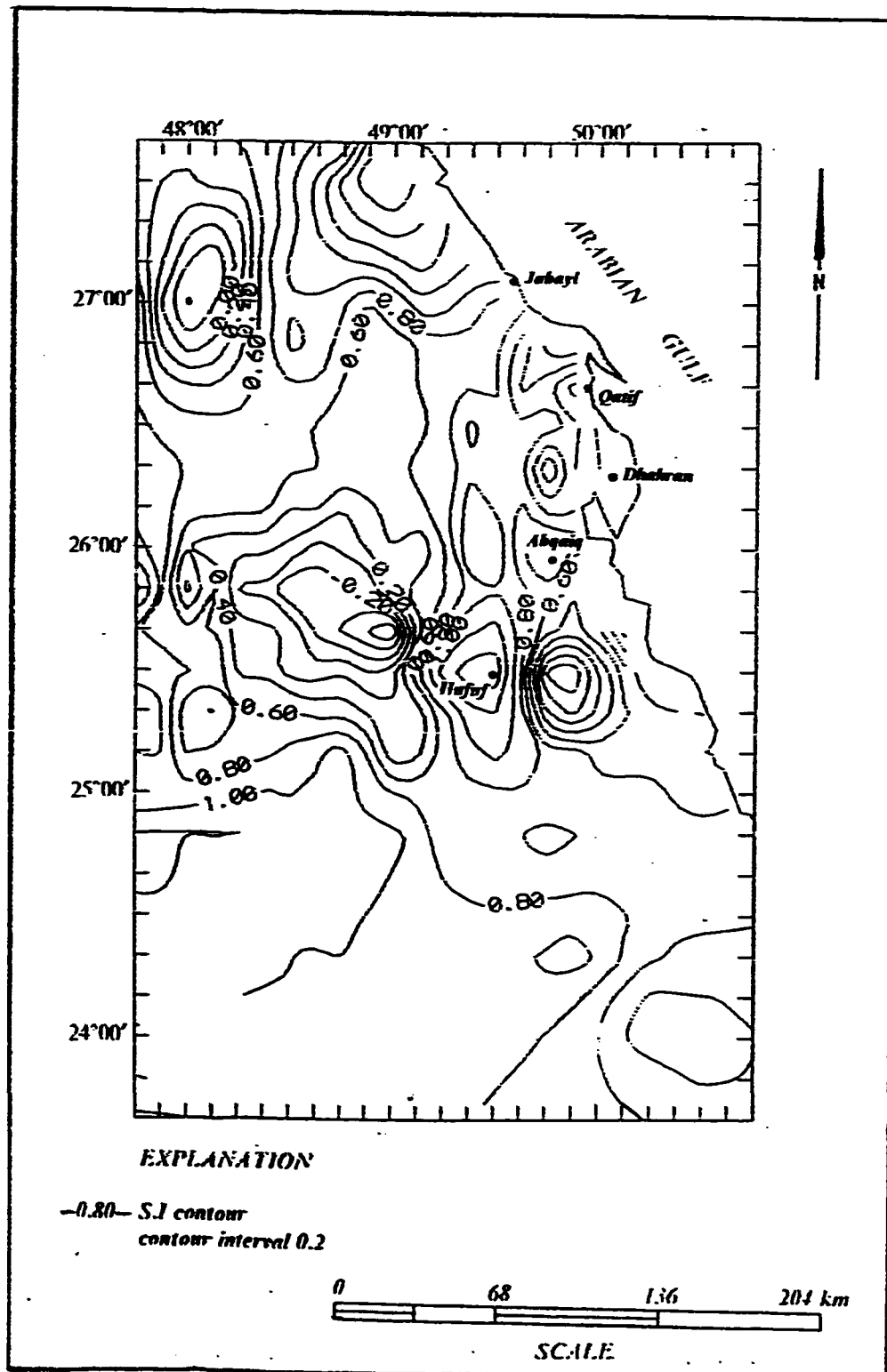


Figure 4.5 Dolomite saturation index map of the Khobar aquifer.

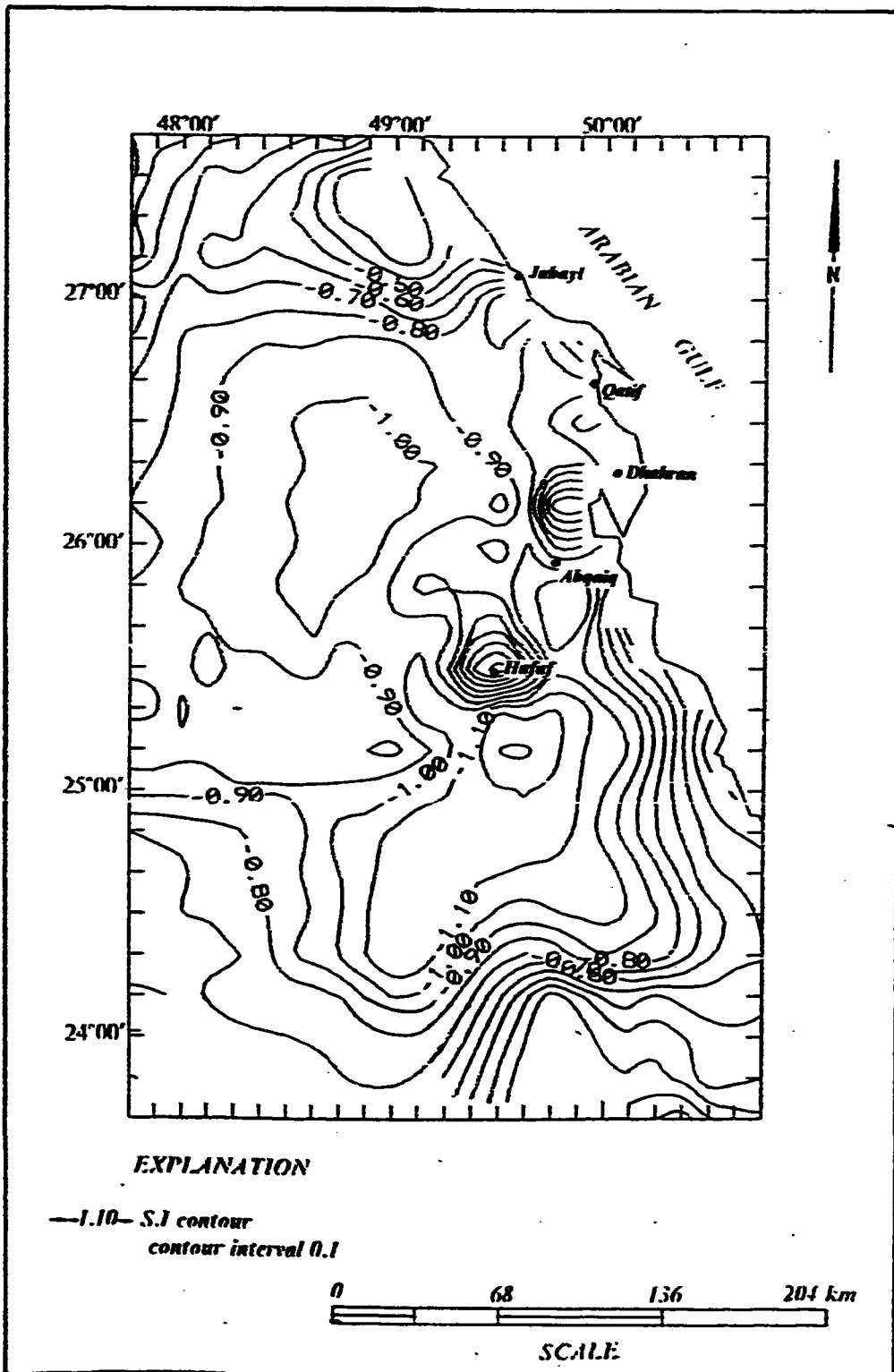


Figure 4.6 Gypsum saturation index map of the Khobar aquifer.

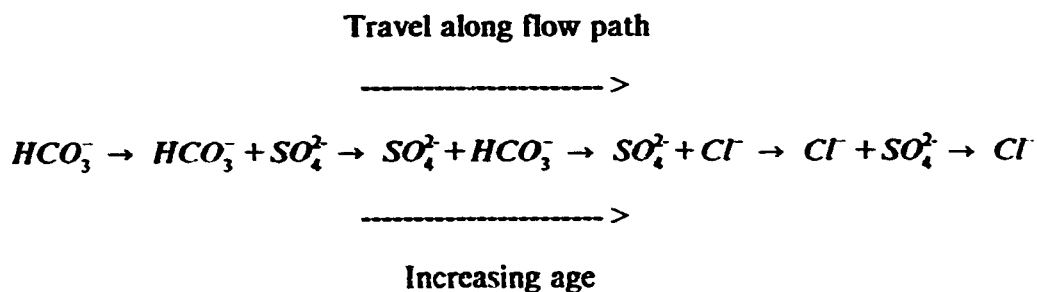
## CHAPTER 5

### HYDROGEOCHEMICAL PROCESSES

#### 5.1 Introduction

Total dissolved solids and most of the major ions increase when groundwater moves along its flow path. Many investigations around the world have shown that shallow groundwater in recharge areas is lower in TDS than deeper zone water in the same area or water in discharge areas.

Chebotarev (1955), in a classic paper, concluded that groundwater tends to evolve chemically towards the composition of seawater. He indicated that the evolution was normally accompanied by regional change in the proportion of major anions along the flow path, as shown below.



From a geochemical view point, the above sequence can be explained in terms of two main variables, mineral availability and mineral solubility (Freeze and Cherry, 1979).

Bicarbonate in groundwater is normally derived from a soil zone and from dissolution of calcite and dolomite. The availability of calcite and dolomite, and their rapid dissolution in contact with  $CO_2$ , makes bicarbonate the dominant anion in recharge areas.

The most common sulfate-bearing minerals are gypsum and anhydrite which dissolve readily in the presence of water. Gypsum and anhydrite are more soluble than calcite and dolomite but less soluble than chloride-bearing minerals. However, in most sedimentary basins a groundwater has to travel a considerable distance before sulfate becomes the dominant anion (Freeze and Cherry, 1979); the reason is due to the scarcity of gypsum and anhydrite in the porous medium.

Chloride minerals of sedimentary origin dissolve readily in water. However, they are scarce in sedimentary basins. In clastic and carbonate rocks, chloride minerals occur in trace amounts, so chloride dissolution is mainly controlled by the process of diffusion. Due to the sluggish nature of diffusion process and the scarcity of chloride- and sulfate-bearing minerals, the chemical evolution of groundwater from  $HCO_3^-$  to  $Cl^-$  proceeds very gradually rather than by distinct steps over short distances (Freeze and Cherry, 1979).

Generally, chloride is the predominant anion in deep groundwater and in discharge areas. Freeze and Cherry (1979) attributed this to the paucity of chloride-bearing minerals along the flow path. However, regardless of flow distance and presence of other minerals in the system, if groundwater comes into



contact with halite, the water will evolve directly to a chloride type. Generalization of major cation evolution sequence is not advisable, because cation exchange process causes large unexpected variations in the predicted sequence.

### ***5.2 Alat Aquifer***

At the extreme north of the study area, the calcium concentration (Fig. 3.1) increases seaward. This increase becomes sharp around 27°00' latitude. The cause of this increase is not related to a recharge, as indicated by the relatively low bicarbonate concentration (Fig. 3.6), the absence of Dammam formation outcrops, and high TDS (Fig. 3.7). Also the high calcium and sodium concentrations and the presence of calcite oversaturation make unlikely the role of cation exchange.

In fact, the oversaturation with respect to calcite (Fig. 4.1), the high magnesium concentration (Fig. 3.2), the high chloride concentration (Fig. 3.4) and the increase in dolomite saturation index (Fig. 4.2) provide a clear evidence of seawater intrusion. The plots of samples #56 and #27 (Fig. 5.1) show that the relatively high sulfate concentration is due to the Arabian gulf seawater intrusion. The trend lines of figure 5.1 were drawn by using assumed  $SO_4$  and Cl (mg/l) concentrations in dilute groundwater (Sprinkle, 1989). The points A and C represent the initial concentrations while lines AB and CD indicate the gypsum dissolution trend. Samples #56 and # 27 plot somewhere around the Arabian gulf seawater plot. So to the north of Jubayl, seawater intrusion is the

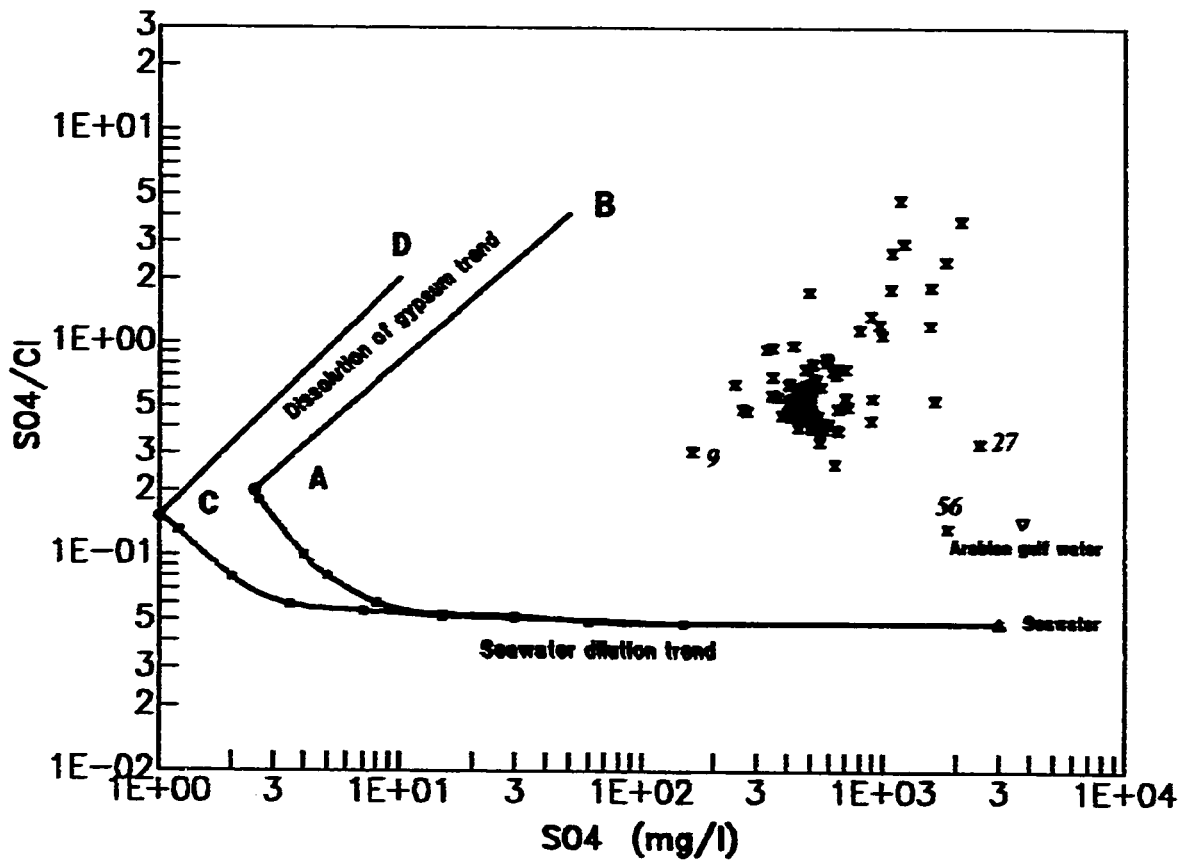


Fig. 5.1 Relation of Sulfate / Chloride ratio to Sulfate (mg/l) in the Alat Aquifer (The base diagram is modified from Sprinkle, 1989; Rightmire and others, 1974).

Points A and C represent assumed  $SO_4^{2-}$  and  $Cl^-$  concentrations in dilute groundwater.

main process that controls the hydrogeochemistry of the aquifer. Italconult (1969) and Rasheeduddin (1988) plotted the contour maps of the piezometric surface of the Alat aquifer. They showed the absence of hydraulic gradient dependent seawater intrusion. However, Freeze and Cherry (1979) explained how in the absence of the other gradients (hydraulic gradient and temperature gradient), the chemical gradient can cause the flow of water from regions of high salinity to regions of low salinity. Instead of the solely hydraulic gradient dependent flow, the authors established the following more general flow law :

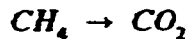
$$v = -L_1 \frac{dh}{dl} - L_2 \frac{dT}{dl} - L_3 \frac{dC}{dl}$$

Where  $v$  is specific discharge,  $h$  is hydraulic head,  $l$  is distance,  $T$  is temperature and  $C$  is chemical concentration;  $L_1$ ,  $L_2$  and  $L_3$  are constants of proportionality. The nature of seawater intrusion in the north of Jubayl is a chemical gradient dependent rather than a hydraulic gradient dependent.

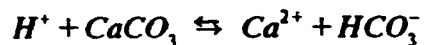
In the area extending from Ras Tanura to Qatif all the way to Dhahran there is no evident variation in calcium. Also the TDS maintains a constant value of about 3000 mg/l and the calcite saturation index increases slightly (from 0.4 to 0.5). This indicates the absence of noticeable recharge even though the aquifer around the Dammam dome assumes semi-confined behavior. Likewise, the relatively low chloride concentration (500 - 1000 mg/l) suggests the absence of seawater intrusion. The effect of cation exchange, in this area, is not evident; the fact that calcium concentration maintains a constant to slightly increasing value accompanied by relatively low (400 mg/l) sodium concentration and the relative decrease in bicarbonate testifies the absence of cation exchange

process.

In the Abqaiq - Al Hufuf area the TDS drops from 3000 to 2000 mg/l. Also sodium and chloride assume relatively low concentration values. At the west of Abqaiq a sharp increase of bicarbonate is shown on figure 3.6 . The increase is associated with relative decrease in calcite and dolomite saturation indices (Figures 4.1 and 4.2), and drop in TDS (Fig. 3.7). Although the predominant water type in this area is Na-Cl facies (Fig. 3.10), there is a localized *Na-HCO<sub>3</sub>* facies which can be explained by groundwater mixing process. The area of interest falls on the Ghawar structure, well 9 (Fig. 5.2). On the structural highs generally the intervening confining layers decrease in thickness (Edgell, 1990) whereby through leakage water passes from one aquifer to another. The high bicarbonate could be explained by three different processes. The first possibility is recharge by upwelling water from Umm Er Radhuma on the structural highs. This is supported by Low TDS. The second possibility is heterotrophic oxidation of organic matter. This is the oxidation of deep source *CH<sub>4</sub>*, probably from the oil fields, according to the reaction :



by bacteria. The third possibility is anaerobic reduction of *SO<sub>4</sub>* and concomitant oxidation of organic matter by a reaction of the form:



the drop in sulfate and the increase in bicarbonate could be explained by this process. Since recharge would have contributed both *Ca* and *HCO<sub>3</sub>*, the high

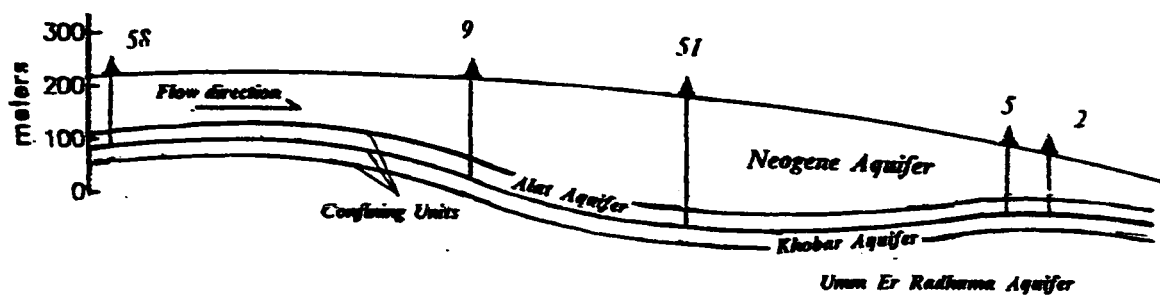
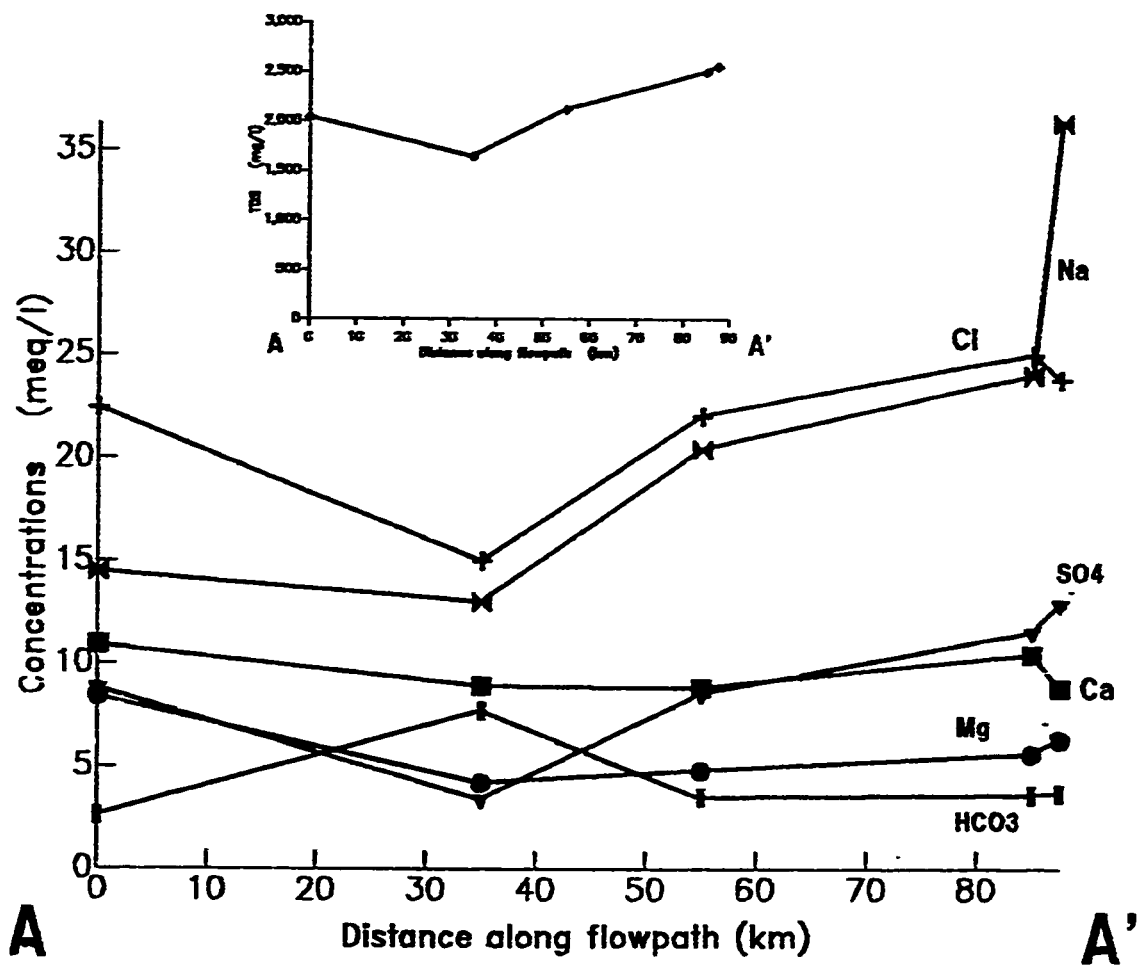


Figure 5.2 Profiles of hydrogeochemical parameters along Almaty aquifer flowpath (For the location of the profile see Fig. 1.2).

bicarbonate value is most likely related to bacterial activity.

Between well no. 5 and well no. 2 (Fig. 5.2), the drop of calcium concentration and the sharp increase in sodium concentration could be explained by a cation exchange process. In outcrop the lower unit of Alat member is argillaceous whereas the upper unit is composed of a dolomitic limestone. It is quite possible that the upper unit itself might contain localized shaly layers in the subsurface. The interlayer monovalent cations (Na) of these clay minerals might have exchanged with divalent cations (Ca).

The hydrogeochemical evolving pattern of Alat aquifer is clearly shown on figure 5.3. The major ions concentrations of five wells along Alat aquifer flowpath are represented by Stiff diagrams. Also the Arabian gulf seawater composition is plotted for comparison. Generally, the shape of the diagrams evolves towards the seawater plot. For instance the shape (the Stiff diagram) of sample no. 58 is more different than the seawater plot compared with samples no. 51, 5 and 2. The change (increase) of the concentration scales is also another indication that the Alat aquifer water along its percourse evolves towards the seawater composition. Along the flowpath AA' (Fig. 5.2) the only disturbing pattern is the shape of sample no. 9. As explained previously here probably the change is due to anaerobic reduction of sulfate and concomitant oxidation of organic matter.

The possible origin of sulfate in the aquifer is analyzed (Fig. 5.1) by checking the contributions of seawater dilution and gypsum dissolution.

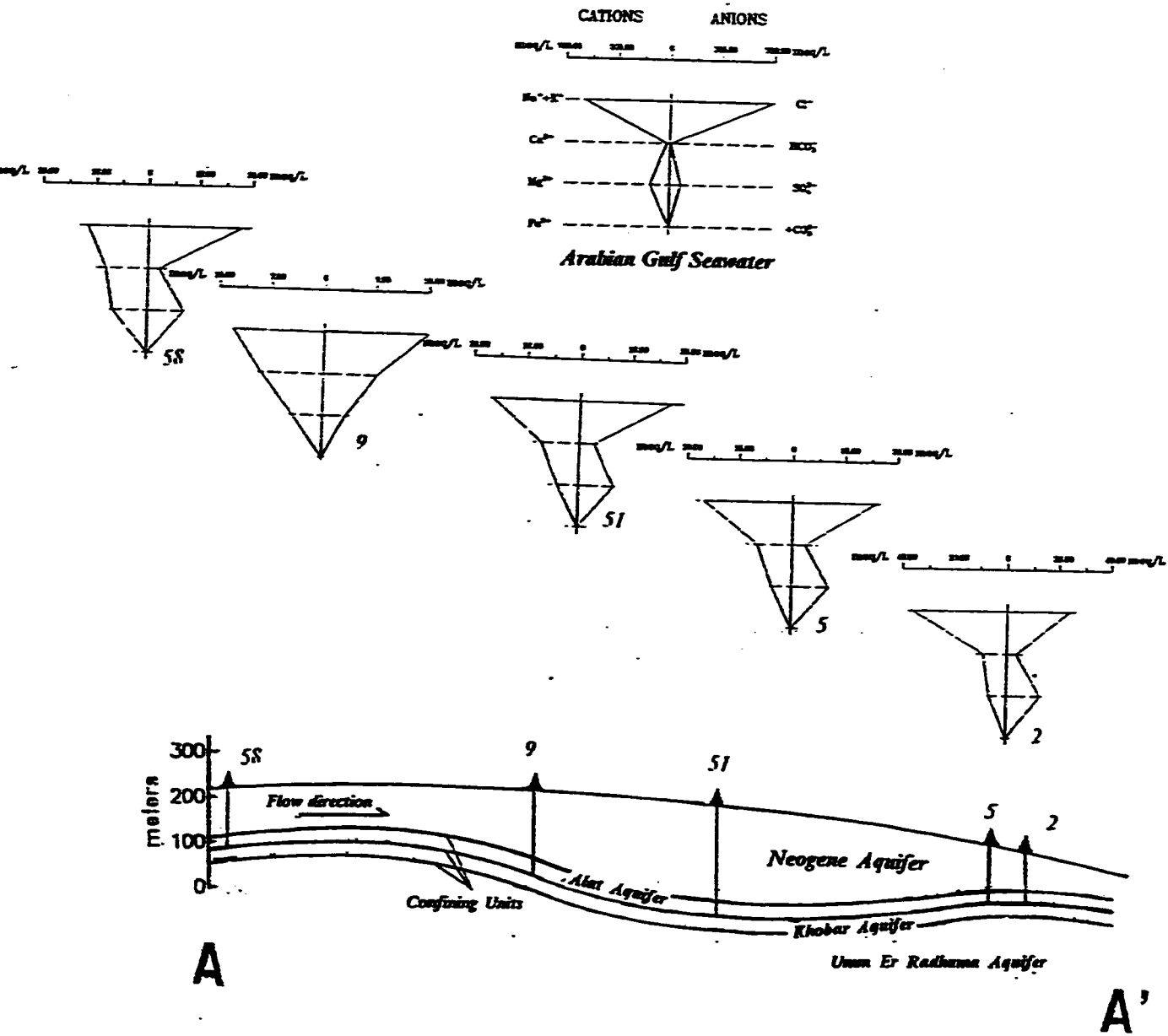


Figure 5.3 Stiff diagrams showing changes in major ions along Alat aquifer flowpath.

Sample no. 56 plots with  $SO_4/Cl$  ratio which is equal to that of the Arabian gulf seawater and the sample falls within the seawater intrusion influence zone. Sample no. 9 plots with lowest sulfate concentrations. In contrast, samples with high sulfate and  $SO_4/Cl$  ratio are found on the extreme north of the study area. In this area the degree of gypsum undersaturation is low (Fig. 4.3).

### **5.3. Khobar Aquifer**

In Al Hufuf area, the concentrations of major cations are reasonably low and increase seaward. The same is valid in the case of the TDS which increases seaward from a low of 1000 mg/l value upto more than 6000 mg/l.

The chloride concentration follows the pattern of the sodium concentration, and their meq/l (Na/Cl) ratio is generally greater than 1 (Fig. 3.15). Sulfate, though low, has a pattern which is similar to the other ions. Bicarbonate on the other hand has a different pattern and assumes its highest concentration level (400 mg/l) in an area situated between Al Hufuf and Abqaiq. Profiles of hydrogeochemical parameters along a flowline BB' (Fig. 5.4) is useful for discussion of the possible hydrogeochemical processes. Well no. 232 is located some distance away from the recharge area and contains water that is somewhat rich in sodium and chloride. Well no. 203 has a low TDS with a relative increase in its bicarbonate content. Surprisingly, in this well chloride decreases gently and sodium remains constant. This well is located right over the Ghawar structure, whereby the confining units decrease in thickness allowing the interaction of different aquifers. Here the mixing of water from the Khobar



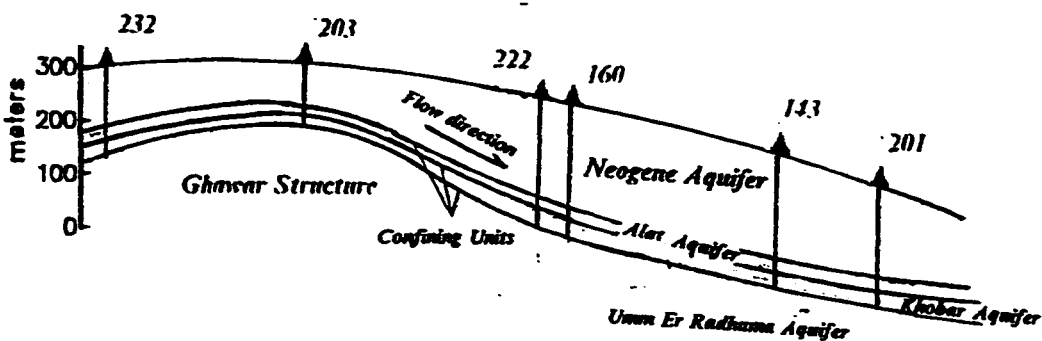
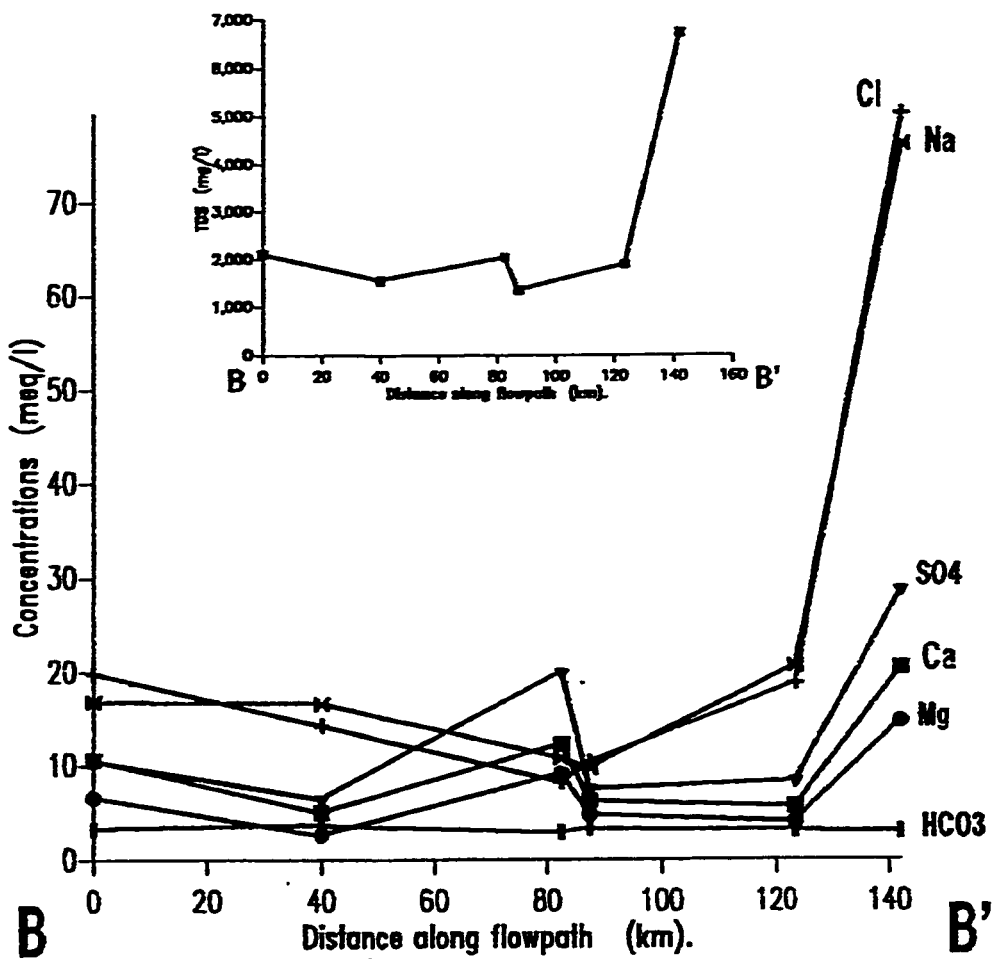


Figure 5.4 Hydrogeochemical parameters along Al-Hufuf flowpath in Khobar aquifer (Schematic profile, see Fig. 1.3 for the location of the profile BB').

aquifer with the underlying better quality water from Umm Er Radhuma aquifer explains the dilution effect and the resultant drop in the most major ion concentrations.

In well no. 222 the concentrations of calcium, magnesium and sulfate increase while sodium, chloride and bicarbonate concentrations decrease. The  $SO_4/Cl$  ratio of this well is greater than 3 and it follows the gypsum dissolution trend (Fig. 5.5). The gypsum dissolution and the concomitant dedolomitization would result in the high sulfate, calcium and magnesium concentrations (Sprinkle, 1989). Although the aquifer in general is undersaturated with respect to gypsum, the degree of undersaturation is considerably lower in this area, thus supporting the gypsum dissolution process (Fig. 4.6). From well no. 160 downgradient, the water body resumes its normal evolution towards the seawater composition. Although the bicarbonate increase and the drop in the TDS at well no. 160 could be explained by an aquifer interaction, a more plausible cause is the pH decrease and the  $PCO_2$  increase associated with gypsum dissolution, dedolomitization and calcite precipitation at well no. 222 (Sprinkle, 1989).

The groundwater evolution along flowpath BB' is clearly illustrated by Stiff diagrams (Fig. 5.6). The chemistry of the flowing water body evolves from a reasonably fresh water composition in well no. 232 to a mixed water composition rich in sulfate, magnesium and calcium in well no. 203. The evolution is in perfect accordance with the hydrogeochemical evolutionary sequence discussed in section 5.1. However, the change in the plot shape and the

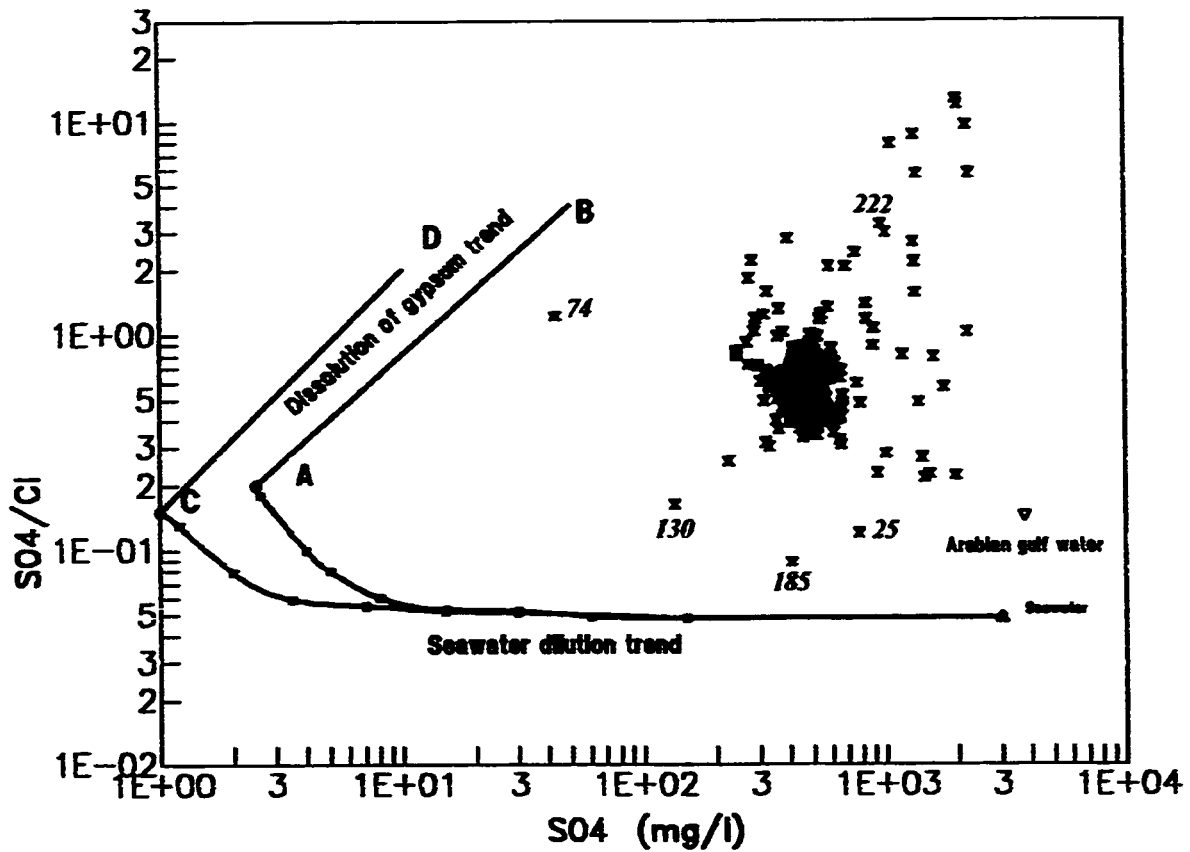
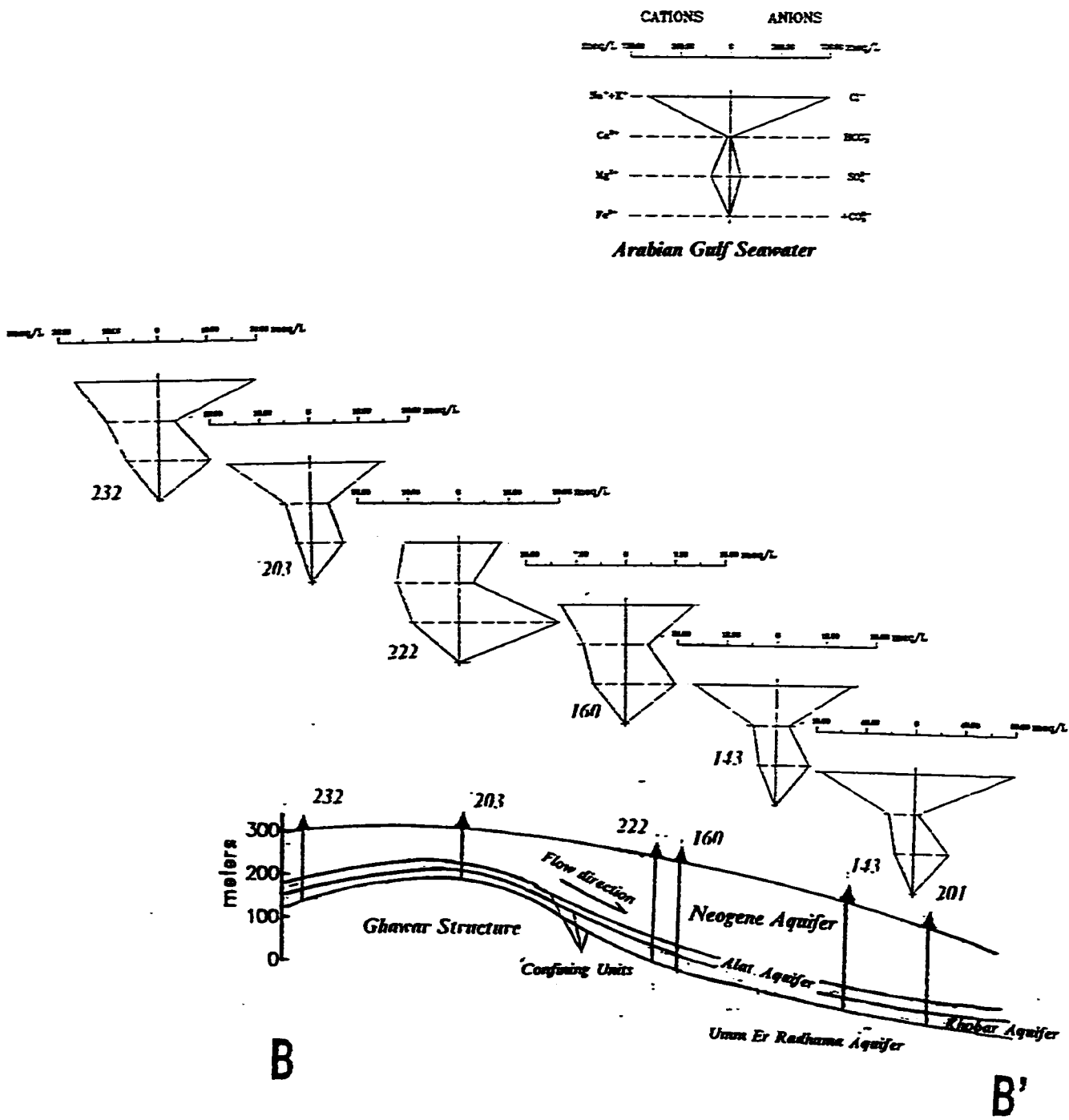


Fig. 5.5 Relation of Sulfate / Chloride ratio to Sulfate (mg/l) in the Khobar Aquifer (The base diagram is modified from Sprinkle, 1989; Rightmire and others, 1974). Points A and C represent assumed  $SO_4^{2-}$  and  $Cl^-$  concentrations in dilute groundwater.



**Figure 5.6** Stiff diagrams showing changes in major ions along Al-Hufuf flowpath in Khobar aquifer.

increase in concentrations are interrupted at well no. 222 whereby gypsum dissolution and dedolomitization takes place. The water body, eventually, resumes its normal evolutionary trend beyond well no. 160.

Hydrogeochemical profiles along the flowpath CC' near Abqaiq (Fig. 5.7) depicts the possible hydrogeochemical processes that are taking place in the aquifer. A normal groundwater evolution is evident in the upgradient part of the flow. The drop in bicarbonate and increase in other ions at well no. 13 is a part of the evolutionary sequence. However, in well no. 113, which is adjacent to well no. 13, there is a dilution effect. Here, the aquifer most likely receives recharge. Since there is no outcrop for the aquifer in this area, an upward leakage probably comes from the adjacent Umm Er Radhuma aquifer. As explained previously, well no. 113 is located over the Abqaiq structural high where the confining layers decrease in thickness and allow some upward leakage from the Umm Er Radhuma aquifer. Such a leakage would explain the drop in the concentrations of most of the major ions since the Umm Er Radhuma water is low in TDS relative to the Khobar aquifer water (Table 5.1). The similarity between the ion concentrations of well no. 13 and 113, along a flow line, with the Umm Er Radhuma aquifer water (MAW, 1984) supports the upward leakage (Table 5.1). The major differences in sulfate is due to the high sulfate content of Umm Er Radhuma aquifer water.

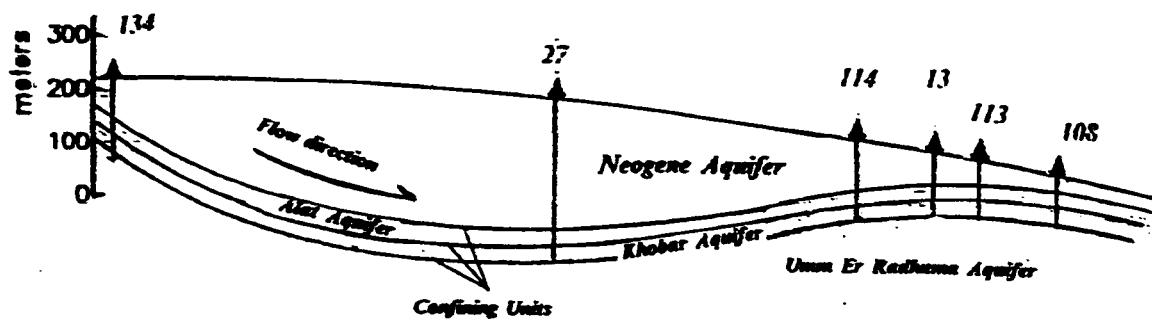
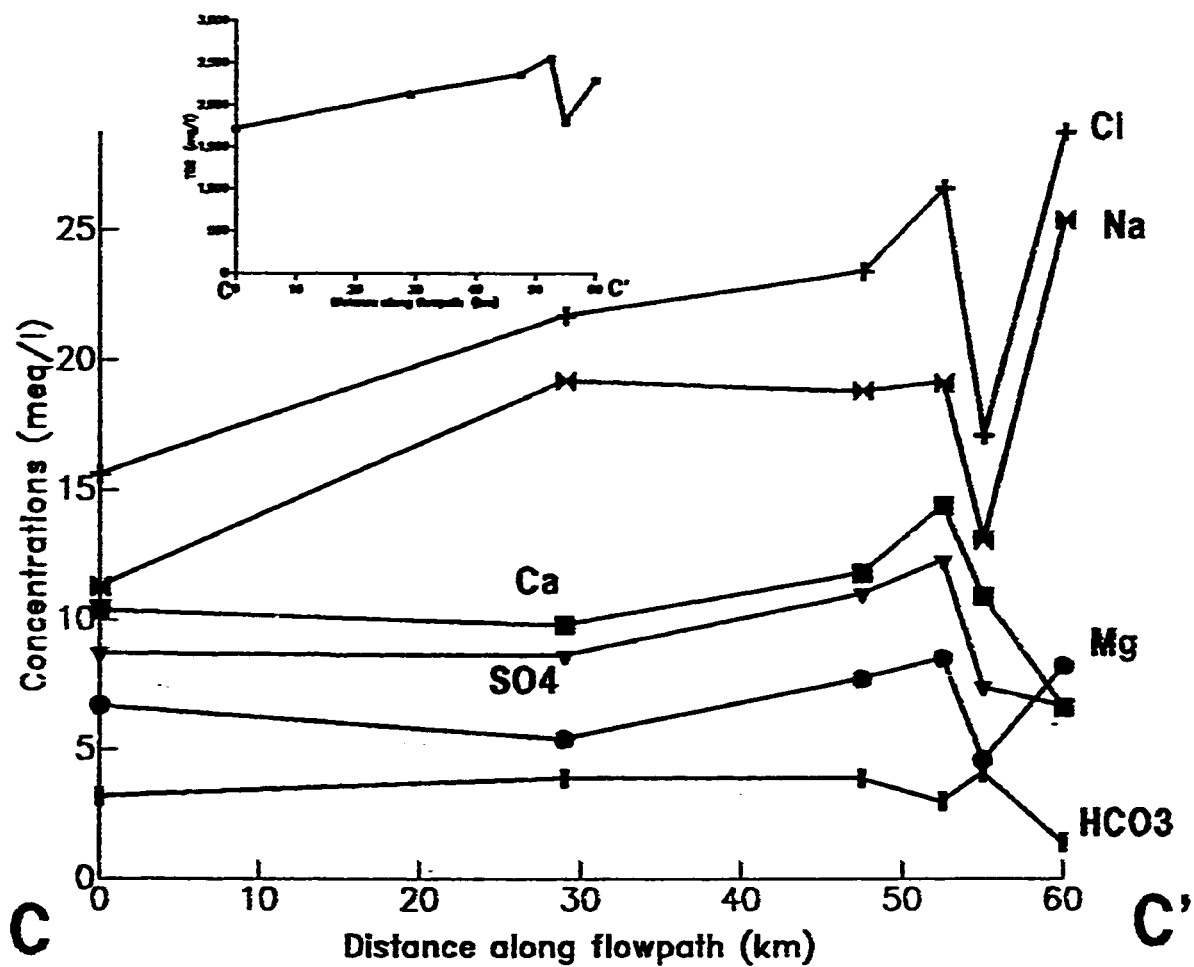


Figure 5.7 Hydrogeochemical profiles along Abqaiq flowpath in Khobar aquifer (see Fig. 1.3 for the location of the profile CC).

**TABLE 5.1 Comparison between Khobar and Umm Er Radhuma Aquifers in Abqaiq Area. (The concentrations are in mg/l).**

<b>Aquifer</b>	<b>Khobar</b>	<b>Khobar</b>	<b>UER</b>	<b>UER</b>	<b>UER</b>	<b>UER</b>
<b>Well</b>	<b>13</b>	<b>113</b>	<b>I</b>	<b>II</b>	<b>III</b>	<b>IV</b>
<b>Depth</b>	<b>76m</b>	<b>107m</b>	<b>219m</b>	<b>338m</b>	<b>233m</b>	<b>329m</b>
<b>TDS</b>	<b>2148</b>	<b>1802</b>	<b>1784</b>	<b>1708</b>	<b>1783</b>	<b>1833</b>
<b>Ca</b>	<b>132</b>	<b>219</b>	<b>205</b>	<b>131</b>	<b>130</b>	<b>143</b>
<b>Mg</b>	<b>100</b>	<b>56</b>	<b>56</b>	<b>71</b>	<b>46</b>	<b>68</b>
<b>Na</b>	<b>583</b>	<b>302</b>	<b>315</b>	<b>314</b>	<b>409</b>	<b>383</b>
<b>Cl</b>	<b>1022</b>	<b>605</b>	<b>589</b>	<b>497</b>	<b>568</b>	<b>515</b>
<b>SO<sub>4</sub></b>	<b>324</b>	<b>354</b>	<b>405</b>	<b>437</b>	<b>398</b>	<b>672</b>
<b>HCO<sub>3</sub></b>	<b>226</b>	<b>254</b>	<b>214</b>	<b>238</b>	<b>232</b>	<b>195</b>

**Well no. Latitude Longitude**

**13 26° 01' 41" 49° 38' 09"**

**113 25° 58' 01" 49° 40' 53"**

**I 25° 52' 43" 49° 14' 44"**

**II 25° 43' 45" 49° 25' 57"**

**III 25° 58' 13" 49° 14' 00"**

**IV 25° 53' 21" 49° 25' 34"**

Job (1978) noticed high relative sulfate concentrations in Umm Er Raduma water samples, while Dincer et al. (1973) based the difference in origin between Umm Er Radhuma and the overlying Eocene aquifers on the high sulfate concentrations. The rise in the bicarbonate concentration is probably due to the biogenic oxidation of methane migrating upward along the same leakage channels. The Stiff plots of wells along the traverse CC' shows how water in the aquifer evolves from a Ca-Na-Cl type water with moderate concentrations of sulfate, at well no. 134, towards a more seawater like concentrations, at well no. 108 (Fig. 5.8).

In the northern part of the study area (around Jubayl), the major ions with the exception of bicarbonate, assume high values and increase sharply seaward. In this part of the study area along traverse DD' there is an absence of geological structures and no evidence of recharge related to the possible aquifer interactions (Fig. 5.9). Also there is a clear absence of an appreciable ion-exchange process. All along the flowpath the water body undergoes a normal hydrogeochemical evolution. In well no. 24 sulfate is the major anion indicating the second stage of Chebotarev's sequence (Chebotarev, 1955). In accordance with the sequence, along the flowpath sulfate ceases to be the predominant anion and is replaced by chloride the major constituent of anions. This fact depicts the existence of the third stage of Chebotarev's sequence. It is clear that the boundary between the two stages lies somewhere around well no. 163. The Stiff diagrams (Fig 5.10) show the hydrogeochemical changes along the traverse DD'. Between well no. 2 and well no. 25 the effect of seawater intrusion is evident. The high sulfate, magnesium, sodium and chloride concentrations as



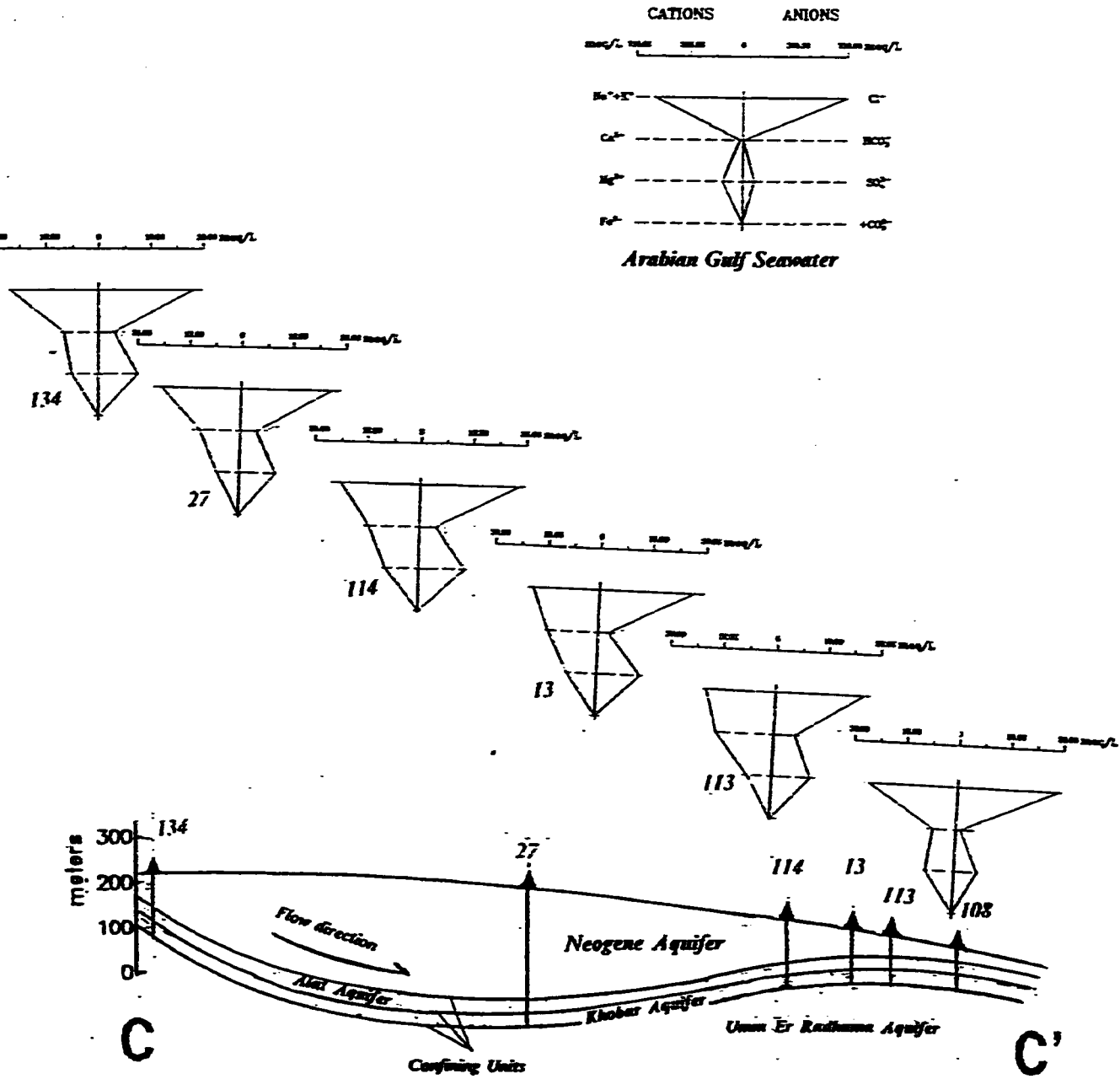


Figure 5.8 Stiff diagrams showing the major ions changes along Abqaiq flowpath in Khobar aquifer.

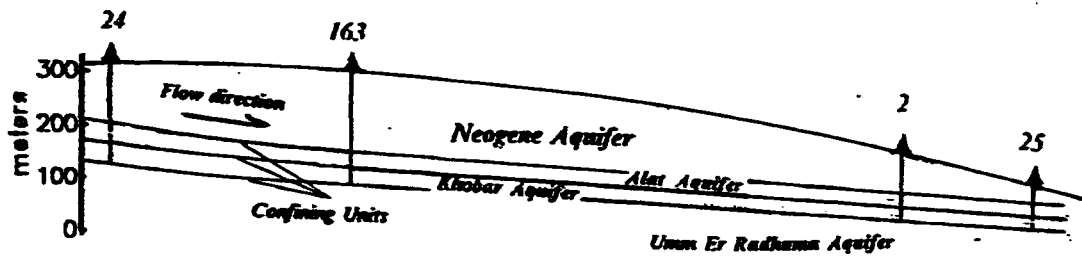
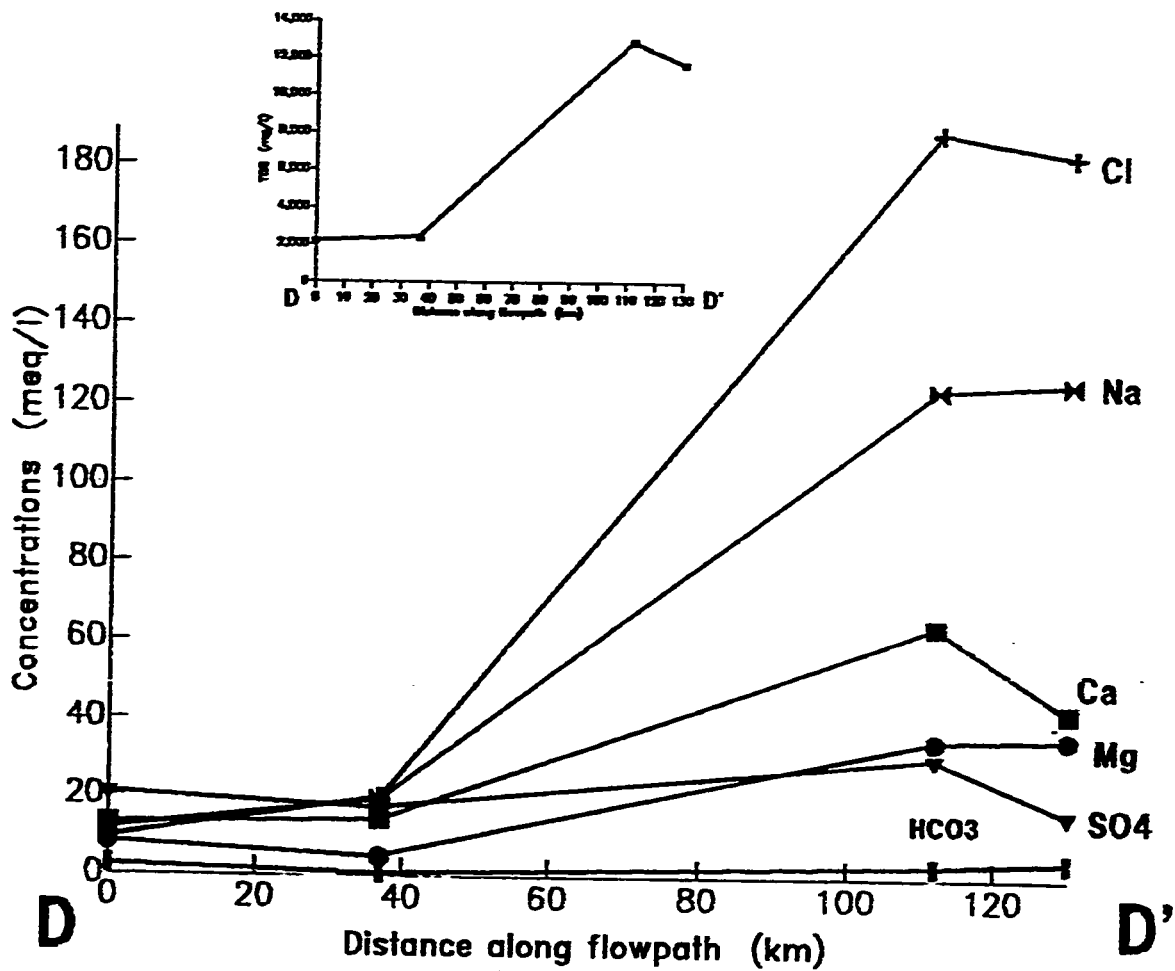


Figure 5.9 Hydrogeochemical profiles along a flowpath at the north of Jubayl in Khobar aquifer (See Fig. 1.3 for the location of the profile DD').

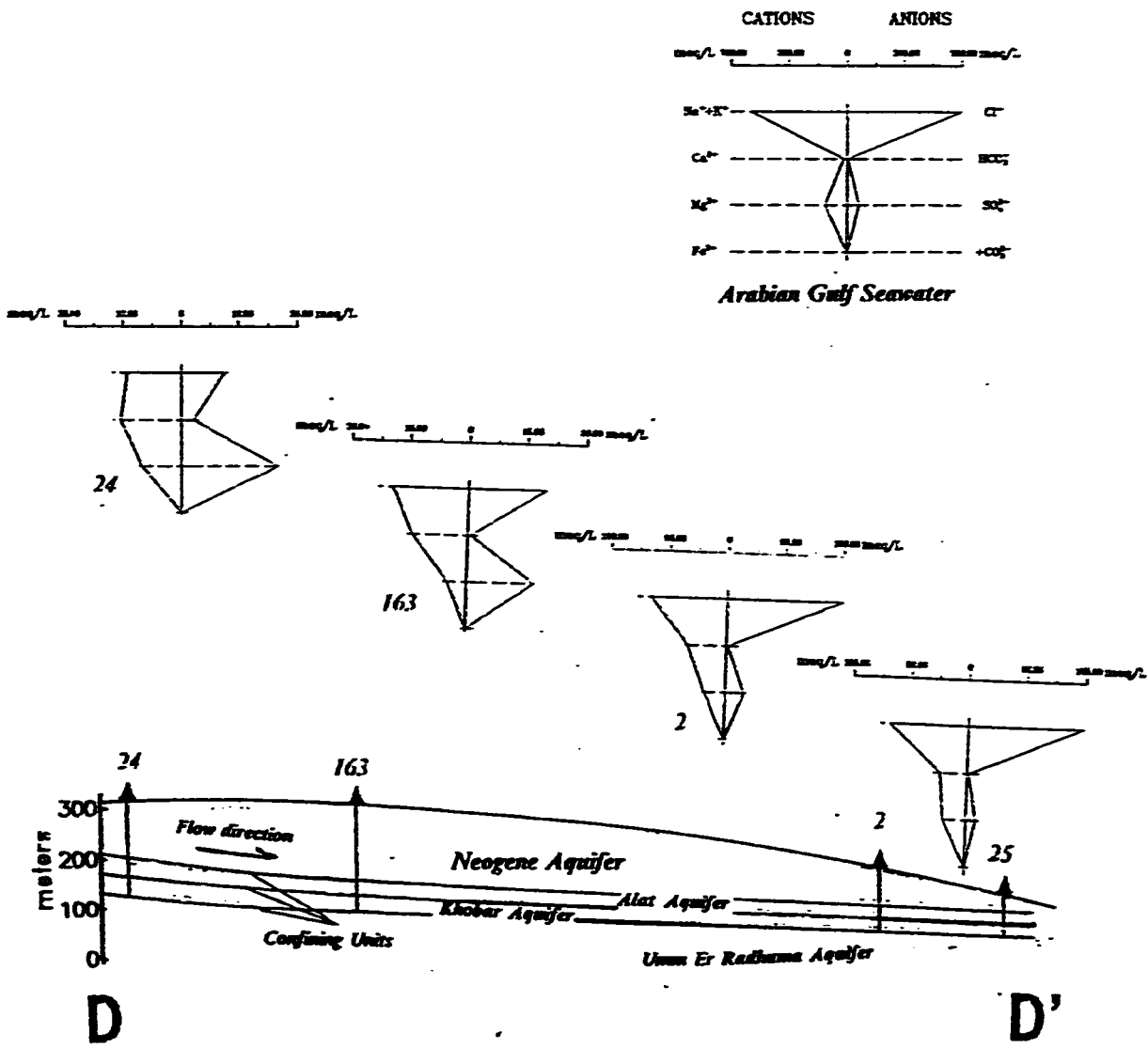


Figure 5.10 Stiff Diagrams showing changes in major ions along a flowpath at the north of Jubayl in Khobar Aquifer.

well as the increased dolomite and calcite saturation indices in this area are strong evidence of the seawater intrusion from the Arabian gulf. Moreover, the seawater mixing model (Fig. 5.5) indicates that if a dilution model consisting of Arabian gulf seawater and the ideal groundwater concentrations A and C were considered, the water samples from wells #25, #2, #156 and #157 would plot around the mixing trend curve. This indicates the presence of a seawater intrusion related to a concentration (chemical) gradient with NE-SW direction. In the north of Jubayl, both the Alat and Khobar aquifers are affected by a seawater intrusion from the Arabian gulf.

## **CHAPTER 6**

### **POTABILITY AND AGRICULTURAL USE**

#### **6.1 Domestic Use and Public Supply**

Recommended limits for concentration of inorganic constituents in drinking water have existed for many years. The most important of these standards are those established by the U.S. Environmental Protection Agency (EPA) in 1975 (Freeze and Cherry, 1979). The Agency lists permissible limits for TDS and major ions such as sulfate and chloride (Table 6.1).

Nitrate is the most common contaminant in groundwater. Its recommended limit is 45 mg/l expressed as  $NO_3$  or 10 mg/l expressed as N. However, due to lack of nitrate data, the nitrate contamination effect is not discussed in this study. Similarly, the effect of minor constituents and the bacteriological aspects are beyond the scope of the study.

The TDS, chloride, and sulfate concentrations of Alat aquifer water exceed more than double the recommended concentration limits for drinking water. Freeze and Cherry (1979) pointed out that in many regions around the world, the groundwater used for drinking-water supply exceeds the recommended limits. Even though Alat aquifer can not be mostly exploited for drinking,

**TABLE 6.1 Recommended Concentration Limits for Human Consumption (after Hem, 1989; USPHS, 1962).**

<b>Constituent</b>	<b>Recommended concentration limit (mg/l)</b>
<b>TDS</b>	<b>500</b>
<b>Chloride</b>	<b>250</b>
<b>Sulfate</b>	<b>250</b>
<b>Nitrate</b>	<b>45</b>

Hem (1989) pointed out that in some countries, water containing more than 1000 mg/l of total dissolved solids has been used.

The TDS in Khobar aquifer is also more than the recommended limit for drinking water. The only area where the TDS is below 1000 mg/l and chloride and sulfate are in acceptable concentration is near Al-Hufuf. Seaward and northward, the TDS, chloride and sulfate increase in concentration. So, the water in these areas has to be either treated before it is domestically used or mixed with desalinated water. However, in most areas, Khobar and Alat aquifers waters are suitable for general municipal use.

The relatively good quality of water in Umm Er Radhuma aquifer places little demand on Alat and Khobar aquifers. However, future improvement in water treatment technology, accompanied with increasing water demand, would place more demand on these aquifers.

## ***6.2 Livestock Consumption***

Water for domestic animals should have quality limitations equivalent to the ones for drinking water (Table 6.1). Most animals, however, can tolerate water having higher total dissolved solids (TDS) than that considered adequate for humans. Hem (1989) mentioned that some cattle in the Western United States are accustomed to highly mineralized water containing as much as 10,000 mg/l TDS. Such water contains mostly sodium and chloride, whereas the sulfate rich waters are less desirable. Hem (1989) recommended an average upper limit of around 5,000 mg/l TDS for livestock consumption.

The upper concentration limit for camel is not included in (Table 6.2). However, it is expected that camels can tolerate drinking water with a very high TDS. In some countries whenever high TDS water is not in hand, camel breeders feed their flocks common salt or a NaCl rich clay to compensate mineral deficiency that could damage the animal health.

Both Alat and Khobar aquifers provide water that is acceptable for camels, sheep, and cattle. As for poultry, these aquifers in the coastal areas contain inadequately high TDS. However, the Alat and Khobar water in some coastal areas such as Dammam, Qatif, Jubayl (Khobar aquifer only), and Ras Tanura (Alat aquifer only) contain about 3500 mg/l and these areas could be good livestock farming sites.



**TABLE 6.2 Recommended TDS Concentration Limits for Livestock consumption (after McKee and Wolf, 1963).**

<b>Stock</b>	<b>Concentration (mg/l)</b>
<b>Poultry</b>	<b>2,860</b>
<b>Horses</b>	<b>6,435</b>
<b>Cattle (diary)</b>	<b>7,150</b>
<b>Cattle (beef)</b>	<b>10,100</b>
<b>Sheep (adult)</b>	<b>12,900</b>

### **6.3 Agricultural Use**

The quality of water is equally important as the quantity of the groundwater supplies that are used for irrigation. Hence, the chemical aspect is an important factor in evaluating the usefulness of a given water body for irrigation. These qualities include the total dissolved solids, the toxic constituents, and the relative proportion of Na, Ca, and Mg.

Boron which could be present in groundwater at neutral pH as  $H_2BO_3^-$  is toxic to certain plants. However, the problem of toxic constituents is beyond the scope of this study due to the lack of relevant data. Hem (1989) pointed out that crops tolerant to boron are also tolerant to high salinity. Table 6.3 indicates the tolerance level of different crops to boron, which is also applicable to salinity (Hem, 1989).

Alat and Khobar aquifers are suitable for irrigating tolerant crop plants, except in the north of Jubayl (Manifa) where the salinity is very high. The tolerant and semi-tolerant plants could grow well in the upgradient parts of the aquifers, namely in the western part of the study area where the TDS is low. As for the sensitive crop plants, the water of the two aquifers must undergo some pre-irrigation treatments.

**TABLE 6.3 Salinity tolerance level of crop plants  
(after U.S Salinity Lab Staff, 1954).**

<b>Sensitive</b>	<b>Semi-tolerant</b>	<b>Tolerant</b>
<b>Lemon</b>	<b>Sweetpotato</b>	<b>Date Palm</b>
<b>Grape</b>	<b>Potato</b>	<b>Palm</b>
<b>Orange</b>	<b>Pumpkin</b>	<b>Carrot</b>
<b>Apricot</b>	<b>Oat</b>	<b>Cabbage</b>
<b>Apple</b>	<b>Corn</b>	<b>Turnip</b>
<b>Cherry</b>	<b>Wheat</b>	<b>Onion</b>
<b>Pear</b>	<b>Barley</b>	<b>Alfalfa</b>
	<b>Tomato</b>	<b>Sugar beat</b>
	<b>Cotton</b>	

The sodium adsorption ratio ( SAR ) is an overall index for the suitability of irrigation water. It can be defined as the tendency of a water to replace adsorbed calcium and magnesium with sodium. It is given by the equation :

$$SAR = \frac{Na^+}{\left\{ \frac{Ca^{2+} + Mg^{2+}}{2} \right\}^{0.5}}$$

An irrigation water having a high proportion of sodium to total cations tends to place sodium ions in the exchange sites on the soil-mineral particles, while water having mostly divalent cations reverses this process.

Clay minerals have high exchange capacity per unit weight and they preferentially adsorb divalent ion because of their high charge. With their exchange sites occupied with calcium and magnesium, the physical properties of the clay-bearing soil is optimal. In contrast, when their exchange sites are saturated with sodium, the soil tends to become deflocculated and impermeable to water.

Fetter (1988) subdivided irrigation water into different classes according to their SAR values (Table 6.4).

**TABLE 6.4 Water classes based on SAR**  
**(after Fetter, 1988).**

<b>Hazard</b>	<b>SAR</b>
<b>Low</b>	<b>2 - 10</b>
<b>Medium</b>	<b>7 - 18</b>
<b>High</b>	<b>11 - 26</b>
<b>Very high</b>	<b>&gt; 26</b>

The SAR values of Alat and Khobar aquifers are calculated in this study and the results are shown on Figures 6.1 and 6.2. The sodium hazard level of Alat aquifer is generally medium to high. The only area with the objectionable very high SAR values coincides with the previously mentioned high TDS area to the north of Jubayl (Fig 3.7).

Khobar aquifer has SAR values ranging from low to very high. The low SAR values are situated in the extreme south of the study area, Al Jafurah. For obvious reasons in Al Jafurah, the SAR increases seaward. Near Al Hufuf, the SAR ranges from 6 to 12, indicating low to medium hazard. A relatively low sodium hazard is evident (Fig 6.2) in Qatif. However, the SAR increases sharply in Ras Tanura to a value of 12 but drops to about 8 around Jubayl. North of Jubayl (Manifa), where the SAR attains its maximum value of more than 26, the aquifer becomes unsuitable for irrigation purposes. For irrigation, regarding SAR and TDS, the two aquifers could be utilized within a treatable range. The U.S. Salinity Laboratory Staff (1954) diagram is used in this study to classify the Alat and Khobar waters for the irrigation use (Fig. 6.3, 6.4). Appendix 4 includes the classification of individual water samples. According to these diagrams, most of the Alat water falls in the medium to high sodium hazard and in the very high salinity hazard, whereas the Khobar water ranges from low to very high in terms of sodium hazard and from high to very high in terms of salinity hazard.

The electrical conductivity of a water body is generally a parameter which is related to the dissolved solids and more precisely to the dissolved major ions.

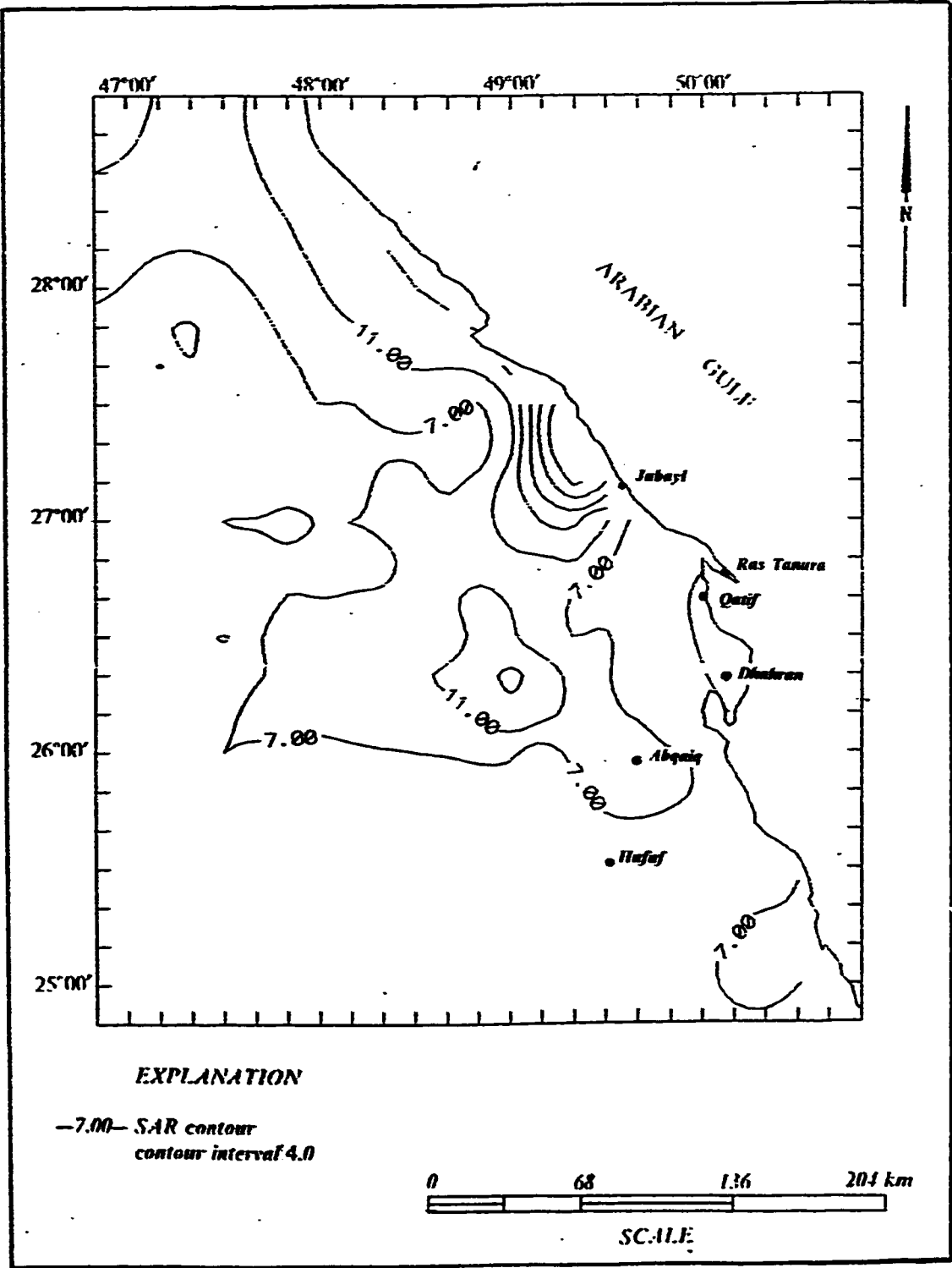


Figure 6.1 Sodium adsorption ratio map of the Alat aquifer.

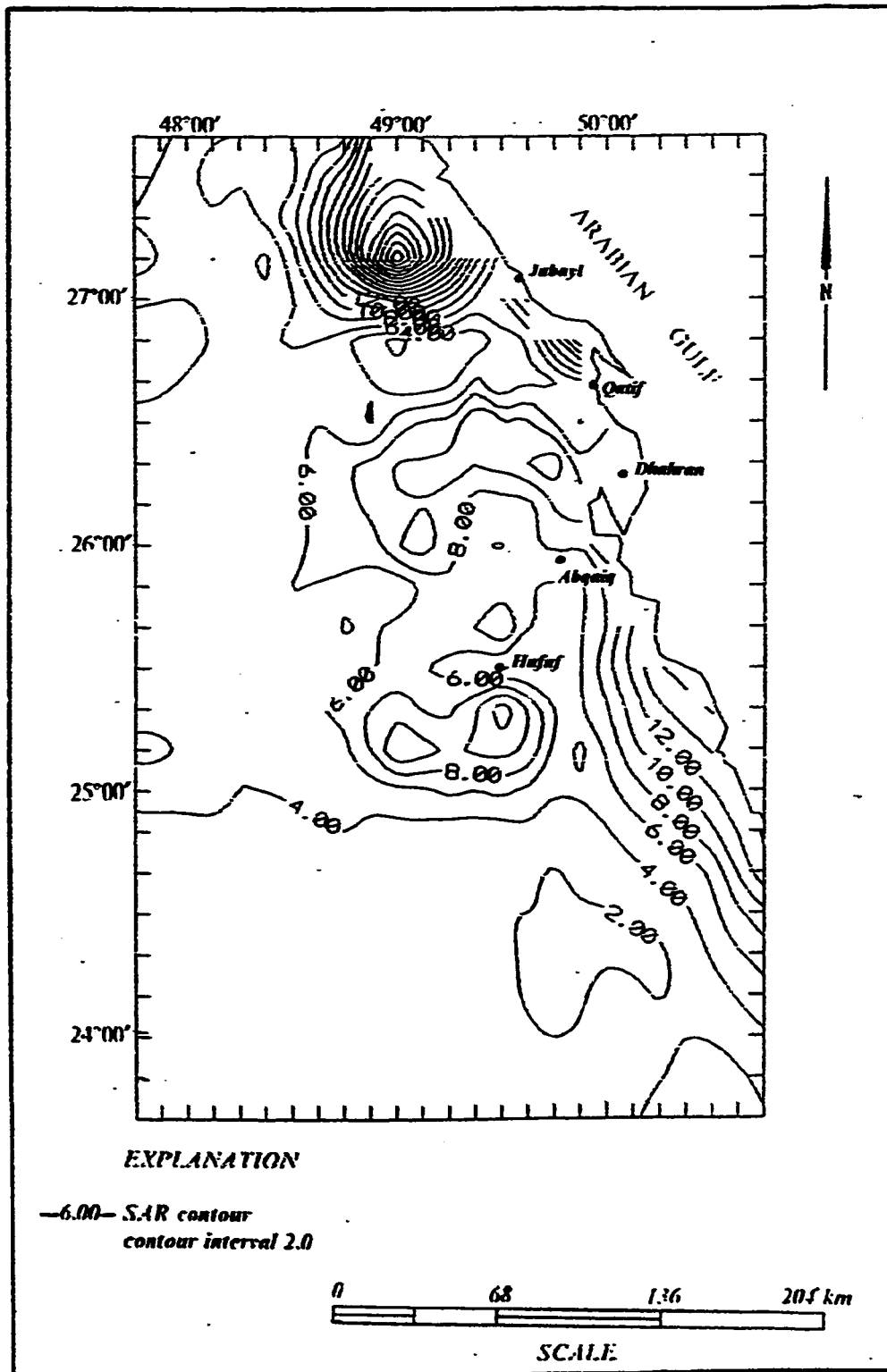
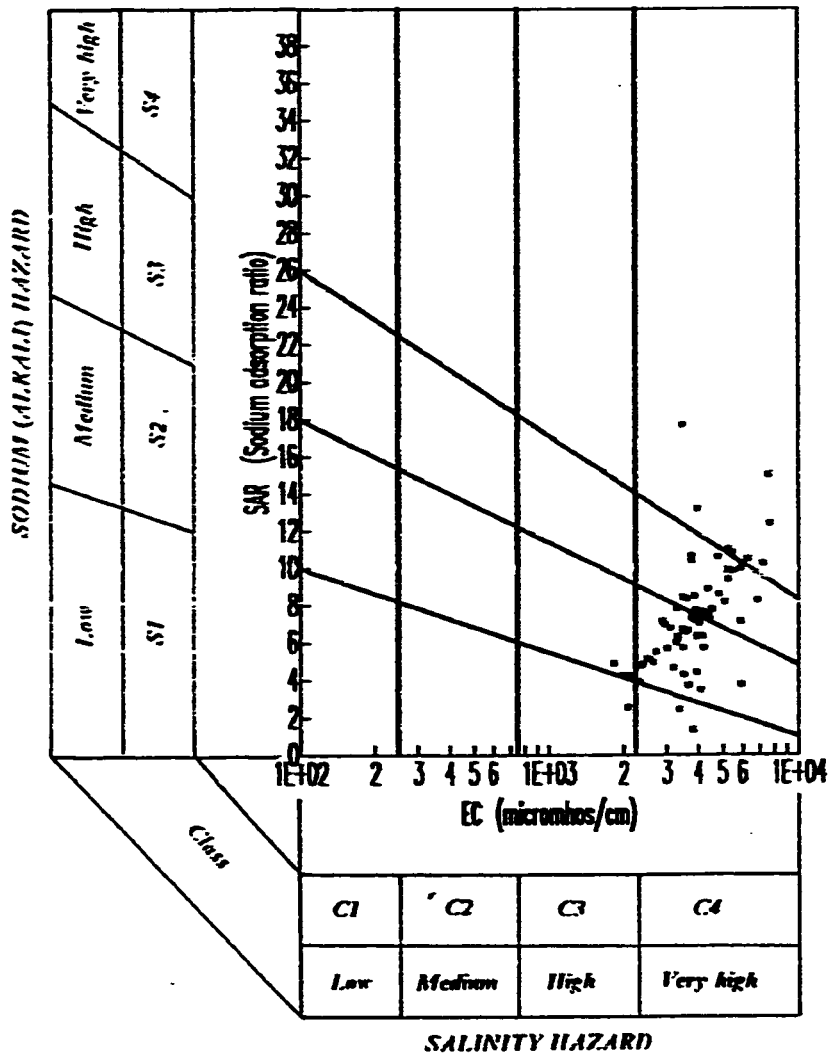
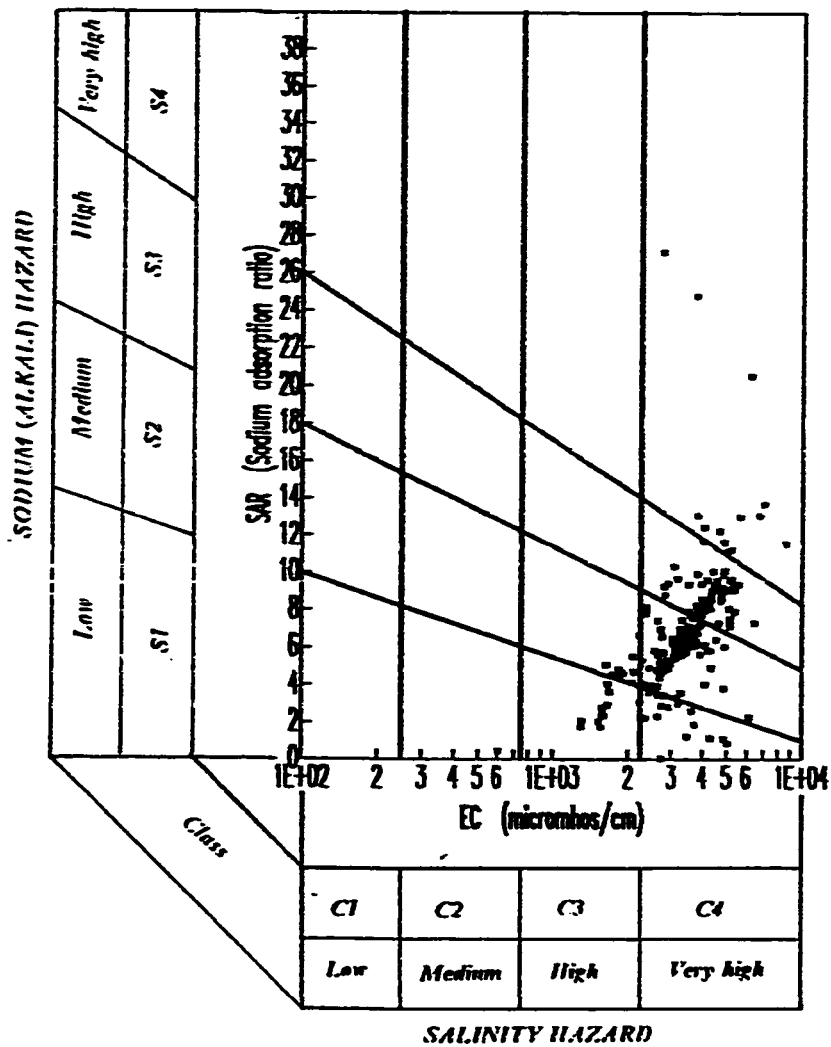


Figure 6.2 Sodium adsorption ratio map of the Khobar aquifer.





**Figure 6.3** Diagram showing irrigation water classification of Alat aquifer (After U.S. Salinity Lab Saff, 1954).



**Figure 6.4** Diagram showing irrigation water classification of Khobar aquifer (After U.S. Salinity Lab Saff, 1954).

The measurement of electrical conductivity (EC) is very practical and inexpensive. A diagram is devised for quick and inexpensive determination of the SAR values for the Khobar aquifer waters and its evaluation for irrigational purpose.

The diagram is a contour plot of SAR as a function of EC versus TDS (Fig. 6.5). It can be adequately used when sodium is more abundant than calcium and magnesium, which is the case in Khobar aquifer except for Al Hufuf area, where calcium increases sharply. In order to use this diagram, it is necessary to measure the EC and then get the corresponding TDS value from the EC-TDS relationship shown in Fig. 3.20. Then, the SAR value of the water body could be estimated by using the diagram (Fig. 6.5).

Calcium is not a direct hazard in irrigation water, but the use of water oversaturated with calcite could precipitate calcite and form calcrete (Falciai, 1981). However, the effect of other cations present in the system controls the precipitation.

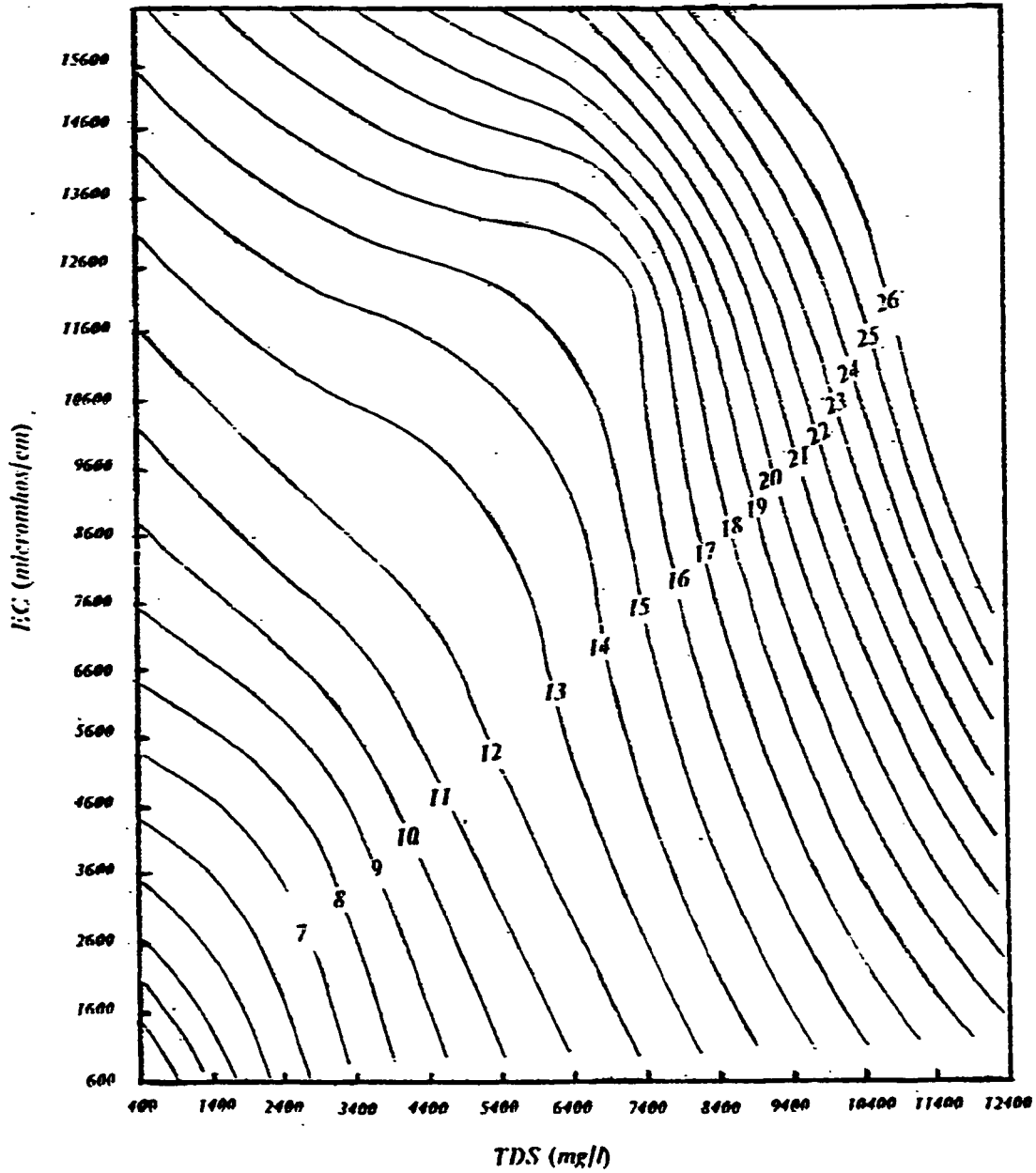


**Figure 6.5** Diagram for quantitative estimation of SAR from EC and TDS values of the Khobar aquifer.

#### **6.4 Industrial Use**

For industrial use, the quality of water ranges widely and almost every industrial application has its own standards. The chemical quality, for some uses, is not critical and almost any water could be used. In other cases, very low TDS is required for processes such as the manufacture of high-grade paper, pharmaceuticals and cosmetics. The water quality requirements for various industries are summarized in Table 6.5 (Hem, 1989).

It is a common practice to treat water before using it for most industrial purposes. Hence, water from Alat and Khobar aquifers, at least for soft drinks, canned fruits, petroleum products and hydraulic cement industries, needs some treatment. However, the type and the degree of treatment should strictly depend on the desired objective.

**TABLE 6.5 Recommended concentration limits for some selected industries (after Hem, 1989).**

<b>Constituent</b>	<b>Soft drinks mg/l</b>	<b>Canned fruits mg/l</b>	<b>Petroleum products mg/l</b>	<b>Hydraulic cement mg/l</b>
<b>Calcium</b>	<b>100</b>	<b>—</b>	<b>75</b>	<b>—</b>
<b>Magnesium</b>	<b>—</b>	<b>—</b>	<b>30</b>	<b>—</b>
<b>Chloride</b>	<b>500</b>	<b>250</b>	<b>300</b>	<b>250</b>
<b>Sulfate</b>	<b>500</b>	<b>250</b>	<b>—</b>	<b>250</b>
<b>TDS</b>	<b>—</b>	<b>500</b>	<b>1000</b>	<b>600</b>

## **CHAPTER 7**

### **CONCLUSIONS**

The following conclusions have been drawn from the hydrogeochemical studies of the Alat and Khobar aquifers.

1 - In the Alat aquifer, three hydrogeochemical facies namely Na-Cl, Na-Ca-Cl, Na-Ca-Cl-  $SO_4$  are present. The Na-Ca-Cl facies and the Na-Cl facies, which are located along the coastal belt, are the two major water types.

2 - Four hydrogeochemical facies, which are Na-Cl, Na-Ca-Cl, Na-Cl-Ca- $SO_4$  and Ca- $SO_4$ , are identified in Khobar aquifer. The predominant water type is the Na-Cl facies.

3 - The TDS in Alat aquifer varies from 2000 mg/l to more than 9000 mg/l The lowest TDS values being located in the southern part of the study area, in Al Hufuf and its surrounding areas. A TDS-EC relationship :

$$\text{TDS} = 0.64 \text{ EC}$$

is established for estimating the TDS from the EC measurements.

4 - The TDS in Khobar aquifer varies from less than 1000 mg/l to more than 7000 mg/l. The lowest TDS values are found in the southern part of the study area, while the TDS increases northward. The relationship for TDS estimation in Khobar aquifer is:

$$\text{TDS} = 0.65 \text{ EC.}$$

5 - Alat aquifer is generally oversaturated with respect to calcite and dolomite, and it is undersaturated with respect to gypsum. However, the degree of gypsum

undersaturation decreases in the northeast direction.

6 - Khobar aquifer is oversaturated with respect to calcite and dolomite, and undersaturated with respect to gypsum. However, the degree of oversaturation with respect to calcite and dolomite is more higher than in Alat aquifer. The undersaturation with respect to gypsum, in both aquifers, is generally similar.

7 - In the north of Jubayl, a seawater intrusion is evident in both aquifers. It is more likely caused by chemical gradient rather than hydraulic gradient.

8 - In both aquifers, there is no conspicuous hydrogeochemical process in the area stretching from Ras Tanura in the north to Dhahran in the south. Although, both aquifers are semi-confined near Dhahran, there is no evident recharge. This is supported by the scarcity of the rainfall in the region.

9 - In the west of Abqaiq, in Alat aquifer, anaerobic bacteria reduces sulfate with the concomitant oxidation of organic matter. This is displayed by the decrease in sulfate and the increase in the bicarbonate concentrations (Fig. 5.2). Since this area falls in the Ghawar structure, the possibility of recharge water from the prolific Umm Er Radhuma aquifer could not be ruled out. Along the Abqaiq flowpath, there is a dilution effect in Khobar aquifer. Over the Abqaiq structure, the Khobar aquifer receives water, through upward leakage, from the underlying Umm Er Radhuma aquifer.

10 - In Alat aquifer, near Abqaiq, there is an indication of a cation exchange process. Here, sodium is being exchanged by calcium. Subsurface shaly layers with limited thickness and lateral extent are the probable cause of this process . Such process is absent in the area in the Khobar aquifer.

11 - Sulfate concentration in both aquifers seems to be controlled by gypsum



dissolution in the southern part of the study area. In the north, particularly north of Jubayl, the high sulfate concentration is mainly due to seawater intrusion. In the central part of the study area, sulfate has a mixed origin with contribution from seawater and gypsum dissolution.

12 - An evolutionary pattern from sulfate rich water to chloride predominant water is evident in the northern part of the study area. However, in the southern part, the evolutionary sequence is superimposed by the sulfate reduction and biogenic carbon dioxide production.

13 - The TDS in both aquifers is above the recommended limit for human consumption. So the waters are not suitable for domestic purposes.

14 - For animal breeding farms both aquifers do not pose any problem. Moreover, water in the southern part of the study area is good for use of livestock breeding farms.

15 - The highly saline nature of the waters in these aquifers limits their irrigational use. Plants such as date palm, palm, onion, carrot, cabbage, turnip, alfalfa and sugar beats could grow in most parts of the study area.

16 - For industrial purposes, the use heavily depends on the targeted manufacture-material. The waters of Alat and Khobar aquifers are not suitable for processing food stuffs, but they could be used in heavy industries.

## **REFERENCES**

- 1. Abderrahman, W. A., 1990, Effects of Groundwater Use on the Chemistry of Spring Water in Al-Hassa, The First Saudi Symposium on Earth Sciences, Special Issue, Scientific Publication Center, King Abdulaziz University, Jeddah, pp. 259-264.**
- 2. Al-Sayyari, S. S., and Zottle, J. G., 1978, Quaternary Period in Saudi Arabia, vol. 2, Springer-Verlag, Wein, New York.**
- 3. Al-Tamimi, M. H., 1985, Stratigraphical and microfacies analyses of Early Paleogene succession in Dammam dome, Eastern Saudi Arabia: M.Sc. thesis, King Fahd University of Petroleum and Minerals, Dhahran, Saudi Arabia, 92 p.**
- 4. Bazuhair, A. A., M. T. Hussein and M. S. Hamza, 1990, Comparative Hydrochemical Study of Water Springs in Saudi Arabia, Water Resource Development, vol. 6, No. 2, pp: 143-150.**
- 5. Bureau de Recherches Geologiques et Mineres (BRGM), 1977, Al-Hassa Development Project: Groundwater Resources Study and Management Program, Unpublished Report to Ministry of Agriculture and Water, Riyadh, Saudi Arabia.**
- 6. Brinkley, S.R., 1947, Calculation of the Equilibrium Composition of Systems of Many Constituents, J. Chem. Physics. 15, pp: 107-110.**

7. Cagatay, M. N., 1990, Palygorskite in the Eocene Rocks of the Dammam Dome, Saudi Arabia, *Clays and Clay minerals*, vol. 38, No. 3, pp: 299-307.
8. Cavalier, C, 1975, *Le Tertiaire du Qatar en affleurement : Lexique Strat.Int.* 3, pp: 89-120.
9. Department of Water Resources Development, 1984, *Water Quality Data for the Period 1939-1970. Areas 4,5,6,7 & 9; Division of Water Research and Studies, DWRD, Ministry of Agriculture and Water, Pub. No.2, v.2, pp. 5-79.*
10. Doornkamp, J.C., Brunnsden, D., and Jones, D. K. C., 1980, *Geology, Geomorphology and Pedology of Bahrain : Geo. Abstracts Ltd., Norwich, United Kingdom, 15-85.*
11. Drever, J. I., 1982, *The Geochemistry of Natural Waters*, Prentice-Hall Inc., Englewood Cliffs, New Jersey, 388 p.
12. Edgell, H.S, 1990, *Geological Framework of Saudi Arabia Groundwater Resources, The First Saudi Symposium on Earth Sciences, special issue, Scientific Pub. Center, King Abdulaziz University, Jeddah, pp. 278-285.*
13. Falciai, M., 1981, *Appunti di Idraulica Agraria, Cooperativa Culturale Studio e Lavoro, Firenze, 261 p.*
14. Feldman, H. F., Simons, W. H. and Bienstock, D., 1969, *Calculating*

**Equilibrium Compositions of Multicomponent, Multiphase, Chemical Reacting Systems, U.S. Bur. Mines Rep. Invest. 7257, 22 p.**

- 15. Fetter, C. W., 1988, Applied Hydrogeology, second edition, Merrill Publishing Company, Columbus, Ohio, 592 p.**
- 16. Freeze, R. A. and Cherry, J. A., 1979, Groundwater, Prentice-Hall, Englewood Cliffs, New Jersey, 604 p.**
- 17. Groundwater Development Consultants (GDC), 1980, Umm Er Radhuma study: Bahrain Assignment, Demeter House, Report Ministry of Agriculture and Water, Riyadh, Kingdom of Saudi Arabia.**
- 18. Hem, John D., 1989, Study and Interpretation of Chemical Characteristics of Natural Water, third edition, U.S. Geological Survey Water-Supply Paper 2255, Washington D.C., 264 p.**
- 19. ITALCONSULT, 1969, Water and Agricultural Development Studies for Area IV., Eastern Province, Saudi Arabia, Unpublished Report to Ministry of Agriculture and Water, Riyadh, Kingdom of Saudi Arabia.**
- 20. Job, C., 1978, Hydrochemical Investigations in the Areas of Al Qatif and Al Hassa, Quaternary Period in Saudi Arabia, vol.I, Springer-Verlag, Wien, New York, pp. 93-119.**
- 21. Kandiner, H. J. and Brinkley, S. R., 1950, Calculation of Complex Equilibrium Relations, Ind. Eng. Chem. 42, pp: 850-855.**

22. Kaprov, I. K. and Kaz'min, L. A., 1972, Calculation of Geochemical Equilibria in Heterogeneous Multicomponent Systems, *Geochem. Intl.* 9, pp : 252-265.
23. Kharaka, Y. K and Barnes, I., 1973, SOLMNEQ : Solution-mineral equilibrium computations, NTIS Tech. Rept. PB214-899, Springfield, VA., 82 p.
24. McKee, J. E. and Wolf, H. W., 1963, Water Quality Criteria, California State Water Quality Control Board Publication 3-A, 548 p.
25. Naimi, A.I, 1965, The Groundwater of North Eastern Saudi Arabia, Fifth Arab petrol. Congress Cairo, Egypt.
26. Nordstrom, D.K, et al, 1979, A Comparison of Computerized Chemical Models for Equilibrium Calculations in Aqueous Systems, Chapter 38, pp. 857-894, *Chemical Modeling in Aqueous Systems*, E.A. Jenne, editor, American Chemical Society.
27. Pagenkopf, G. K., 1978, Introduction to natural water chemistry, Environmental science and technology series, volume 3., Marcel Dekker Inc, New York, pp. 55-60.
28. Piper, A.M, 1944, A Graphical Procedure in Geochemical Interpretation for Water Analyses, *Trans American Geophysical Union*, v.25, pp.914-923.
29. Plummer, L.N, B.F. Jones and A.H. Truesdell, 1976 (revised 1978,

- 1984) WATEQF, a FORTRAN IV version of WATEQ, A Computer Program for Calculating Chemical Equilibria of Natural Waters. U.S Geological Survey Water Resources Investigations paper 76-13.
30. Powers, R. W., Ramirez, L. F., Redmond, C. D. and Elberg, E. L., 1966, Geology of Arabian Peninsula, U.S. Geological Survey, Professional Paper 560-D, 1-147, New York.
31. Rasheeduddin, M., 1988, Numerical Modeling of Alat, Khobar and Umm Er Radhuma Aquifer Systems in Eastern Saudi Arabia, M.S. Thesis Dhahran, Saudi Arabia.
32. Rightmire, C. T., Pearson, F. J., Jr., Back, William, Rye, R.O., and Hanshaw, B. B., 1974, Distribution of sulphur isotopes of sulphates in groundwaters from the principal artesian aquifer of Florida and the Edwards aquifer of Texas, U.S.A., in Isotope techniques in groundwater hydrology, 1974, v. 2: Vienna, Austria, International Atomic Energy Agency, p. 191-207.
33. Rollins, L., 1990, Users Guide to DATAGEN/PCWATEQ, A Software Manual, ShadoWare, 215 Cedar Lane Woodland, Ca. 95695
34. Sen, Z and A. Al-Dakheel, 1986, Hydrochemical Facies Evaluation in Umm Er Radhuma, Eastern Saudi Arabia, Groundwater, Vol. 24, No. 5, pp: 626-635.
35. Sprinkle, Craig L., 1989, Geochemistry of the Floridan Aquifer

- System in Florida and in Parts of Georgia, South Carolina and Atlanta, U.S.G.S. Professional Paper 1403-I, Washington D.C, 105 p.
36. Tleel, J. W., 1973, Surface Geology of Dammam Dome, Eastern Province, Sudi Arabia, M.S. Thesis, Texas Christian University.
  37. Truesdell, A.H. and B.F. Jones, 1974, WATEQ, A Computer Program for Calculating Chemical Equilibria of Natural Waters. U.S. Geological Survey Journal of Research, v. 2, No. 2, pp. 233-248.
  38. U.S. Federal Water Pollution Control Administration, 1968, Report of the Committee on Water-Quality Criteria, Washington D.C., 234 p.
  39. White, W. B., Johnson, S. M. and Dantzig, G. B., 1958, Chemical Equilibrium in Complex Mixtures, J. Chem. Phys. 28, PP : 751-755.
  40. Wigley, T. M. L., 1977, WATSPEC: A Computer Program for Determining the Equilibrium Speciation of Aqueous Solutions, Brit. Geomorph. Res. Group Tech. Bull. 20, 48 p.
  41. Willis, R. P., 1976, Geology of the Arabian Peninsula: Bahrain: U.S.Geol. Surv. Prof. Pap. 560-E, pp: 1-4.
  42. Wolery, T. J., 1978, Some chemical aspects of hydrothermal processes at mid-oceanic ridges - a theoretical study. I. Basalt - seawater reaction and chemical cycling between the oceanic crust and the oceans. II. Calculations of chemical equilibrium between aqueous solutions and minerals, Ph.D. dissertation, Northwestern Univ.,

Evanston, IL.

43. Yazicigil, H., R.I. Al-Layla and R.L. DeJong, 1986, Numerical Modeling of the Dammam aquifer in Eastern Saudi Arabia. The Arabian Journal for Science and Engineering, vol. 11, pp.349-362.



***APPENDIX 1***  
***HYDROGEOCHEMICAL DATA***  
***ALAT AQUIFER***

Appendix 1. Hydrogeochemical Data of the Alat Aquifer.

Sample No.	TDS mg/l	Ca meq/l	Mg meq/l	Na + K meq/l	Cl meq/l	SO <sub>4</sub> meq/l	HCO <sub>3</sub> meq/l
1	3784	29.5	12.8	17.4	20.8	37.5	1.6
2	2545	8.8	6.3	36.3	23.8	12.9	3.7
3	3076	9.7	6.9	30.5	25.6	20.6	3.3
4	3777	19.6	11.7	28.2	24.0	32.7	2.8
5	2486	10.4	5.6	24.0	25.0	11.5	3.6
6	2415	9.6	5.2	29.0	23.0	9.4	3.7
7	2313	9.0	5.6	22.5	22.9	10.6	3.7
8	4399	20.9	15.1	35.0	36.1	32.4	2.6
9	1637	8.9	4.2	13.0	15.0	3.4	7.7
10	1849	7.7	4.2	17.4	18.5	7.6	3.7
11	1511	8.0	4.4	11.9	15.3	5.5	3.5
12	1529	8.0	4.5	12.1	16.2	5.7	3.5
13	2410	11.1	1.0	25.5	19.4	16.6	1.7
14	4603	31.9	10.5	47.2	15.6	43.4	1.9
15	4021	14.6	13.4	39.2	46.5	18.8	1.8
16	2337	15.1	8.4	12.8	11.4	22.6	2.4
17	2531	14.6	9.4	15.3	11.6	25.3	2.4
18	2508	10.1	8.2	23.4	29.0	10.4	2.3
19	1978	8.5	5.4	17.8	18.2	10.7	2.8
20	2685	14.8	9.4	19.8	26.2	14.6	3.0
21	3495	13.3	8.7	35.8	40.4	14.9	2.4
22	2210	3.4	2.1	29.3	22.1	10.9	1.9
23	1592	8.2	4.1	12.8	14.2	7.3	3.7
24	1341	6.3	4.7	10.0	10.4	7.3	3.4
25	1258	6.2	4.0	9.6	10.8	5.1	3.6
26	1166	4.8	3.5	10.0	10.0	6.9	1.7
27	15769	34.3	33.7	197.9	210.0	52.0	2.8
28	7357	35.7	18.6	68.3	85.9	34.0	2.4
29	2160	10.5	7.0	17.2	19.5	12.2	3.1
30	2295	9.4	11.9	21.4	22.9	9.7	2.9
31	2229	10.3	1.8	20.7	23.6	10.5	2.8
32	1494	8.0	5.7	10.3	12.4	8.9	2.6
33	2098	10.4	6.3	17.3	21.0	9.5	3.5
34	2872	13.7	9.5	24.6	33.5	11.1	3.2
35	1736	8.2	5.5	14.4	17.6	7.3	3.2
36	2577	11.9	8.3	22.4	29.6	9.7	3.4
37	3345	13.6	8.9	33.1	40.1	12.3	3.1
38	3563	15.4	9.6	34.7	45.1	11.4	3.2
39	1690	8.4	5.5	13.0	17.3	7.3	3.1
40	2655	12.0	7.9	24.1	31.3	9.3	3.4

Appendix 1. Hydrogeochemical Data of the Alat Aquifer.

Sample No.	TDS mg/l	Ca meq/l	Mg meq/l	Na + K meq/l	Cl meq/l	SO <sub>4</sub> meq/l	HCO <sub>3</sub> meq/l
41	2834	13.0	9.1	25.1	33.4	10.6	3.2
42	2130	10.0	6.7	18.3	23.7	8.0	3.3
43	2538	11.5	7.6	22.9	29.0	9.8	3.2
44	2918	13.6	8.9	26.2	35.2	10.5	3.2
45	2480	11.5	7.4	22.2	28.5	9.4	3.1
46	2810	15.5	4.2	27.8	36.4	10.6	0.1
47	2736	13.2	7.6	24.4	31.5	10.6	3.2
48	3379	15.0	8.9	32.4	41.3	11.9	3.1
49	4904	20.6	12.3	50.2	66.9	13.2	3.0
50	2332	11.1	7.0	20.0	26.3	8.7	3.2
51	2107	8.8	4.8	20.4	22.0	8.5	3.5
52	2622	17.6	10.9	13.3	16.8	22.4	2.7
53	4874	14.4	11.9	54.4	58.5	18.6	3.7
54	3368	14.3	7.2	36.1	35.9	14.6	3.0
55	2523	13.0	7.8	20.5	25.6	13.4	2.3
56	25034	77.4	44.3	309.4	390.0	38.5	2.6
57	2438	12.9	22.2	5.7	18.6	18.5	3.7
58	2035	10.9	8.4	14.5	22.4	8.8	2.6
59	2247	12.9	7.6	13.7	7.0	24.5	2.6
60	1925	9.7	5.8	15.8	17.9	10.0	2.9
61	2232	10.8	6.7	19.9	24.1	9.5	2.7
62	3770	16.9	9.5	36.1	46.8	13.4	3.0
63	3251	15.7	8.9	28.7	37.4	13.6	3.0
64	3108	14.9	8.9	29.6	37.2	10.9	2.9
65	3855	17.2	9.7	37.5	47.8	13.6	2.98
66	2657	10.9	6.7	18.8	22.1	20.0	2.95
67	2129	10.6	7.0	18.3	21.3	9.6	3.2
68	2234	11.5	7.1	17.4	20.4	12.3	3.3
69	2419	11.4	6.0	21.7	25.2	10.4	3.7
70	2431	11.9	5.9	21.9	26.0	9.6	3.8
71	2524	12.8	7.8	20.3	24.1	13.5	3.3
72	2600	13.9	8.9	21.4	29.6	10.2	2.95
73	2534	12.1	7.1	22.3	27.3	10.7	3.5
74	1887	9.0	5.5	18.7	17.9	8.5	2.7
75	1330	9.0	5.4	6.9	8.0	10.3	2.4

***APPENDIX 2***  
***HYDROGEOCHEMICAL DATA***  
***KHOBAR AQUIFER***

Appendix 2. Hydrogeochemical Data of the Khobar Aquifer.

Sample No.	TDS mg/l	Ca meq/l	Mg meq/l	Na + K meq/l	Cl meq/l	SO <sub>4</sub> meq/l	HCO <sub>3</sub> meq/l
1	3454	14.4	9.2	31.6	24.0	27.8	3.3
2	12872	63.6	34.8	123.7	188.7	30.3	3.0
3	2228	11.4	6.5	18.6	22.5	11.2	2.6
4	2078	10.8	5.9	16.9	20.1	10.1	3.3
5	1759	9.2	5.4	13.9	16.1	9.6	2.6
6	1787	9.5	5.4	13.9	16.2	9.8	2.7
7	2467	11.2	9.5	20.3	26.2	12.9	1.8
8	2734	14.5	9.7	20.1	23.6	18.7	2.1
9	852	5.4	3.2	4.3	4.2	5.7	3.0
10	1019	6.9	4.4	4.1	4.0	8.3	3.1
11	2789	15.4	9.9	20.7	28.9	13.5	3.5
12	1575	8.9	6.5	10.0	13.8	8.8	2.8
13	2549	14.4	8.5	19.1	26.6	12.3	3.0
14	2457	11.7	6.6	24.9	30.9	6.9	2.3
15	2000	5.8	3.7	22.5	20.2	9.4	2.5
16	1080	5.8	4.0	6.5	6.9	6.1	3.6
17	2223	11.3	7.7	17.5	23.9	9.2	3.4
18	2220	11.4	7.7	17.6	23.9	9.6	3.0
19	2160	10.1	4.8	20.3	23.7	10.1	1.7
20	2197	10.4	7.0	18.0	23.0	11.3	1.9
21	2829	11.9	7.5	27.2	31.4	11.8	3.2
22	2012	10.5	6.6	16.1	19.7	10.6	3.3
23	3343	13.9	9.2	32.6	40.1	12.9	2.7
24	2133	13.0	8.4	11.6	9.4	20.9	2.7
25	11689	42.3	35.5	125.6	182.9	16.2	4.2
26	1748	10.0	5.9	12.3	15.9	9.5	2.8
27	2130	9.8	5.4	19.2	21.7	8.6	3.9
28	995	6.5	4.2	4.7	5.8	6.8	2.8
29	1615	7.9	7.4	11.0	13.8	10.2	2.2
30	5621	22.2	18.3	51.9	56.6	33.1	2.7
31	2156	10.6	6.3	19.4	22.1	9.5	3.0
32	2025	10.7	5.8	16.7	19.8	10.2	2.7
33	2064	10.7	6.1	16.5	20.4	10.0	3.2
34	2061	10.8	6.3	16.3	20.2	10.5	2.9
35	1982	9.8	6.0	17.5	20.3	9.4	2.3
36	2348	10.5	6.5	22.5	27.6	10.0	1.3
37	3207	14.5	8.4	30.4	35.8	13.9	2.9
38	2474	12.4	6.9	21.0	26.3	11.3	3.0
39	3080	14.3	8.2	28.4	36.4	12.0	2.9
40	3487	16.3	9.4	32.3	40.8	13.9	3.1

Appendix 2. Hydrogeochemical Data of the Khobar Aquifer.

Sample No.	TDS mg/l	Ca meq/l	Mg meq/l	Na + K meq/l	Cl meq/l	SO <sub>4</sub> meq/l	HCO <sub>3</sub> meq/l
41	3083	14.2	8.4	30.5	37.8	10.0	2.9
42	3603	16.6	9.5	33.6	43.7	13.6	3.0
43	3374	10.7	9.1	35.2	43.4	10.9	2.9
44	2311	11.8	6.4	19.2	23.4	11.4	3.0
45	3082	14.5	8.1	28.8	36.5	11.5	3.0
46	3606	16.8	9.4	33.8	44.2	13.8	3.0
47	2280	11.8	6.7	18.7	22.8	11.3	3.0
48	2365	11.4	6.9	21.4	25.5	10.0	2.9
49	3151	14.5	7.8	30.7	38.2	11.2	2.7
50	2687	12.5	7.6	25.8	31.6	9.5	2.9
51	1815	9.9	5.8	13.4	15.7	10.1	3.2
52	2314	1.7	7.2	18.9	23.9	11.0	3.0
53	1876	10.1	5.7	14.3	16.8	10.2	3.1
54	1730	8.9	5.1	14.8	16.1	7.9	3.3
55	1790	9.6	5.1	14.0	16.0	9.2	3.3
56	1815	9.9	5.3	13.9	15.8	10.0	3.2
57	1900	10.1	6.2	14.5	17.0	10.4	3.1
58	1883	10.0	5.9	14.5	16.9	10.2	3.1
59	2420	11.8	7.7	19.9	23.1	12.8	3.3
60	2097	11.2	6.9	17.4	21.3	9.5	2.95
61	2362	12.1	6.8	19.7	24.2	11.2	3.1
62	2359	11.9	7.1	19.4	23.1	12.1	3.0
63	2318	11.9	7.2	18.7	23.1	11.7	2.98
64	2338	11.9	7.0	19.3	23.3	11.8	2.96
65	2241	11.9	6.7	17.8	22.0	11.4	3.0
66	2034	11.5	6.3	16.1	18.9	10.9	3.0
67	2530	12.2	7.2	22.2	26.7	11.6	2.98
68	2613	11.8	6.9	24.3	30.9	10.5	2.2
69	2655	12.5	7.4	25.0	30.6	10.0	2.9
70	2641	12.2	7.5	25.0	30.6	10.0	2.7
71	3267	15.3	9.0	31.6	40.0	11.0	2.9
72	3392	15.8	9.1	31.8	40.0	13.2	2.96
73	394	4.2	0.82	0.74	1.0	0.9	3.3
74	3106	14.2	8.8	30.6	39.2	9.6	2.6
75	2236	11.2	6.7	20.0	25.0	8.5	2.9
76	3132	14.5	8.4	29.3	36.7	12.2	2.9
77	2060	10.4	5.7	17.1	20.1	9.8	3.4
78	3331	15.0	9.4	31.6	40.6	11.9	2.95
79	3498	10.2	6.1	22.5	25.5	8.5	2.7
80	2275	10.2	6.1	22.5	25.5	8.5	2.7

Appendix 2. Hydrogeochemical Data of the Khobar Aquifer.

Sample No.	TDS mg/l	Ca meq/l	Mg meq/l	Na + K meq/l	Cl meq/l	SO <sub>4</sub> meq/l	HCO <sub>3</sub> meq/l
81	2420	11.3	9.1	19.7	24.5	11.1	3.6
82	2097	10.7	5.9	17.4	20.7	10.1	3.1
83	2194	10.9	5.9	18.5	21.7	10.2	3.5
84	2212	11.1	6.3	18.3	21.7	10.6	3.5
85	2186	11.1	6.3	18.2	22.2	9.8	3.5
86	2396	10.8	6.7	18.6	27.8	8.5	2.9
87	2593	12.3	6.5	23.7	28.5	10.5	3.4
88	2113	10.8	5.9	17.3	20.7	10.1	3.4
89	2299	11.5	6.5	19.5	23.8	10.5	3.2
90	2312	11.7	6.3	19.4	23.5	10.5	3.6
91	2266	11.4	6.3	19.2	23.0	10.6	3.2
92	2054	10.5	5.8	16.7	19.7	9.9	3.6
93	1874	10.0	5.7	14.3	16.7	9.9	3.4
94	2168	11.0	6.3	17.7	21.7	10.5	3.2
95	2107	11.1	5.8	16.9	20.3	10.4	3.3
96	2365	11.4	6.5	20.6	24.4	10.7	3.4
97	2570	12.9	6.7	22.6	27.6	10.8	3.4
98	1895	10.0	5.6	14.8	17.1	9.7	3.5
99	1999	10.5	5.7	15.7	18.5	10.0	5.6
100	1763	10.0	5.6	13.0	16.2	9.8	2.5
101	2060	10.4	6.3	16.4	19.7	10.1	3.5
102	2218	10.9	6.9	18.0	22.0	10.5	3.5
103	2152	13.3	6.1	17.4	21.2	10.5	3.2
104	1848	10.1	5.5	14.6	16.7	10.2	2.6
105	2250	11.3	6.7	18.7	22.4	11.2	3.0
106	2807	16.9	9.6	17.8	13.6	27.3	2.4
107	2373	12.6	6.3	20.0	25.8	9.8	3.2
108	2286	6.6	8.2	25.4	28.8	6.7	1.4
109	2795	6.6	8.2	21.9	28.8	6.7	1.1
110	2908	14.2	3.5	27.7	30.4	11.5	3.5
111	3346	15.1	13.1	28.1	40.8	12.0	3.5
112	1808	8.7	5.3	15.1	17.5	7.5	4.0
113	1790	10.9	4.6	13.1	17.1	7.4	4.1
114	2358	11.8	7.7	18.8	23.4	11.0	3.9
115	2645	7.2	4.9	30.5	28.2	10.2	4.1
116	2049	6.5	4.0	22.1	20.2	8.1	4.2
117	1845	10.5	5.7	14.2	20.0	7.5	2.9
118	1980	9.4	5.3	17.4	20.4	7.8	3.8
119	1840	5.9	3.8	19.3	16.8	8.0	4.1
120	1824	9.5	9.7	10.7	17.6	8.4	3.9

Appendix 2. Hydrogeochemical Data of the Khobar Aquifer.

Sample No.	TDS mg/l	Ca meq/l	Mg meq/l	Na + K meq/l	Cl meq/l	SO <sub>4</sub> meq/l	HCO <sub>3</sub> meq/l
121	4586	15.5	11.4	50.1	59.9	13.7	3.4
122	3173	9.9	8.1	34.8	39.5	10.1	3.1
123	3025	12.6	11.2	25.1	28.3	18.6	2.7
124	4407	15.5	10.8	47.4	56.5	13.5	3.7
125	6639	29.5	18.8	59.9	60.1	45.8	1.8
126	2984	11.3	8.1	29.7	36.1	9.8	3.4
127	2343	14.2	2.7	20.2	21.4	12.0	3.7
128	1670	7.9	4.3	14.4	15.5	7.5	3.6
129	1784	5.9	4.9	15.2	16.0	8.8	3.4
130	1537	4.3	4.9	17.4	23.2	2.8	0.6
131	1709	10.4	6.7	11.3	15.6	8.7	3.2
132	1761	6.6	5.1	16.8	18.0	7.5	3.0
133	1438	9.2	0.2	14.4	16.4	6.9	0.1
134	3680	10.6	9.5	41.1	44.9	13.6	2.7
135	1538	8.5	0.6	16.6	16.0	7.9	0.1
136	2718	9.0	7.9	27.9	31.5	10.2	3.1
137	3338	15.8	10.2	29.1	36.0	15.9	3.1
138	2970	11.4	8.1	29.6	35.1	10.4	3.6
139	1527	7.7	6.6	10.6	14.0	8.8	2.1
140	1705	7.7	7.1	13.0	15.0	10.9	1.9
141	1212	4.8	4.8	9.7	10.6	5.7	3.0
142	2627	7.3	5.9	29.9	30.4	10.0	2.7
143	1887	5.6	4.0	20.6	18.8	8.3	3.1
144	2361	5.0	4.4	11.9	10.4	7.9	3.0
145	1191	4.4	4.0	9.9	7.8	7.6	3.0
146	846	7.5	1.3	3.7	3.6	5.9	3.0
147	2407	20.1	9.8	7.2	6.7	28.3	2.0
148	3169	31.3	11.7	5.1	4.4	41.5	2.2
149	3178	12.6	11.9	21.1	4.7	42.0	2.0
150	1774	15.8	8.5	3.0	3.8	22.1	1.4
151	3404	34.8	17.9	0.3	6.4	45.5	1.1
152	4188	17.6	13.3	37.7	41.1	24.6	2.8
153	2374	11.0	6.7	21.7	28.4	7.6	3.3
154	2493	12.6	5.6	22.8	29.3	8.5	3.3
155	2450	10.9	6.3	23.1	28.2	8.5	3.5
156	13241	39.6	35.6	151.8	192.3	31.9	2.9
157	17369	33.9	27.2	232.7	250.4	40.9	2.8
158	4039	12.2	4.9	48.6	46.1	16.4	3.2
159	3983	36.0	12.4	11.1	11.0	46.7	3.5
160	1343	6.3	4.8	9.7	10.3	7.5	3.3



Appendix 2. Hydrogeochemical Data of the Khobar Aquifer.

Sample No.	TDS mg/l	Ca meq/l	Mg meq/l	Na + K meq/l	Cl meq/l	SO <sub>4</sub> meq/l	HCO <sub>3</sub> meq/l
161	1099	5.5	3.5	7.7	7.8	6.0	3.2
162	3269	0.8	2.0	50.6	40.0	12.6	1.2
163	2374	14.1	4.9	19.3	19.9	17.4	0.8
164	1714	9.8	6.2	9.8	12.4	11.4	3.3
165	1788	12.8	6.0	8.8	8.8	15.7	3.1
166	2395	12.1	7.2	19.4	23.4	12.9	2.7
167	2485	9.7	3.9	25.9	29.3	8.9	2.7
168	2652	10.7	19.7	23.9	29.5	8.7	2.8
169	2011	9.6	5.8	17.2	19.8	9.3	3.3
170	2063	9.2	5.1	17.2	19.0	10.6	3.9
171	1904	9.6	7.4	14.9	18.0	8.5	3.8
172	3103	11.8	11.4	29.5	37.7	12.1	2.9
173	2096	10.4	7.4	16.5	21.2	10.3	2.8
174	2607	12.0	6.0	24.4	28.0	10.9	3.5
175	1788	8.4	5.0	14.9	17.3	7.5	4.0
176	3193	11.8	8.7	32.3	37.2	11.6	3.8
177	2223	11.0	6.4	19.2	24.6	9.5	2.5
178	2135	8.1	9.5	17.7	22.4	10.0	2.9
179	2879	17.3	10.4	37.4	49.2	12.8	3.0
180	1916	16.9	0.4	14.4	24.7	4.7	2.3
181	1773	8.6	4.9	14.8	16.0	8.5	3.7
182	10764	33.8	14.2	132.9	148.4	29.6	2.8
183	2714	10.0	8.9	25.4	27.2	13.7	3.2
184	7271	28.0	23.1	73.5	101.6	21.0	2.1
185	8366	36.7	23.3	95.6	130.2	8.5	2.1
186	7994	22.1	20.9	93.7	114.6	19.3	2.2
187	2243	19.9	9.6	4.7	4.3	27.6	2.2
188	2097	9.1	8.1	17.2	21.4	10.0	3.0
189	1043	6.6	4.4	5.5	7.2	6.6	2.6
190	1824	9.6	6.5	13.5	16.8	10.2	2.5
191	2452	12.2	7.0	18.9	16.8	17.4	4.2
192	3175	12.3	6.2	30.0	17.0	27.6	3.8
193	3254	14.6	2.6	32.7	26.8	13.6	9.4
194	2538	11.5	6.3	24.1	29.8	8.6	3.4
195	2154	10.7	6.7	18.2	25.0	7.4	3.2
196	2485	4.6	5.9	29.9	28.3	8.5	3.6
197	2518	11.5	6.7	23.3	29.1	9.2	3.3
198	2544	11.5	6.1	24.3	29.6	8.9	3.3
199	2120	12.9	3.0	18.5	23.2	7.9	3.2

Appendix 2. Hydrogeochemical Data of the Khobar Aquifer.

Sample No.	TDS mg/l	Ca meq/l	Mg meq/l	Na + K meq/l	Cl meq/l	SO <sub>4</sub> meq/l	HCO <sub>3</sub> meq/l
200	2280	9.8	7.2	19.9	23.2	9.7	4.1
201	6725	20.4	14.7	76.3	79.5	28.7	3.0
202	1125	5.6	4.1	10.1	8.6	5.1	3.0
203	1545	5.0	2.6	16.6	14.2	6.4	3.6
204	1994	9.5	4.9	16.9	18.0	6.6	6.6
205	1033	6.5	4.4	5.5	8.2	5.1	3.1
206	2855	11.9	7.4	28.0	34.4	9.3	3.5
207	1583	7.9	5.3	12.6	16.0	6.9	2.8
208	1829	5.4	3.7	19.7	16.2	8.8	3.7
209	1032	6.2	4.0	6.2	8.2	5.6	2.6
210	1718	6.1	4.0	16.6	12.2	12.1	2.4
211	2666	11.7	6.7	25.4	30.7	10.3	2.95
212	2605	11.0	7.0	25.6	30.5	10.2	2.3
213	2727	12.2	7.2	25.6	31.1	10.7	3.0
214	2583	10.1	6.2	26.8	31.2	10.7	1.1
215	2787	1071.9	7.5	26.7	32.8	10.3	2.9
216	2777	12.6	7.1	26.6	32.6	10.2	2.9
217	2768	12.2	7.2	26.6	32.8	10.2	2.8
218	2672	11.7	6.9	25.8	31.3	10.2	2.6
219	2809	12.5	7.3	26.9	32.7	10.7	2.9
220	3033	12.2	8.0	38.8	36.9	11.5	1.98
221	2273	10.6	6.3	20.7	24.8	10.1	2.3
222	2029	12.2	9.1	10.8	8.2	20.0	2.9
223	1494	8.2	5.9	10.7	14.5	7.0	2.6
224	1928	9.8	6.6	14.6	17.0	10.5	3.4
225	2219	12.4	5.8	17.3	19.6	12.5	3.4
226	1787	1.0	0.8	25.7	12.8	11.2	2.2
227	1087	5.0	3.4	8.3	8.3	5.1	3.2
228	7423	31.5	19.9	72.6	86.4	36.5	1.1
229	1477	5.6	5.0	12.2	13.4	6.7	3.2
230	1370	6.0	4.3	10.7	11.7	6.2	3.2
231	1241	8.8	5.5	12.4	14.3	8.9	2.7
232	2102	10.5	6.6	16.8	19.8	10.4	3.2
233	1720	12.4	6.8	7.2	9.3	14.3	2.9
234	1527	11.0	5.7	6.4	7.9	12.2	3.0

***APPENDIX 3***

***PCWATEQ DATABASE***

Appendix 3 Thermodynamic Database of PCWATEQ Computer Program.

I	NReact.	$\Delta H_R$	Log K
1	$Fe^{3+}$	9.7000	-13.0380
2	$FeH^{2+}$	20.1150	-15.2280
3	$FeOH^+$	13.2180	-9.5000
4	$FeOH_3^-$	30.3000	-31.0000
5	$FeSO_4^+$	13.6100	-9.1180
6	$FeCl^{2+}$	18.1520	-11.6000
7	$FeCl_2^+$	0.0000	-10.9190
8	$FeCl_3$	0.0000	-11.9250
9	$FeSO_4$	3.2300	2.2500
10	Siderite	-6.1400	-10.5700
11	Magnesite	-6.1690	-8.2400
12	Dolomite	-9.4360	-17.0900
13	Calcite	-2.2970	-8.4800*
14	$H_3SiO_4^-$	8.9350	-9.9290*
15	$H_2SiO_4^{2-}$	29.7170	-21.6170*
16	$HPO_4^{2-}$	-3.5300	12.3460
17	$H_2PO_4^-$	-4.5200	19.5530
18	Anhydrite	-4.3000	-4.3840
19	Gypsum	-0.0280	-4.6020*
20	Brucite	0.8500	-11.4100
21	Chrysoitile	27.5850	-51.8000
22	Aragonite	-2.5890	-8.3360*
23	$MgF^-$	4.6740	1.8200
24	$CaSO_4$	1.5000	2.3090
25	$MgOH^+$	2.0900	2.2100*
26	$H_3BO_3$	3.2190	-9.2350*
27	$NH_3$	12.4770	-9.2440*
28	Forsterite	4.8700	-28.1100
29	Diopside	21.1000	-36.2200
30	Clinoenstatite	6.6750	-16.8700
31	$NaHPO_4^-$	0.0000	0.2900
32	Tremolite	90.2150	-140.30
33	$KHPO_4^-$	0.0000	0.2900
34	$MgHPO_4^-$	3.3000	2.8700
35	$CaHPO_4^-$	3.3000	2.7390

\*\* Denotes that an analytical expression has been used for K(T).

Appendix 3 Thermodynamic Database of PCWATEQ Computer Program.

I	NReact.	$\Delta H_R$	Log K
36	$H_2CO_3$	-2.1770	6.3520*
37	Sepiolite	26.5320	-40.1000
38	Talc	45.0650	-62.2900
39	Hydromagnesite	-25.5200	-37.8200
40	Adularia	30.8200	-20.5700
41	Albite	25.8960	-18.0000
42	Anorthite	17.5300	-19.3300
43	Analcime	18.2060	-12.7000
44	K mica	67.8600	-49.0900
45	Phlogopite	0.0000	-63.5300
46	Illite	54.6840	-40.3100
47	Kaolinite	49.1500	-36.9100
48	Halloysite	44.6800	-32.8200
49	Beidellite	60.3550	-45.2600
50	Chlorite	54.7600	-90.6100
51	Alunite	29.8200	-85.3200
52	Gibbsite (crys)	14.4700	-32.7700
53	Boehmite	11.9050	-33.4100
54	Pyrophyllite	0.0000	-42.4300
55	Phillipsite	0.0000	-19.8600
56	Erionite	0.0000	0.0000
57	Clinoptilolite	0.0000	0.0000
58	Mordenite	0.0000	0.0000
59	Nahcolite	3.7200	-0.5480
60	Trona	-18.0000	-0.7950
61	Natron	15.7450	-1.3110
62	Thermonatrite	-2.8020	0.1250
63	Fluorite	4.7100	-10.9600
64	Ca Montmorillonite	58.3730	-45.0000
65	Halite	0.9180	1.5820
66	Thenardite	-0.5720	-0.1790
67	Mirabilite	18.9870	-1.1130
68	Mackinawite	0.0000	-4.6310
69	$HCO_3^-$	-3.5610	10.3290*
70	$NaCO_3^-$	8.9110	1.2680
71	$NaHCO_3$	0.0000	-0.2500
72	$NaSO_4^-$	1.1200	0.7200

Appendix 3 Thermodynamic Database of PCWATEQ Computer Program.

I	NReact.	$\Delta H_R$	Log K
73	$KSO_4$	2.2500	0.8470*
74	$MgCO_3$	2.7100	2.9800*
75	$MgHCO_3^+$	1.0770	1.0660*
76	$MgSO_4$	4.6000	2.2380
77	$CaOH^+$	1.1900	1.4000
78	$CaHCO_3^+$	4.1100	1.0950*
79	$CaCO_3$	3.5560	3.2240*
80	$CaF^+$	4.1200	0.9400
81	$AlOH^{2+}$	1.4300	9.0300
82	$Al(OH)_2^+$	0.0000	18.7000
83	$Al(OH)_4^-$	-11.1600	33.0000
84	$AlF^{2+}$	0.0000	7.0100
85	$AlF_2^+$	20.0000	12.7500
86	$AlF_3$	2.5000	17.0200
87	$AlF_4^-$	0.0000	19.7200
88	$AlSO_4^+$	2.1500	3.0200
89	$Al(SO_4)_2^-$	2.8400	4.9200
90	$HSO_4^-$	4.9100	1.9870*
91	$H_2S$ (crs)	-65.4400	40.6440
92	$H_2S$	5.2990	-6.9420*
93	$HS^-$	12.1000	-12.9180
94	$O_2$ (gas)	34.1570	-20.7800
95	$CH_4$ (gas)	-57.4350	30.7410
96	OH Apatite	17.2250	-59.3500
97	F Apatite	19.6950	-66.7900
98	Chalcedony	4.6150	-3.5230
99	Magadiite	0.0000	-14.3000
100	Silica Gel	5.5000	-2.7000
101	Silica Glass	4.4400	-3.0170
102	Quartz	6.2200	-4.0050
103	$Fe(OH)_2^+$	0.0000	-18.7080
104	$Fe(OH)_3$	0.0000	-26.6380
105	$Fe(OH)_4^-$	0.0000	-34.6380
106	$Fe(OH)_2$	28.5650	-20.5700

Appendix 3 Thermodynamic Database of PCWATEQ Computer Program.

I	NReact.	$\Delta H_R$	Log K
107	Vivianite	0.0000	-36.0000
108	Magnetite	-40.6600	-9.5650
109	Hematite	-30.8450	-4.0070
110	Maghemite	0.0000	6.3700
111	Goethite	25.5550	-44.1970
112	Greenalite	0.0000	-63.1900
113	$Fe(OH)_3$ (amorph.)	0.0000	4.8850
114	Annite	62.4800	-84.2400
115	Pyrite	11.3000	-18.4800
116	Montmo. (Belle Fourche)	0.0000	-34.9700
117	Montmo. (Aberdeen)	0.0000	-29.7800
118	Huntite	-25.7600	-30.5100
119	Gregite	0.0000	-17.9700
120	FeS (ppt)	0.0000	-3.9150
121	$FeH_2PO_4^+$	0.0000	2.7000
122	$CaPO_4^-$	3.1000	6.4590
123	$CaH_2PO_4^+$	3.4000	1.4080
124	$MgPO_4^-$	3.1000	6.5890
125	$MgH_2PO_4^+$	3.4000	1.5130
126	LiOH	4.8320	0.2000
127	$LiSO_4$	0.0000	0.6400
128	$NO_3^-/NH_4^+$	-187.0550	119.0770
129	Laumontite	9.6100	-30.9600
130	$SrOH^+$	1.1500	0.8200
131	$BaOH^+$	1.7500	0.6400
132	$NH_4SO_4^-$	0.0000	1.1100
133	HCl	0.0000	-30.0000
134	NaCl	0.0000	-30.0000
135	KCl	0.0000	-30.0000
136	$H_2SO_4$	0.0000	-30.0000
137	$H_2O/O_2$	0.0000	-11.3850
138	$CO_2$ (gas)	-4.7760	-1.4680
139	$FeHPO_4$	0.0000	3.6000
140	$FeHPO_4^+$	0.0000	-7.6130
141	$Al(OH)_3$ (amorph.)	12.9900	-31.6100
142	Prehnite	10.3900	-11.5200

Appendix 3 Thermodynamic Database of PCWATEQ Computer Program.

I	NReact.	$\Delta H_R$	Log K
143	Strontianite	-0.4000	-9.2710*
144	Celestite	0.2280	-6.5780*
145	Barite	6.1410	-9.9780
146	Witherite	6.9500	-8.5850
147	Strengite	-2.0300	-26.4000
148	Leonhardite	90.0700	-69.5700
149	$SrHCO_3^+$	6.0500	1.1800*
150	Nesquehonite	-5.7890	-5.2110
151	Artinite	-1.8420	-18.4000
152	$O_2(aqu)$	33.4570	-21.4950
153	W	13.3410	-13.9920*
154	Sepiolite (ppt)	0.0000	-37.2120
155	Diaspore	-15.4050	-35.0600
156	Wairakite	26.1400	-26.6200
157	$FeH_2PO_4^{2+}$	0.0000	-7.5830
158	$Mn^{3+}$	25.7600	-25.5070
159	$MnCl^+$	0.0000	0.6070
160	$MnCl_2$	0.0000	0.0410
161	$MnCl^2$	0.0000	-0.3050
162	$MnOH^+$	0.0000	3.4490
163	$Mn(OH)_3$	0.0000	7.7820
164	$MnF^+$	0.0000	0.8500
165	$MNSO^4$	3.7000	1.7080
166	$MN(NO_3)_2$	-0.3960	0.0590
167	$MnHCO_3$	0.0000	1.7160
168	$MNO_4^-$	176.6200	-127.8240
169	$MnO_4^{2-}$	150.0200	-118.4400
170	$SrCO_3$	5.2200	2.8100*
171	$KHMnNO_2^2$	0.0000	-34.4400
172	Manganosite	-24.0250	17.9380
173	Pyrolusite	-29.1800	15.8610
174	Birnsite	0.0000	18.0910



Appendix 3 Thermodynamic Database of PCWATEQ Computer Program.

I	NReact.	$\Delta H_R$	Log K
175	Nustite	0.0000	17.5040
176	Bixbyite	-15.2450	-0.6110
177	Hausmite	-80.1400	61.5400
178	$MnOH_2$	4.1000	-12.9120
179	$MnOH_3$	20.0900	-35.6440
180	Manganosite	0.0000	-0.2380
181	Rhodochrosite	-2.0790	-10.5390
182	$SrSO_4$	1.6000	2.5500
183	$MnCl_2$	-17.6220	8.7600
184	$MnCl_2 \cdot H_2O$	-7.1750	5.5220
185	$MnCl_2 \cdot 2H_2O$	1.7100	3.9740
186	$MnCl_2 \cdot 4H_2O$	17.3800	2.7100
187	Tephroite	-40.0600	23.1220
188	Rhoconit.	-21.8850	9.5220
189	MnS grn	-5.7900	3.8000
190	$MnSO_4$	-15.4800	2.6690
191	$Mn_2(SO_4)_3$	-39.0600	-5.7110
192	$Mn_3(PO_4)_2$	2.1200	-23.8270
193	$MnHPO_4$	0.0000	-12.9470

I = identifier (in the program).  
 NReact. = name of the reactant.  
 $\Delta H_R$  = Enthalpy of the reaction.  
 K = Equilibrium constant.

Appendix 3 Thermodynamic Database of PCWATEQ Computer Program.

I	NSpec.	Z	a	GFW
1	Ca	2	6.0	40.0800
2	Mg	2	6.5	24.3120
3	Na	1	4.0	22.9898
4	K	1	3.0	39.1020
5	Cl	-1	3.0	35.4530
6	SO <sub>4</sub>	-2	4.0	96.0616
7	HCO <sub>3</sub>	-1	5.4	61.0173
8	Fe	2	6.0	55.8470
9	Fe	3	9.0	55.8470
10	FeOH	2	5.0	72.8544
11	FeOH	1	5.0	72.8549
12	Fe(OH) <sub>3</sub>	-1	5.0	106.8690
13	FeHPO <sub>4</sub>	1	5.4	151.8200
14	H <sub>2</sub> S (aqu)	0	0.0	34.0799
15	FeSO <sub>4</sub>	1	5.0	151.9086
16	FeCl	2	5.0	91.3000
17	Ana. H <sub>2</sub> S	0	0.0	34.0799
18	CO <sub>3</sub>	-2	5.4	60.0094
19	MgOH	1	6.5	41.3194
20	MgF	1	4.5	43.3104
21	MgCO <sub>3</sub> (aqu)	0	0.0	84.3214
22	MgHCO <sub>3</sub>	1	4.0	85.3293
23	MgSO <sub>4</sub> (aqu)	0	0.0	120.3736
24	H <sub>4</sub> SiO <sub>4</sub> (aqu)	0	0.0	96.1155
25	H <sub>3</sub> SiO <sub>4</sub>	-1	4.0	95.1075
26	H <sub>2</sub> SiO <sub>4</sub>	-2	5.4	94.0995
27	OH	-1	3.5	17.0074
28	FeCl <sub>2</sub>	1	5.0	126.7530
29	CaOH	1	6.0	57.0874
30	CaHCO <sub>3</sub>	1	6.0	101.0973
31	CaCO <sub>3</sub> (aqu)	0	0.0	100.0890
32	CaSO <sub>4</sub> (aqu)	0	0.0	136.1416
33	FeCl <sub>3</sub>	0	0.0	162.2060
34	FeSO <sub>4</sub>	0	0.0	151.9086
35	SiO <sub>2</sub> (tot.)	0	0.0	60.0848

Appendix 3 Thermodynamic Database of PCWATEQ Computer Program.

I	NSpec.	Z	a	GFW
36	$H_3BO_3$ (aqu)	0	0.0	61.8331
37	$H_2BO_3$	-1	2.5	60.8251
38	$NH_3$ (aqu)	0	0.0	17.0306
39	$NH_4$	1	2.5	18.0386
40	$MgPO_4$	-1	5.4	119.2834
41	$MgH_2PO_4$	1	5.4	121.2993
42	$NaCO_3$	-1	5.4	82.9992
43	$NaHCO_3$	0	0.0	83.9909
44	$NaSO_4$	-1	5.4	119.0514
45	$PO_4$	-3	5.0	94.9714
46	$KSO_4$	-1	5.4	135.1636
47	$HPO_4$	-2	5.0	95.9794
48	$H_2PO_4$	-1	5.4	96.9873
49	CaF	1	5.0	59.0784
50	$NaHPO_4$	-1	5.4	118.9692
51	Al	3	9.0	26.9815
52	AlOH	2	5.4	43.9889
53	$Al(OH)_2$	1	5.4	60.9962
54	$Al(OH)_4$	-1	4.5	95.0110
55	AlF	2	5.4	45.9799
56	$AlF_2$	1	5.4	64.9783
57	$AlF_3$	0	0.0	83.9767
58	$AlF_4$	-1	4.5	102.9751
59	$AlSO_4$	1	4.5	123.0431
60	$Al(SO_4)_2$	-1	4.5	219.1047
61	$KHPO_4$	-1	5.4	135.0814
62	F	-1	3.5	18.9984
63	$HSO_4$	-1	4.5	97.0696
64	H	1	9.0	1.0080
65	$FeH_2PO_4$	1	5.4	152.8340
66	$H_2S$ calcu.	0	0.0	34.0799
67	HS	-1	3.5	33.0720
68	S	-2	5.0	32.0640
69	$SrHCO_3$	1	5.4	148.6373
70	$PO_2$	0	0.0	31.9988

Appendix 3 Thermodynamic Database of PCWATEQ Computer Program.

I	NSpec.	Z	a	GFW
71	$PCH_4$	0	0.0	16.0430
72	$AH_2O$	0	0.0	18.0153
73	$MgHPO_4$	0	0.0	120.2914
74	$CaHPO_4$	0	0.0	136.0594
75	$CaPO_4$	-1	5.4	135.0514
76	$CaH_2PO_4$	1	5.4	137.0673
77	$Fe(OH)_2$	1	5.4	89.8616
78	$Fe(OH)_3$	0	0.0	106.8689
79	$Fe(OH)_4$	-1	5.4	123.8762
80	$Fe(OH)_2$	0	0.0	89.8616
81	Li	1	6.0	6.9390
82	LiOH	0	0.0	23.9464
83	$LiSO_4$	-1	5.0	103.0006
84	$NH_4$ <i>calcu.</i>	1	2.5	18.0386
85	$NO_3$	-1	3.0	62.0049
86	$H_2CO_3$	0	0.0	62.0253
87	B tot.	0	0.0	10.8100
88	Sr	2	5.0	87.6200
89	SrOH	1	5.0	104.6274
90	Ba	2	5.0	137.3400
91	BaOH	1	5.0	154.3474
92	$NH_4SO_4$	-1	5.0	114.1002
93	HCl	0	0.0	36.4610
94	NaCl	0	0.0	58.4428
95	KCl	0	0.0	74.5550
96	$H_2SO_4$	0	0.0	98.0775
97	$SrCO_3$	0	0.0	147.6294
98	Br	-1	4.0	79.9090
99	$FeH_2PO_4$	2	5.4	152.8340
100	$FeHPO_4$	0	0.0	151.8200
101	Mn	2	6.0	54.9400
102	Mn	3	9.0	54.9400
103	MnCl	1	5.0	90.3970
104	$MnCl_2$	0	0.0	125.8540

Appendix 3 Thermodynamic Database of PCWATEQ Computer Program.

I	NSpec.	Z	a	GFW
105	<i>MnCl<sub>3</sub></i>	-1	5.0	161.3110
106	<i>MnOH</i>	1	5.0	71.8480
107	<i>Mn(OH)<sub>3</sub></i>	-1	5.0	105.9640
108	<i>MnF</i>	1	5.0	73.9400
109	<i>MnSO<sub>4</sub></i>	0	0.0	151.0060
110	<i>Mn(NO<sub>3</sub>)<sub>2</sub></i>	0	0.0	178.9560
111	<i>MnHCO<sub>3</sub></i>	1	5.0	115.9590
112	<i>MnO<sub>4</sub></i>	-1	3.0	118.9400
113	<i>MnO<sub>4</sub></i>	-2	5.0	118.9400
114	<i>SrSO<sub>4</sub></i>	0	0.0	183.6800
115	<i>HMnO<sub>2</sub></i>	-1	5.0	87.9480

I = identifier (in the program)

NSpec. = name of the species.

Z = valance

a = denotes the "a" value used for activity coefficient calculation.

GFW = weight in grams.

Appendix 3 Thermodynamic Database of PCWATEQ Computer Program.

Summary of analytical expressions of the form:  
 $\log K = A + BT + C/T + DT^2 + E/T^2 + F \log T$   
 used in PCWATEQ program are listed below.

I	NReact.	Expression
13	Calcite	$\log K = -171.9065 - 0.077992998T + 2839.3191/T + 71.595001 \log T$
14	$H_2SiO_4$	$\log K = 6.368 - 0.016346T - 3405.899/T$
15	$H_2SiO_4$	$\log K = 39.478 - 0.065926999T - 12355.0996/T$
19	Gypsum	$\log K = 82.0904 - 3853.9360/T - 29.81148 \log T$
22	Aragonite	$\log K = -171.9773 - 0.077992998T + 2903.2930/T - 71.595001 \log T$
25	MgOH	$\log K = 0.6840 + 0.0051295T$
26	$H_3BO_3$	$\log K = 28.6059 - 0.012078T + 1573.21/T - 13.2258 \log T$
27	$NH_3$	$\log K = 0.6322 - 0.001225T + 2835.76/T$
36	$H_2CO_3$	$\log K = 356.3094 - 0.06091964T - 21834.3691/T + 1684915/T^2 - 126.8339 \log T$
69	$HCO_3^-$	$\log K = 107.8871 - 0.03252849T - 5151.79/T + 563713.9/T^2 - 38.92561 \log T$
73	$KSO_4$	$\log K = 3.106 - 673.6/T$
74	$MgCO_3$	$\log K = 0.991 + 0.00667T$
75	$MgHCO_3$	$\log K = 2.319 - 0.011056T + 22981T^2$
78	$CaHCO_3$	$\log K = 1209.12 + 0.312940001T - 34765.0508/T - 478.78201 \log T$
79	$CaCO_3$	$\log K = -1228.7321 - 0.299439996T + 35512.75/T + 485.81799 \log T$
90	$H_2SO_4$	$\log K = -5.3505 + 0.0183412T + 557.2461/T$
92	$H_2S$	$\log K = 11.17 - 0.02386T - 3279/T$
143	Strontianite	$\log K = 155.0305 - 7239.5942/T - 59.58638 \log T$
144	Celestite	$\log K = 73.415 - 3603.3411/T - 27.443701 \log T$
149	$SrHCO_3$	$\log K = -3.248 - 0.014867T$
153	W	$\log K = -606.522 - 0.097611003T - 31286/T - 2170870/T^2 + 21.868434 \log T$
170	$SrCO_3$	$\log K = -1.0190 + 0.012826T$

***APPENDIX 4***  
***IRRIGATION CLASSES***  
***ALAT AQUIFER***

Appendix 4. The Irrigation Classes of Alat Aquifer Water.

Sample No	TDS mg/l	EC micromhos/cm	SAR	Irrigation Class
1	3784.000	5912.500	3.78	C4 S2
2	2545.000	3976.563	13.2	C4 S4
3	3076.000	4806.250	10.58	C4 S3
4	3777.000	5901.563	7.12	C4 S3
5	2486.000	3884.375	8.48	C4 S3
6	2415.000	3773.438	10.66	C4 S3
7	2313.000	3614.063	8.33	C4 S3
8	4399.000	6873.438	8.25	C4 S3
9	1637.000	2557.813	5.09	C4 S2
10	1849.000	2889.063	7.13	C4 S2
11	1511.000	2360.938	4.78	C4 S2
12	1529.000	2389.063	4.84	C4 S2
13	2410.000	3765.625	10.41	C4 S3
14	4603.000	7192.188	10.25	C4 S4
15	4021.000	6282.813	10.48	C4 S4
16	2337.000	3651.563	3.73	C4 S1
17	2531.000	3954.688	4.42	C4 S2
18	2508.000	3918.750	7.74	C4 S2
19	1978.000	3090.625	6.75	C4 S2
20	2685.000	4195.313	5.69	C4 S2
21	3495.000	5460.938	10.79	C4 S3
22	2210.000	3453.125	17.67	C4 S4
23	1592.000	2487.500	5.16	C4 S2
24	1341.000	2095.313	4.26	C3 S1
25	1258.000	1965.625	4.25	C3 S1
26	1166.000	1821.875	4.91	C3 S1
27	5769.000	24639.063	33.94	C4 S4
28	7357.000	11495.313	13.11	C4 S4
29	2160.000	3375.000	2.43	C4 S1
30	2295.000	3585.938	6.56	C4 S2
31	2229.000	3482.813	8.42	C4 S3
32	1494.000	2334.375	3.94	C4 S1
33	2098.000	3278.125	5.99	C4 S2
34	2872.000	4487.500	7.22	C4 S3
35	1736.000	2712.500	5.5	C4 S2
36	2577.000	4026.563	7.05	C4 S2
37	3345.000	5226.563	9.87	C4 S4
38	3563.000	5567.188	9.82	C4 S4
39	1690.000	2640.625	4.93	C4 S2
40	2655.000	4148.438	7.64	C4 S2



Appendix 4. The Irrigation Classes of Alat Aquifer Water.

Sample No	TDS mg/l	EC micromhos/cm	SAR	Irrigation Class
41	2834.000	4428.125	7.55	C4 S2
42	2130.000	3328.125	6.33	C4 S2
43	2538.000	3965.625	7.41	C4 S2
44	2918.000	4559.375	7.75	C4 S2
45	2480.000	3875.000	7.22	C4 S2
46	2810.000	4390.625	8.86	C4 S3
47	2736.000	4275.000	7.57	C4 S2
48	3379.000	5279.688	9.37	C4 S3
49	4904.000	7662.500	12.38	C4 S4
50	2332.000	3643.750	6.65	C4 S2
51	2107.000	3292.188	7.82	C4 S3
52	2622.000	4096.875	3.5	C4 S2
53	4874.000	7615.625	15.0	C4 S4
54	3368.000	5262.500	11.01	C4 S4
55	2523.000	3942.188	6.36	C4 S2
56	25034.000	39115.625	39.66	C4 S4
57	2438.000	3809.375	1.36	C4 S1
58	2035.000	3179.688	4.67	C4 S2
59	2247.000	3510.938	4.28	C4 S2
60	1925.000	3007.813	5.67	C4 S2
61	2232.000	3487.500	6.7	C4 S2
62	3770.000	5890.625	9.94	C4 S3
63	3251.000	5079.688	8.18	C4 S3
64	3108.000	4856.250	8.58	C4 S3
65	3855.000	6023.438	10.22	C4 S3
66	2657.000	4151.563	6.34	C4 S2
67	2129.000	3326.563	6.17	C4 S2
68	2234.000	3490.625	5.71	C4 S2
69	2419.000	3779.688	7.36	C4 S2
70	2431.000	3798.438	7.34	C4 S2
71	2524.000	3943.750	6.33	C4 S2
72	2600.000	4062.500	6.34	C4 S2
73	2534.000	3959.375	7.2	C4 S2
74	1887.000	2948.438	6.95	C4 S2
75	1330.000	2078.125	2.57	C3 S1

***APPENDIX 5***  
***IRRIGATION CLASSES***  
***KHOBAR AQUIFER***

Appendix 5. The Irrigation Classes of Khobar Aquifer Water.

Sample No	TDS mg/l	EC micromhos/cm	SAR	Irrigation Class
1	3454.000	5313.844	9.199	C4 S3
2	12872.000	19803.074	17.635	C4 S4
3	2228.000	3427.692	6.217	C4 S2
4	2078.000	3196.923	5.848	C4 S2
5	1759.000	2706.154	5.145	C4 S2
6	1787.000	2749.231	5.093	C4 S2
7	2467.000	3795.385	6.31	C4 S2
8	2734.000	4206.152	5.778	C4 S2
9	852.000	1310.769	2.074	C3 S1
10	1019.000	1567.692	1.725	C3 S1
11	2789.000	4290.766	5.82	C4 S2
12	1575.000	2423.077	3.604	C4 S1
13	2549.000	3921.539	5.645	C4 S2
14	2457.000	3780.000	8.232	C4 S2
15	2000.000	3076.923	10.324	C4 S3
16	1080.000	1661.538	2.936	C3 S1
17	2223.000	3420.000	5.678	C4 S2
18	2220.000	3415.385	5.695	C4 S2
19	2160.000	3323.077	7.437	C4 S2
20	2197.000	3380.000	6.103	C4 S2
21	2829.000	4352.305	8.733	C4 S2
22	2012.000	3095.385	5.506	C4 S2
23	3343.000	5143.074	9.592	C4 S3
24	2133.000	3281.539	3.546	C4 S1
25	11689.000	17983.074	20.138	C4 S4
26	1748.000	2689.231	4.361	C4 S1
27	2130.000	3276.923	6.965	C4 S2
28	995.000	1530.769	2.032	C3 S1
29	1615.000	2484.615	3.977	C3 S1
30	5621.000	8647.691	11.533	C4 S4
31	2156.000	3316.923	6.674	C4 S2
32	2025.000	3115.385	5.814	C4 S2
33	2064.000	3175.385	5.693	C4 S2
34	2061.000	3170.769	5.574	C4 S2
35	1982.000	3049.231	6.226	C4 S2
36	2348.000	3612.308	7.717	C4 S2
37	3207.000	4933.844	8.984	C4 S3
38	2474.000	3806.154	6.76	C4 S2
39	3080.000	4738.461	8.467	C4 S3
40	3487.000	5364.613	9.011	C4 S3

Appendix 5. The Irrigation Classes of Khobar Aquifer Water.

Sample No	TDS mg/l	EC micromhos/cm	SAR	Irrigation Class
41	3083.000	4743.074	9.073	C4 S3
42	3603.000	5543.074	9.301	C4 S3
43	3374.000	5190.766	11.187	C4 S3
44	2311.000	3555.385	6.365	C4 S2
45	3082.000	4741.535	8.567	C4 S3
46	3606.000	5547.691	9.339	C4 S3
47	2280.000	3507.692	6.149	C4 S2
48	2365.000	3638.462	7.075	C4 S2
49	3151.000	4847.691	9.194	C4 S3
50	2687.000	4133.844	8.138	C4 S3
51	1815.000	2792.308	4.783	C4 S2
52	2314.000	3560.000	6.148	C4 S2
53	1876.000	2886.154	5.088	C4 S2
54	1730.000	2661.538	5.594	C4 S2
55	1790.000	2753.846	5.164	C4 S2
56	1815.000	2792.308	5.042	C4 S2
57	1900.000	2923.077	5.079	C4 S2
58	1883.000	2896.923	5.143	C4 S2
59	2420.000	3723.077	6.373	C4 S2
60	2097.000	3226.154	5.784	C4 S2
61	2362.000	3633.846	6.408	C4 S2
62	2359.000	3629.231	6.294	C4 S2
63	2318.000	3566.154	6.051	C4 S2
64	2338.000	3596.923	6.278	C4 S2
65	2241.000	3447.692	5.837	C4 S2
66	2034.000	3129.231	5.397	C4 S2
67	2530.000	3892.308	7.128	C4 S2
68	2613.000	4020.000	7.947	C4 S2
69	2655.000	4084.615	7.926	C4 S2
70	2641.000	4063.077	7.966	C4 S2
71	3267.000	5026.152	9.066	C4 S3
72	3392.000	5218.461	9.012	C4 S3
73	394.000	606.154	0.467	C2 S1
74	3106.000	4778.461	9.023	C4 S3
75	2236.000	3440.000	6.685	C4 S2
76	3132.000	4818.461	8.659	C4 S3
77	2060.000	3169.231	6.027	C4 S2
78	3331.000	5124.613	9.047	C4 S3
79	3498.000	5381.535	7.881	C4 S3
80	2275.000	3500.000	7.881	C4 S2

Appendix 5. The Irrigation Classes of Khobar Aquifer Water.

Sample No	TDS mg/l	EC micromhos/cm	SAR	Irrigation Class
81	2420.000	3723.077	6.168	C4 S2
82	2097.000	3226.154	6.04	C4 S2
83	2194.000	3375.385	6.383	C4 S2
84	2212.000	3403.077	6.204	C4 S2
85	2186.000	3363.077	6.17	C4 S2
86	2396.000	3686.154	6.288	C4 S2
87	2593.000	3989.231	7.73	C4 S2
88	2113.000	3250.769	5.987	C4 S2
89	2299.000	3536.923	6.5	C4 S2
90	2312.000	3556.923	6.467	C4 S2
91	2266.000	3486.154	6.454	C4 S2
92	2054.000	3160.000	5.85	C4 S2
93	1874.000	2883.077	5.104	C4 S2
94	2168.000	3335.385	6.018	C4 S2
95	2107.000	3241.539	5.831	C4 S2
96	2365.000	3638.462	6.886	C4 S2
97	2570.000	3953.846	7.219	C4 S2
98	1895.000	2915.385	5.299	C4 S2
99	1999.000	3075.385	5.516	C4 S2
100	1763.000	2712.308	4.655	C4 S2
101	2060.000	3169.231	5.675	C4 S2
102	2218.000	3412.308	6.034	C4 S2
103	2152.000	3310.769	5.587	C4 S2
104	1848.000	2843.077	5.228	C4 S2
105	2250.000	3461.539	6.233	C4 S2
106	2807.000	4318.461	4.89	C4 S2
107	2373.000	3650.769	6.506	C4 S2
108	2286.000	3516.923	9.337	C4 S3
109	2795.000	4300.000	8.051	C4 S3
110	2908.000	4473.844	9.311	C4 S3
111	3346.000	5147.691	7.483	C4 S3
112	1808.000	2781.538	5.707	C4 S2
113	1790.000	2753.846	4.706	C4 S2
114	2358.000	3627.692	6.021	C4 S2
115	2645.000	4069.231	12.4	C4 S4
116	2049.000	3152.308	9.645	C4 S3
117	1854.000	2852.308	4.989	C4 S2
118	1980.000	3046.154	6.418	C4 S2
119	1840.000	2830.769	8.764	C4 S2
120	1824.000	2806.154	3.453	C4 S1

Appendix 5. The Irrigation Classes of Khobar Aquifer Water.

Sample No	TDS mg/l	EC micromhos/cm	SAR	Irrigation Class
121	4586.000	7055.383	13.661	C4 S4
122	3173.000	4881.535	11.6	C4 S3
123	3025.000	4653.844	7.276	C4 S2
124	4407.000	6780.000	13.071	C4 S4
125	6639.000	10213.844	12.202	C4 S4
126	2984.000	4590.766	9.536	C4 S3
127	2343.000	3604.615	6.949	C4 S2
128	1670.000	2569.231	5.83	C4 S2
129	1784.000	2744.615	6.541	C4 S2
130	1537.000	2364.615	8.113	C4 S2
131	1709.000	2629.231	3.946	C4 S1
132	1761.000	2709.231	6.946	C4 S2
133	1438.000	2212.308	6.642	C3 S2
134	3680.000	5661.535	12.965	C4 S4
135	1538.000	2366.154	7.782	C4 S2
136	2718.000	4181.535	9.598	C4 S3
137	3338.000	5135.383	8.071	C4 S3
138	2970.000	4569.230	9.48	C4 S3
139	1527.000	2349.231	3.964	C4 S1
140	1705.000	2623.077	4.779	C4 S2
141	1212.000	1864.615	4.427	C3 S1
142	2627.000	4041.539	11.639	C4 S3
143	1887.000	2903.077	9.403	C4 S3
144	1361.000	2093.846	5.489	C3 S2
145	1191.000	1832.308	4.831	C3 S1
146	846.000	1301.538	1.764	C3 S1
147	2407.000	3703.077	1.862	C4 S1
148	3169.000	4875.383	1.1	C4 S1
149	3187.000	4903.074	6.029	C4 S2
150	1774.000	2729.231	0.058	C4 S1
151	4188.000	6443.074	7.294	C4 S2
152	2374.000	3652.308	7.558	C4 S2
153	2493.000	3835.385	7.877	C4 S2
154	2450.000	3769.231	24.756	C4 S4
155	13241.000	20370.770	42.101	C4 S4
156	17369.000	26721.539	16.621	C4 S4
157	4039.000	6213.844	20.491	C4 S1
158	3983.000	6127.691	2.256	C4 S1
159	1343.000	2066.154	4.117	C3 S1
160	1099.000	1690.769	3.63	C3 S1

Appendix 5. The Irrigation Classes of Khobar Aquifer Water.

Sample No	TDS mg/l	EC micromhos/cm	SAR	Irrigation Class
161	3269.000	5029.230	42.765	C4 S4
162	11476.000	17655.383	21.071	C4 S4
163	2374.000	3652.308	6.262	C4 S3
164	1714.000	2636.923	3.465	C4 S1
165	1788.000	2750.769	2.87	C4 S1
166	2395.000	3684.615	6.245	C4 S2
167	2485.000	3823.077	9.932	C4 S3
168	2652.000	4080.000	6.13	C4 S2
169	2011.000	3093.846	6.198	C4 S2
170	2063.000	3173.846	6.432	C4 S2
171	1904.000	2929.231	5.111	C4 S2
172	3103.000	4773.844	8.662	C4 S3
173	2096.000	3224.615	5.531	C4 S2
174	2607.000	4010.769	8.133	C4 S3
175	1788.000	2750.769	5.756	C4 S2
176	3193.000	4912.305	10.089	C4 S3
177	2223.000	3420.000	6.509	C4 S2
178	2135.000	3284.615	5.967	C4 S2
179	2879.000	4429.230	10.05	C4 S3
180	1916.000	2947.692	4.869	C4 S2
181	1773.000	2727.692	5.697	C4 S2
182	10764.000	16560.000	27.128	C4 S4
183	2714.000	4175.383	8.263	C4 S3
184	7271.000	11186.152	14.541	C4 S4
185	8366.000	12870.770	17.454	C4 S4
186	7994.000	12298.461	20.208	C4 S4
187	2243.000	3450.769	1.224	C4 S1
188	2097.000	3226.154	5.865	C4 S2
189	1043.000	1604.615	2.345	C3 S1
190	1824.000	2806.154	4.758	C4 S2
191	2452.000	3772.308	6.1	C4 S2
192	3175.000	4884.613	9.864	C4 S3
193	3254.000	5006.152	11.151	C4 S3
194	2538.000	3904.615	8.078	C4 S3
195	2154.000	3313.846	6.17	C4 S2
196	2485.000	3823.077	13.049	C4 S4
197	2518.000	3873.846	7.724	C4 S2
198	2544.000	3913.846	8.192	C4 S2
199	2120.000	3261.539	6.561	C4 S2
200	2280.000	3507.692	6.826	C4 S2

Appendix 5. The Irrigation Classes of Khobar Aquifer Water.

Sample No	TDS mg/l	EC micromhos/cm	SAR	Irrigation Class
201	6725.000	10346.152	18.213	C4 S4
202	1125.000	1730.769	4.586	C3 S1
203	1545.000	2376.923	8.003	C4 S2
204	1994.000	3067.692	6.298	C4 S2
205	1033.000	1589.231	2.356	C3 S1
206	2855.000	4392.305	9.014	C4 S3
207	1583.000	2435.385	4.905	C4 S2
208	1829.000	2813.846	9.236	C4 S3
209	1032.000	1587.692	2.745	C3 S1
210	1718.000	2643.077	7.387	C4 S2
211	2666.000	4101.535	8.374	C4 S3
212	2605.000	4007.692	8.533	C4 S3
213	2727.000	4195.383	8.22	C4 S3
214	2583.000	3973.846	9.388	C4 S3
215	2787.000	4287.691	1.149	C4 S1
216	2777.000	4272.305	8.475	C4 S3
217	2768.000	4258.461	8.541	C4 S3
218	2672.000	4110.766	8.46	C4 S3
219	2809.000	4321.535	8.549	C4 S3
220	3033.000	4666.152	12.209	C4 S4
221	2273.000	3496.923	7.121	C4 S2
222	2029.000	3121.539	3.309	C4 S2
223	1494.000	2298.461	4.03	C3 S1
224	1928.000	2966.154	5.099	C4 S2
225	2219.000	3413.846	5.735	C4 S2
226	1787.000	2749.231	27.09	C4 S4
227	1081.000	1663.077	4.05	C3 S1
228	7423.000	11420.000	14.321	C4 S4
229	1477.000	2272.308	5.299	C3 S2
230	1370.000	2107.692	4.715	C3 S1
231	1240.000	1907.692	4.637	C3 S1
232	2101.000	3232.308	5.745	C4 S2
233	1720.000	2646.154	2.324	C4 S1
234	1527.000	2349.231	2.215	C4 S1